

Mälardalen University Press Dissertations
No. 190

SIMULATION OF INDOOR RADON AND ENERGY RECOVERY VENTILATION SYSTEMS IN RESIDENTIAL BUILDINGS

Keramatollah Akbari

2015



School of Business, Society and Engineering

Copyright © Keramatollah Akbari, 2015
ISBN 978-91-7485-236-3
ISSN 1651-4238
Printed by Arkitektkopia, Västerås, Sweden

Mälardalen University Press Dissertations
No. 190

SIMULATION OF INDOOR RADON AND ENERGY RECOVERY
VENTILATION SYSTEMS IN RESIDENTIAL BUILDINGS

Keramatollah Akbari

Akademisk avhandling

som för avläggande av teknologie doktorsexamen i energi- och miljöteknik vid
Akademin för ekonomi, samhälle och teknik kommer att offentligen försvaras
fredagen den 18 december 2015, 10.00 i Pi, Mälardalens högskola, Västerås.

Fakultetsopponent: Associate Prof. Anestis Kalfas, Aristotle University of Thessaloniki



Akademin för ekonomi, samhälle och teknik

Abstract

This study aims to investigate the effects of ventilation rate, indoor air temperature, humidity and using a heat recovery ventilation system on indoor radon concentration and distribution.

Methods employed include energy dynamic and computational fluid dynamics simulation, experimental measurement and analytical investigations. Experimental investigations primarily utilize a continuous radon meter and a detached house equipped with a recovery heat exchanger unit.

The results of the dynamic simulation show that the heat recovery unit is cost-effective for the cold Swedish climate and an energy saving of about 30 kWh per floor area per year is possible, while it can be also used to lower radon level.

The numerical results showed that ventilation rate and ventilation location have significant impacts on both radon content and distribution, whereas indoor air temperature only has a small effect on radon level and distribution and humidity has no impact on radon level but has a small impact on its distribution.

*In the world, there is only one excellence and
one sin, the knowledge and the ignorance.*

(J.M. Rumi, 1207–1273)

Acknowledgments

This thesis has been carried out at the Future Energy Center at Mälardalen University. I wish to express my gratitude to my previous main supervisor, Prof. Jafar Mahmoudi and my current main supervisor, Associate Prof. Konstantinos Kyprianidis for their continued encouragement and valuable suggestions during this work, for offering the possibility to do my PhD. studies in this field and for their support. I am also grateful to my co-supervisor Dr Robert Öman who supported me with many informative discussions. I would also like to include my gratitude for friendly cooperation to Prof. Erik Dahlquist, Bengt Arnryd and Adel Karim. Also, I am grateful to Dr David Ribé for the English language corrections, Mikael Gustafsson and Dr Jan Pourian and Dr Hamid Nabati for their valuable advice and assistance.

I would like to thank the Academic Center for Education, Culture and Research (ACECR) and the Technology Development Institute (TDI) for financial support of this thesis. Furthermore, I am deeply indebted to cooperation from the environment section of Västerås Municipality, JBS, AB Company and EQUA AB for the use of IDA ICE, the Indoor Air Climate and Energy software program. I would also like to show my appreciation towards Hamid Afshar for providing supports and helping to test radon and obtain measurement data in his house for an extended period.

Finally, I want to thank my family – the encouragement and support from my beloved wife and our always positive and joyful sons is a powerful source of inspiration and energy. I would like to dedicate a special thought to my parents for their never-ending support.

Abstract

This study aims to investigate the effect on indoor radon concentration and distribution of ventilation rate, indoor air temperature, and humidity when using a heat recovery ventilation system.

Methods employed include energy dynamic simulations and computational fluid dynamics, experimental measurements and analytical investigations. Experimental investigations primarily utilize a continuous radon meter and a detached house equipped with a recovery heat exchanger unit.

The results of the dynamic simulation show that the heat recovery unit is cost-effective for the cold Swedish climate and an energy saving of about 30 kWh per m^2 floor area per year is possible, while it can be also used to lower radon level.

The numerical results showed that ventilation rate and ventilation location have significant impacts on both radon content and distribution, whereas indoor air temperature only has a small effect on radon level and distribution and humidity has no impact on radon level but has a small impact on its distribution.

Summary

The main purpose of this doctoral dissertation is to investigate how the radon level and its distribution in indoor air are influenced by both the ventilation and by different conditions indoors. A heat recovery ventilation system could be a good choice from energy saving and indoor radon mitigation standpoints. The study uses two approaches in parallel. In the first approach, dynamic simulation is used to demonstrate the energy recovery potential. In the second approach, a detailed numerical model is developed and utilised to predict the indoor radon level and distribution with varying levels of ventilation rate, indoor air temperature and humidity.

The effect of a heat recovery ventilation system on both energy saving and radon mitigation was investigated in a detached house using IDA, ICE, Indoor Air Climate and Energy software program, analytical investigations and measurements. Then a finite volume method was applied using the computational fluid dynamics (CFD) ANSYS FLUENT software.

Although many research studies have been conducted on the effects of radon in soil and its properties on indoor radon, information about the influence of indoor air conditions on indoor radon behaviour is rather scarce and merits further investigation. Furthermore, traditional methods of measuring indoor radon can only provide rough average values for the whole of a building or a room for an entire year. This is unsafe and unacceptable from the indoor air quality viewpoint. Health organizations also emphasise that any level of radioactive elements such as radon may be carcinogenic.

Through the CFD simulations carried out in this study, the indoor radon level and distribution is predicted throughout a room and particularly in dead zones with insufficient ventilation rate. The simulations provide a good picture of indoor radon distribution and help investigate the effect of different independent variables on indoor radon.

In this study, indoor radon activity concentrations were measured during the cold season for different ventilation rates using a new radon electronic meter (commercially known as R2) which can measure radon, temperature and relative humidity simultaneously. The measurements complement the theoretical analysis performed on the association between indoor radon level and ventilation rate, the height above the floor and economic analysis of installing a heat recovery unit considering life cycle costs.

The results of the dynamic simulation and theoretical analysis confirmed that the heat recovery unit is cost-effective for cold climates like Sweden and an energy saving of about 3,000 kWh per year or about 30 kWh per m² floor area per year is possible.

The numerical simulation results show that ventilation rate and ventilation location have significant impacts on both radon content and radon distribution, whereas indoor air temperature has a small effect on radon level and distribution, and humidity has no impact on radon level but has a small impact on its distribution. There was good agreement between analytical, measurement and simulation results concerning the association between indoor radon level, the height above the floor and ventilation rate.

It should be emphasised that this work represents the first step in the field with regard to using CFD to study the sensitivity of indoor radon level and its distribution in small residential buildings. The research is supported by a number of publications as well as unpublished results which are shown for the first time in the main body of this thesis. It is hoped that the present study will serve as a stepping stone for further work in the field by the other researchers.

Sammanfattning

Huvudsyftet med denna doktorsavhandling är att undersöka hur radonhalt och dess fördelning i inneluft påverkas av både ventilation och av olika förhållanden inomhus. Ett fläktstyrt ventilationssystem med en värmeväxlare mellan från- och tilluft kan bidra till både mindre värmeförluster och lägre radonhalt i inneluften. I denna studie används två metoder parallellt. Den första metoden är dynamisk simulering av energibalans med fokus på värmeväxling. Den andra metoden avser en detaljerad numerisk modell som utvecklats och tillämpats för att förutsäga hur radonhalt och fördelning av radonhalt i inneluft påverkas av uteluftsflöde och inneluftens temperatur och luftfuktighet.

Ett fristående småhus med en värmeväxlare mellan från- och tilluft studerades avseende både energihushållning och radonbegränsning med dataprogrammet IDA ICE (Indoor Climate and Energy), med analytiska undersökningar och med mätningar. För en detaljerad numerisk modell användes sedan en finit volymmetod med CFD (Computational Fluid Dynamics) i dataprogrammet ANSYS FLUENT.

Många studier har gjorts om markradon och dess allmänna påverkan på radonhalten i inneluft. Det finns dock mycket begränsat med information om hur olika förhållanden inomhus kan påverka radon i inneluft och detta motiverar vidare undersökning. Dessutom brukar traditionella mätmetoder för radon bara ge medelvärden för ett visst rum eller en viss byggnad ofta uppskattat för ett helt år. Detta kan sägas vara osäkert och oacceptabelt med hänsyn till den stora betydelsen av inneluftens kvalitet. Hälsoorganisationer betonar också att all joniserande strålning från till exempel radon kan vara cancerframkallande.

Simuleringar med CFD användes i denna studie för att förutsäga radonhalten och dess fördelning i rum som även innehåller stagnationszoner med mycket dålig ventilation. Simuleringarna kan ge en bra uppfattning om radonhaltens fördelning och kan även visa hur olika variabler inverkar på radonhalten.

Samtidiga mätningar av radonhalt, lufttemperatur och relativ luftfuktighet gjordes med olika uteluftsflöde vintertid med en ny elektronisk radonmätare som kommersiellt är känd som R2. Mätningarna kompletterar den teoretiska analysen avseende sambandet mellan radonhalt å ena sidan och uteluftsflöde och höjd över golvet å andra sidan, och även när det gäller en ekonomisk analys med livscykelkostnader avseende värmeväxling.

Resultat från den dynamiska simuleringen och den teoretiska analysen bekräftar att värmeväxlaren i detta fall är kostnadseffektiv för kalla klimat

såsom i Sverige med en möjlig energibesparing om ca 3 000 kWh per år eller ca 30 kWh per m² golvarea och år.

Resultat från de numeriska simuleringarna visar att uteluftsflöde och ventilationsdonens placering har betydande inverkan på både radonhalten och dess fördelning, medan innetemperaturen har en liten inverkan på radonhalten och dess fördelning. Vidare framgår att luftfuktigheten inte inverkar på genomsnittlig radonhalt, men har en liten inverkan på radonhaltens fördelning. Överensstämmelsen var god mellan resultaten från analys, mätningar och simuleringar avseende sambandet mellan radonhalt å ena sidan och uteluftsflöde och höjd över golvet å andra sidan.

Det bör framhållas att det här arbetet utgör ett första steg inom området avseende CFD-simulering för detaljerade studier av radonhalt och dess fördelning i småhus. Forskningen stöds av ett antal publikationer samt opublicerade resultat som visas för första gången i huvuddelen av denna avhandling. En förhoppning är att denna studie kommer att fungera som en språngbräda för fortsatt arbete inom området av andra forskare.

List of Papers included

This thesis is based on the following papers, which are referred to in the text by their Roman numerals.

- I. Akbari, K. & Öman, R. (2013). Impacts of heat recovery ventilators on energy savings and indoor radon level. *Management of Environmental Quality Journal*, Vol. 24, No. 5, pp. 682–694.
- II. Akbari, K., Mahmoudi, J. & Ghanbari, M. (2013). Simulation of Ventilation Effects on Indoor Radon. *Management of Environmental Quality Journal*, Vol. 24, No. 3, pp. 394–407.
- III. Akbari, K. & Mahmoudi, J. (2012). Effects of Heat Recovery Ventilation Systems on Indoor Radon. *Proceedings of ECOS 2012 - the 25th international conference on Efficiency, Cost, Optimization, Simulation and Environmental Impact of Energy Systems, June 26-29, 2012, Perugia, Italy ECOS 2012*. Available at: http://www.ecos2012.unipg.it/public/proceedings/pdf/buces/buces_ecos2012_329.pdf.
- IV. Akbari, K. & Mahmoudi, J. (2013). Influence of Indoor Air Conditions on Radon Concentration in a Detached House. *Journal of Environmental Radioactivity*, No. 116, pp. 166–173.

Reprints were made with permission from the respective publishers.

List of Publications not included

In completion of this thesis and the papers listed above, ideas, data measurements, computations, modeling and simulations, and analyses were carried out by the author. I have been assisted by my main supervisor, co-supervisor, reviewers and co-authors in adding further improvements to the work. Papers and other publications excluded from this thesis are as follows.

Licentiate thesis

- I. Akbari, K. (2009). *Impact of Radon Ventilation on Indoor Air Quality and Building Energy Saving*. Mälardalen University Press. ISBN 978-91-86135-39-3. Available at <http://mdh.diva-portal.org/smash/get/diva2:237857/FULLTEXT01.pdf>

Papers

- II. Akbari, K. & Mahmoudi, J. (2008). Simulation of Radon Mitigation and Ventilation in Residential Building. Printed in *the 49th Scandinavian conference on Simulation and Modeling (SIMS 2008)*. ISBN-13-978-82-579-4632-6.
- III. Akbari, K., Mahmoudi, J. & Öman, R. Ventilation Strategies and Radon Mitigation in Residential Buildings. Submitted to *Indoor Air International Journal of Indoor Environment and Health*. ID: INA-09-09-156.
- IV. Akbari, K. & Mahmoudi, J. (2009). Influence of Residential Ventilation on Radon Mitigation with Energy Saving Emphasis. Scientific Conference on *"Energy system with IT" March 2009, Stockholm*. ISBN 978-91-977493-4-3.

Table of Contents

| | | |
|-------|--|----|
| 1 | INTRODUCTION | 1 |
| 1.1 | Background | 1 |
| 1.2 | Problem description and motivation..... | 3 |
| 1.3 | Aims and objectives | 4 |
| 1.4 | Methods, limitations and research process | 4 |
| 1.5 | Thesis outline | 5 |
| 1.6 | Summary of included papers | 6 |
| 1.7 | Contribution to knowledge | 8 |
| 2 | LITERATURE REVIEW | 9 |
| 2.1 | Indoor radon levels, energy use and heat recovery ventilation system..... | 9 |
| 2.2 | Ventilation effect and Indoor Radon Mitigation..... | 12 |
| 2.3 | Radon transport mechanisms and environmental conditions effects | 12 |
| 2.3.1 | Radon concentration equation in a ventilated room | 14 |
| 2.3.2 | The effects of temperature and humidity on the pressure field .. | 14 |
| 2.4 | Radon modeling methods | 15 |
| 3 | MATERIALS AND METHODOLOGY | 17 |
| 3.1 | Materials | 17 |
| 3.1.1 | Case study house | 17 |
| 3.1.2 | Heat recovery unit | 18 |
| 3.1.3 | Radon detectors | 20 |
| 3.2 | Research methods..... | 21 |
| 3.2.1 | Measurement | 21 |
| 3.2.2 | Analytical analysis | 22 |
| 3.2.3 | Economic analysis..... | 23 |
| 3.2.4 | Heating degree days (HDD) calculations | 23 |
| 3.2.5 | Ventilation loss..... | 24 |
| 3.2.6 | The life cycle cost analysis of heat recovery ventilation system | 25 |
| 3.3 | Energy dynamic simulation | 26 |
| 3.4 | Computational fluid dynamics (CFD) | 27 |
| 4 | NUMERICAL MODELING PROCEDURE..... | 29 |
| 4.1 | Discretization methods | 29 |
| 4.1.1 | Finite control volume analysis | 30 |

| | | |
|-------|---|----|
| 4.2 | Governing equations used | 30 |
| 4.3 | Turbulence model | 34 |
| 4.4 | Boundary conditions and input data | 35 |
| 4.4.1 | Inlet Vent | 35 |
| 4.4.2 | Outlet | 37 |
| 4.4.3 | Outer Surfaces | 37 |
| 4.4.4 | Internal Surfaces | 38 |
| 4.4.5 | Floor Zone | 38 |
| 4.5 | The House Plan Geometry | 39 |
| 4.6 | Parameters Variation Range | 40 |
| 4.7 | Materials Properties | 41 |
| 4.8 | Relative Humidity | 42 |
| 4.9 | Defined Functions | 45 |
| 4.10 | Convergence Criteria | 45 |
| 4.11 | Near-wall treatment | 46 |
| 4.12 | Mesh Independence Study | 50 |
| 4.13 | Examination of convergence criteria | 54 |
| 5 | RESULTS AND DISCUSSION | 63 |
| 5.1 | Radon measurement | 63 |
| 5.2 | Analytical analysis of radon level in the case study house | 68 |
| 5.3 | Dynamic energy simulation and calculation | 68 |
| 5.3.1 | Economic analysis of the heat recovery ventilation unit | 69 |
| 5.4 | Results and discussion of numerical modelling | 71 |
| 5.4.1 | Air Change Rate Effects on Indoor Radon Content | 71 |
| 5.4.2 | Temperature Changes Effects on Indoor Radon Concentration | 76 |
| 5.4.3 | Effects of Relative Humidity Changes on Indoor Radon Concentration | 79 |
| 5.5 | Model validation and result comparison | 81 |
| 6 | CONCLUSIONS AND FUTURE WORK | 83 |
| 6.1 | Dynamic simulation and heat recovery analysis | 83 |
| 6.2 | Numerical Simulation | 84 |
| 6.3 | Future work | 85 |
| | REFERENCES | 87 |
| | APPENDICES | 91 |
| | APPENDIX A: IDA, BOUNDARY CONDITIONS AND INPUT DATA | 93 |
| | APPENDIX B: RADON TRANSPORT EQUATIONS AND INDOOR CONDITIONS | |
| | 97 | |
| | PAPERS | 1 |

List of Figures

| | |
|--|----|
| Figure 1. Ground floor plan and zone divisions of the case study house.... | 18 |
| Figure 2. Air flows through the rotary heat exchanger | 19 |
| Figure 3. The rotary heat exchanger installed in the building | 20 |
| Figure 4. The R2 continuous radon meter | 21 |
| Figure 5. The house plan geometry..... | 39 |
| Figure 6. Room1 geometry | 40 |
| Figure 7. A sample of the meshed model | 50 |
| Figure 8. Average radon concentration for different mesh sizes | 52 |
| Figure 9. Average static temperature for different mesh sizes | 52 |
| Figure 10. Radon flow rate in the outlet for different mesh sizes..... | 53 |
| Figure 11. Radon concentration profile along a vertical line in the middle of the room for different mesh sizes | 53 |
| Figure 12. Average radon concentration versus iterations for the case N11 | 54 |
| Figure 13. Average indoor static temperature versus iterations for the case indicated with N11 | 55 |
| Figure 14. Radon flow rate in the outlet versus iterations for the case indicated with N11 | 56 |
| Figure 15. Residuals versus iterations for the case indicated with N11 | 57 |
| Figure 16. Radon level measurements versus ventilation rate..... | 65 |
| Figure 17. Radon level (green curve) and temperature (purple curve)..... | 66 |
| Figure 18. Radon level changes versus measurement height above the room floor | 66 |
| Figure 19. Average radon levels versus height (0-200 cm from the floor)... | 67 |
| Figure 20. Average radon levels versus height (0-50 cm from the floor)..... | 67 |
| Figure 21. Average radon content for different air change rates at $T = 21^{\circ}\text{C}$ and $\text{RH} = 40\%$ | 72 |
| Figure 22. Radon concentration along a vertical line in the middle of the room for N3 ($\text{Ach} = 0.5\text{hr}$, $T = 21^{\circ}\text{C}$, $\text{RH} = 40\%$)..... | 72 |
| Figure 23. Radon content along a vertical line in the middle of the room for N12 ($\text{Ach} = 0.25\text{ hr}^{-1}$, $T = 21^{\circ}\text{C}$, $\text{RH} = 40\%$)..... | 73 |
| Figure 24. Position of two vertical planes in the middle of room for showing distribution of different quantities within the room..... | 73 |
| Figure 25. Contours of radon concentration (Bqm^{-3}) in two vertical planes in the middle of room for N3 ($\text{Ach}=0.5\text{ hr}^{-1}$, $T=21^{\circ}\text{C}$, $\text{RH}=40\%$).. | 74 |
| Figure 26. Contours of air velocity (ms^{-1}) in two vertical planes in the middle of room for N3 ($\text{Ach} = 0.5\text{ hr}^{-1}$, $T = 21^{\circ}\text{C}$, $\text{RH} = 40\%$)..... | 74 |

| | |
|---|----|
| Figure 27. Contours of radon concentration (Bqm^{-3}) in two vertical planes in the middle of room for N12 ($\text{Ach} = 0.25 \text{ hr}^{-1}$, $T = 21 \text{ }^{\circ}\text{C}$, $\text{RH} = 40\%$)..... | 75 |
| Figure 28. Contours of air velocity (ms^{-1}) in two vertical planes in the middle of room for N12 ($\text{Ach} = 0.25 \text{ hr}^{-1}$, $T = 21 \text{ }^{\circ}\text{C}$, $\text{RH} = 40\%$)..... | 75 |
| Figure 29. Average radon concentration in the room for different temperatures at $\text{Ach} = 0.5 \text{ hr}^{-1}$ and $\text{RH} = 40\%$ | 76 |
| Figure 30. Radon concentration along a vertical line in the middle of room for different temperatures (15 to 23°C) at $\text{Ach} = 0.5 \text{ hr}^{-1}$ and $\text{RH} = 40\%$ | 77 |
| Figure 31. Contours of radon concentration (Bqm^{-3}) in two vertical planes in the middle of room for N3 ($\text{Ach} = 0.5 \text{ hr}^{-1}$, $T = 21 \text{ }^{\circ}\text{C}$, $\text{RH} = 40\%$)..... | 78 |
| Figure 32. Contours of radon concentration (Bqm^{-3}) in two vertical planes in the middle of room for N4 ($\text{Ach} = 0.5 \text{ hr}^{-1}$, $T = 23 \text{ }^{\circ}\text{C}$, $\text{RH} = 40\%$)..... | 78 |
| Figure 33. Contours of radon concentration (Bqm^{-3}) in two vertical planes in the middle of room for N4 ($\text{Ach} = 0.5 \text{ hr}^{-1}$, $T = 21 \text{ }^{\circ}\text{C}$, $\text{RH} = 40\%$)..... | 80 |
| Figure 34. Contours of radon concentration (Bqm^{-3}) in two vertical planes in the middle of room for N7 ($\text{Ach} = 0.5 \text{ hr}^{-1}$, $T = 21 \text{ }^{\circ}\text{C}$, $\text{RH} = 50\%$)..... | 80 |

List of Tables

| | | |
|-----------|---|----|
| Table 1. | Physico-chemical characteristics of radon (Keith S, 2012)..... | 2 |
| Table 2. | Features of the different numerical simulations in the publications..... | 7 |
| Table 3. | Annual radon average concentration in Västerås, Sweden..... | 10 |
| Table 4. | Radon levels and remediation techniques (Radiological Protection Institute of Ireland, 2010) | 12 |
| Table 5. | The operation ratings of the unit | 20 |
| Table 6. | Date and time period of the measurements | 22 |
| Table 7. | Velocity and turbulence intensity for different ventilation rates | 37 |
| Table 8. | Sizes of the building elements..... | 40 |
| Table 9. | Different cases studied in this work | 41 |
| Table 10. | Properties of the fluids (Lide, 2004)..... | 42 |
| Table 11. | Properties of the solids (Lide, 2004) | 42 |
| Table 12. | Mass fraction of water vapor for different relative humidity and temperatures | 45 |
| Table 13. | Average radon concentration, average static temperature and radon flow rate in the outlet for different mesh sizes | 51 |
| Table 14. | The heat rejection to outdoor environment through each outer surface, case N11 | 60 |
| Table 15. | Measured indoor radon levels (Bqm^{-3})..... | 64 |
| Table 16. | Radon level versus ventilation rate by measurement and analytic methods | 68 |
| Table 17. | Dynamic simulation and energy calculation results | 69 |
| Table 18. | Values used for life cycle cost analysis | 70 |
| Table 19. | Ventilation system life cycle cost analysis..... | 70 |
| Table 20. | Average radon content for different air change rates at $T = 21\text{ }^{\circ}\text{C}$ and $\text{RH} = 40\%$ | 71 |
| Table 21. | Average radon concentration in the room for different temperatures at $\text{Ach}=0.5\text{ hr}^{-1}$ and $\text{RH}=40\%$ | 76 |
| Table 22. | Average radon concentration for different relative humidity at $\text{Ach} = 0.5\text{ hr}^{-1}$ and $T = 21\text{ }^{\circ}\text{C}$ | 79 |
| Table 23. | Indoor radon levels obtained by different methods | 81 |
| Table 24. | Indoor radon for different heights above the floor | 82 |
| Table 25. | The impacts of parameters on indoor radon level and distribution..... | 84 |

Nomenclature and abbreviations

Symbols

| | |
|------------------------------|--|
| <i>A</i> | Surface (m^2) |
| <i>Ar</i> | Radium activity (Bq kg^{-1}) |
| <i>C</i> | Radon activity concentration (Bq m^{-3}) |
| <i>C_f</i> | Skin friction |
| <i>C_p</i> | Specific heat capacity ($\text{J kg}^{-1} \text{K}^{-1}$) |
| <i>D</i> | Effective diffusion coefficient ($\text{m}^2 \text{s}^{-1}$) |
| <i>D_h</i> | Hydraulic diameter (m) |
| <i>E</i> | Radon exhalation rate ($\text{Bq m}^{-2} \text{h}^{-1}$) |
| <i>f</i> | Radon emanation coefficient |
| <i>G</i> | Radon generation rate ($\text{Bq m}^{-3} \text{s}^{-1}$) |
| <i>h_c</i> | Heat transfer coefficient ($\text{W m}^{-2} \text{K}^{-1}$) |
| <i>i</i> | Interest rate (%) |
| <i>I</i> | Turbulence intensity |
| <i>I_a</i> | Net present value factor |
| <i>k</i> | Thermal conductivity ($\text{W m}^{-1} \text{K}^{-1}$) |
| <i>K</i> | Turbulent kinetic energy ($\text{m}^2 \text{s}^{-2}$) |
| <i>M_w</i> | Molecular weight |
| <i>m</i> | Mass flow rate (kg s^{-1}) |
| <i>n</i> | Time in year unit |
| <i>P</i> | Pressure (Pa) |
| <i>q</i> | Annual energy cost escalation rate (%) |
| <i>R</i> | Specific gas constant ($\text{J mol}^{-1} \text{K}^{-1}$) |
| <i>T</i> | Temperature (K) |
| <i>V</i> | Volume (m^3) |
| <i>V</i> | Flow velocity vector (m s^{-1}) |
| <i>u, v, w</i> | Velocity components in x, y, and z coordinates (m s^{-1}) |
| <i>η_t</i> | Temperature efficiency |
| <i>η_w</i> | Moisture efficiency |
| <i>λ_v</i> | Air change rate (h^{-1}) |
| <i>ρ</i> | Density (kg m^{-3}) |
| <i>λ_{Rn}</i> | Radon decay constant (s^{-1} or h^{-1}) |
| <i>ε</i> | Turbulent dissipation rate ($\text{m}^2 \text{s}^{-3}$) |
| <i>μ</i> | Molecular viscosity ($\text{kg s}^{-1} \text{m}^{-1}$) |
| <i>μ_t</i> | Turbulent viscosity ($\text{kg s}^{-1} \text{m}^{-1}$) |
| <i>ν</i> | Kinematic viscosity ($\text{m}^2 \text{s}^{-1}$) |
| <i>ε</i> | Porosity |
| <i>τ_w</i> | Wall shear stress |

Abbreviations

| | |
|--------|---|
| Ach | Air change rate |
| ASHRAE | American society of heating, refrigerating and air conditioning engineering |
| ATD | Alpha track detector |
| CFD | Computational fluid dynamics |
| CHTC | Convective heat transfer coefficient |
| CRM | Continuous radon monitor |
| DHW | Domestic hot water |
| HVAC | Heating, ventilation and air conditioning |
| HRV | Heat recovery ventilation |
| HDD | Heat degree days |
| IAQ | Indoor air quality |
| kWh | Kilowatt-hour |
| MF | Mass fraction |
| PDE | Partial differential equations |
| Re | Reynolds number |
| RH | Relative humidity |
| Rn | Radon-222 |
| SST | Shear stress transport |
| TWh | Terawatt-hour |

1 Introduction

1.1 Background

People in developed countries regularly spend more than 90 % of their time in confined and enclosed spaces, i.e. in homes, offices and vehicles. More than two thirds of this time is spent in residential buildings. Buildings act as a shelter and protect people from heat, cold, sunshine, noise, pollutants and other inconveniences. However, these shelters are not as safe as they could be, because they contain many indoor pollutants. Pollutants create indoor air quality (IAQ) problems which affect human health, productivity and comfort. Unfortunately the variety and amount of pollutants are continuously increasing (Zhang Y. , 2004; WHO, 2009).

Radon is one of the major and most harmful indoor pollutants in many countries, such as the Scandinavian countries, the U.S., U.K., etc. Radon is estimated to account for more than 3,000 and 21,000 deaths annually from lung cancer in the UK and US respectively (Nilsson, 2006; EPA, 2008).

Sweden is one of the countries with the highest indoor radon concentrations in the world. This radon originates from uranium-rich soils and rocks such as alum-shale and uranium-rich granites (Sundal, Henriksen, Lauritzen, & Soldal, 2004).

Radon in the environment is present as a radioactive ground gas which exists in soil, water, air and in some natural gas. This radioactive gas mixes with air and is quickly diluted in the atmosphere. However, radon which enters enclosed spaces can accumulate and reach relatively high levels in some places, especially in buildings with insufficient ventilation (Malanca, Cassoni, Dallara, & Pessina, 1992).

General methods to control the levels of indoor pollutants are by source control, e.g. removal, replacement by alternative materials, sealing or dilution, or by removal by ventilation and air cleaning. When the radon regulatory limit is set in the range of 600 Bq/m³ or less, ventilation becomes a cost-effective and applicable method to dilute radon contamination and maintain IAQ in existing under-ventilated buildings (Radiological Protection Institute of Ireland, 2010), i.e. buildings with ventilation below the typical air exchange requirement of 0.5 hr⁻¹. Ventilation blows fresh outdoor air into the room and reduces pollutant concentrations by mixing and dilution. However, building ventilation in turn leads to increased energy consumption in the

building sector. An optimal ventilation rate is therefore important for both people and governing authorities (in the case of housing associations).

Radon-222 (simply referred to as "radon") is a radioactive and inert gas which decays into alpha particles with a half-life of 3.82 days. This radioactive gas is colorless, odorless, tasteless, and is therefore undetectable without the use of specific instruments. It originates from decay chains of uranium and radium and is naturally occurring around the world. Radon in its gaseous form (at normal temperatures) is present throughout the earth's crust at different concentrations which vary as a function of the nature of the soil. Some regions may therefore have serious issues with radon, as is the case in Sweden, while others may have very limited or no concerns at all.

In standard conditions¹, characteristics of radon are as shown in Table 1 (Keith S, 2012). Being a stable gas, radon is chemically neutral, and its half-life is long enough for it to accumulate in confined spaces. This radioactivity half-life also makes radon useful in the physical sciences as a natural tracer. (WHO, 2009).

Table 1. Physico-chemical characteristics of radon (Keith S, 2012)

| Density (kgm ⁻³) | Diffusivity in Air (m ² s ⁻¹) | Decay rate (s ⁻¹) | Atomic weight (gmol ⁻¹) |
|---------------------------------|---|----------------------------------|--|
| 9.73 | 1.1×10 ⁻⁵ | 2.1×10 ⁻⁶ | 222 |

Studies show that there is a direct link between breathing radon and lung cancer. Thus, radon is a significant contaminant and affects IAQ throughout the world. Radon is the main contributor to public exposure to radioactivity. In the United States, radon is the most important cause of lung cancer after cigarette smoking (EPA, 2008).

When radon accumulates in a room, up to 70 % of it decays into metal ions. These decay products are called radon progeny (daughters). Radon itself is an inert gas and does not carry health risks, while its progeny, alpha particles, Po₂₁₄, Pb₂₁₄, Bi₂₁₄, and Po₂₁₈ are harmful to the airways of the human respiratory system. These non-gaseous radon progeny, which settle on airways, are the main routes of exposure. Their ionizing power is 20 times greater than beta rays and gamma rays. Radioactive alpha particles are characterized by low permeability but high ionizing power (Dainius & Aloyzas, 2007).

Radon activity concentration is measured in the SI derived unit Bqm⁻³ (Becquerel per cubic meter). One Becquerel is the quantity of radioactive material that will produce one transformation in one second; 1 Bq is equivalent to 1 event of radiation emission per second. The Becquerel is thus a

¹ At 20 °C and 1 atmosphere.

measure of the activity rate (and not the energy) of radiation emission from a source.

The building sector accounts for almost 40 % of the world's energy use, and exceeds the transportation sector in terms of carbon emissions (Zhang & Cooke, 2010). Most of the energy use in the sector is related to heating, ventilation and air conditioning, which together account for 55 % of the energy use in residential buildings (Zhang & Cooke, 2010). In Sweden for example, about 61 % of energy used in the building sector is used for space heating and domestic hot water (Swedish Energy Agency, 2010). It is important from the energy conservation point of view that ventilation rates are not excessive, but at the same time they should be sufficient to ensure good IAQ. Radon reduction strategies should also aim to consider problems related to radon sources and transport processes to be efficient and cost-effective. Strategies can include active and passive soil depressurization, barriers and membranes, sealing entry routes, sealing building material surfaces and ventilation of occupied spaces.

Sometimes a combination of all these strategies may be necessary, particularly in buildings with highly elevated radon levels. This thesis focuses on ventilation strategy by using a heat recovery ventilation system and describes how to simultaneously improve the complications related to energy use and indoor radon concentration.

1.2 Problem description and motivation

Global energy consumption, particularly in the building sector is growing, and the use of energy-efficient technologies in ventilation systems has an important role to play in energy savings and emissions reduction.

Reducing radon in residential buildings is a significant problem from the viewpoints of IAQ, adverse health effects and energy savings. Reducing radon by means of forced ventilation inevitably leads to higher energy use. Heat recovery ventilation (HRV) systems as an energy-efficient technology can recover energy in exhaust air that would otherwise escape, both reducing energy use and balancing indoor and outdoor pressure to reduce radon concentration.

Earlier studies (Fournier, Groetz, & Jacob, 2005; Narula, Saini, Goyal, & Chauhan, 2009) in this field have focused on factors affecting radon distribution in soil and its characteristics. Some very recent and concurrent studies (Chauhan, Joshi, & Agarwal, 2014; Kumar, Chauhan, & Sahoo, 2014), are focusing on the comparison of CFD simulation results of radon concentration and exhalation rates with experimental measurements indicating the importance of research on the indoor radon problem.

However, these studies do not explain how physical and environmental factors affect indoor radon concentration. The present study considers different indoor temperature and humidity conditions, ventilation rates, and other possibly important parameters to determine their effects on indoor radon distribution and concentration.

HRV systems are a well-known technology in Europe and are used as energy-efficient systems. A HRV system can provide the required indoor conditions in several ways. For instance, it can balance the pressure difference due to supply and exhaust with fans and thus control indoor radon level. This study intends to improve the research community's understanding of the conditions and the extent to which HRV technology can be applicable and cost-effective for indoor radon control relative to other mitigation methods.

In this study I use computational fluid dynamics (CFD) and measurement techniques to show the influence of several parameters on indoor radon level in a detached house. CFD is used to simulate and estimate indoor radon concentrations and dynamic simulation is employed to analyze energy use by means of a rotary heat exchanger installed in the house.

1.3 Aims and objectives

The main aim of this work is to investigate the influence of ventilation, indoor temperature and humidity on radon mitigation using measurement, dynamics and numerical simulation from the viewpoints of energy savings and indoor air radon quality.

The research questions are:

- Is it possible to use CFD to simulate and predict indoor radon distribution in residential buildings with and without HRV?
- What is the indoor radon distribution suggested by the CFD results? Under what conditions is a HRV system economically appropriate for reducing indoor radon in residential buildings relative to other mitigation methods?
- What is the relationship between indoor temperature, indoor humidity, position of the supply and exhaust air terminal devices, and indoor radon level and distribution?

1.4 Methods, limitations and research process

Methods:

In this study, dynamic and CFD simulation, measurement and analytical methods have been used.

Limitations:

In the work described in this thesis, several assumptions have been made for simplicity and to comply with computational limitations (a High Performance Computing facility was not available for this study). These limitations and assumptions have potential to be developed and modified in future studies using other CFD methods and by considering more complicated buildings or rooms. For instance, the effects of residents and their furnishings, as well as the effect of non-ideal airtightness (leakages) in the building have been ignored in this work. Another assumption used throughout the thesis is that ventilation is provided by mechanical means (and with heat recovery) as opposed to other ventilation solutions. Assumptions have also been made regarding constant radon generation rate and outdoor conditions, as well as simplifications in the numerical modeling and intrinsic limitations of CFD techniques because of discretization and semi-empirical turbulence modeling methods.

Research process:

1. Investigating and gathering data on radon in recent years in the case study house.
2. Collecting new measurements with a continuous radon monitor in different situations and under different temperature and relative humidity conditions.
3. Evaluating a heat recovery ventilation system.
4. Dynamic simulation using IDA 4.1 software.
5. CFD simulation using the ANSYS FLUENT 14 package.

1.5 Thesis outline

This thesis is broadly organized on two levels. The first level considers the role of a heat recovery ventilation system in energy saving and indoor radon control using life cycle cost to show its cost-effectiveness (Paper I). The second level considers indoor radon and effects of indoor air conditions including temperature, humidity and ventilation rate (papers II–IV).

The thesis comprises of six chapters and the contents are outlined as follows:

Chapter 1 Introduction: background, problem description, motivation, objectives, thesis scope and outline.

Chapter 2 Literature review: review of heat recovery ventilation system, radon mitigation, radon transport mechanisms and modeling.

Chapter 3 Materials and Methodology: case study house, radon detectors, dynamics and CFD simulation packages.

Chapter 4 Numerical modeling procedure: discretization of radon transport equation, indoor radon modeling, boundaries, geometry and materials.

Chapter 5 Results and discussion: results and discussion of radon measurement, dynamic simulation, economic analysis and numerical modeling.

Chapter 6 Conclusion and future works: dynamic simulation and heat recovery analysis, numerical simulation and future works.

1.6 Summary of included papers

Paper I:

Paper I focuses on dynamic simulation and energy recovery calculations. The results confirm that using a heat recovery unit can meet energy saving and radon mitigation needs simultaneously. It is shown how a heat recovery ventilation system means that an increased outdoor air flow rate can be combined with a comparatively limited increase in the energy demand for space heating in order to dilute and lower indoor radon levels. Life cycle cost analysis also indicates that a heat recovery ventilation system can be cost-effective.

Paper II:

This paper presents the first simple 3-D model to simulate radon generated from soil using CFD and the FLUENT software package. This work investigates the effects of ventilation rate, exhaust fan and supply fan on indoor radon. The results show that the effects of supply air terminal device location on radon level and distribution are distinguishable under different supply air flow rates. Compared to an exhaust fan, a supply fan has a greater impact on radon mitigation. Air leakages through doors and windows can have a similar effect on indoor radon behavior to a supply fan. Of course this by no means a general conclusion, but an example from specific calculations on a particular type of residential building.

Paper III:

In this paper the effects of ventilation rates, temperature, humidity and pressure is investigated on indoor radon. Results of numerical studies indicated that changes of ventilation rate, indoor temperature and moisture by means of ventilation systems have significant effects on indoor radon content. Ventilation rate was inversely proportional to indoor radon concentration. Mini-

imum radon levels were estimated in the range of thermal comfort, i.e. at 21°C and relative humidity between 50–70%.

The approach of this paper is similar to Paper II, but the case study house is modeled without soil section and using fine grids.

Paper IV:

This study uses an improvement over the model described in paper III. A heat recovery ventilation system unit was used to control the ventilation rate. As well as ventilation rate, this model considers the effects of indoor air temperature and relative humidity. The results from analytical solution, measurements and numerical simulation showed that air change rate had a significant effect on indoor radon concentration but indoor air temperature and moisture had little effect.

Overview:

This thesis used the K- ω turbulence model in ANSYS FLUENT 14.0 instead of the K- ϵ model in FLUENT 6.4 used in papers II–IV with the aim of improving the near wall treatment.

The dynamic simulations and calculations on heat recovery presented in Paper I are the same as the results presented in the main body of this thesis. Table 2 presents an overview of the different numerical simulations presented in papers II–IV and in the main body of this thesis.

Table 2. Features of the different numerical simulations in the publications

| Publication | Geometry | Model | Kinds of air conditions | Turbulence and grid cells |
|--------------------|--------------------------|---|--|--|
| Paper II | House without partitions | Soil radon, Mixture of air and radon in species model | Exhaust and supply fans separately | Turbulence k- ϵ model, 200,000 hexahedral cells |
| Paper III | All rooms | Indoor radon, Mixture of air, moisture and radon in species model | Temperature, Humidity, Pressure difference, Balanced ventilation | Turbulence k- ϵ model 370,000 hexahedral cells |
| Paper IV | All rooms | Indoor radon, Mixture of air, moisture and radon in species model | Temperature, Humidity, Balanced ventilation | Turbulence k- ϵ model 700,000 hexahedral cells |
| Thesis | One room | Indoor radon, Mixture of air, moisture and radon in species model | Temperature, Humidity, Balanced ventilation | Turbulence k- ω model 2,700,000 hexahedral cells |

1.7 Contribution to knowledge

The literature survey reveals that there is little or no research available in the public domain regarding the analysis of the effect of heat recovery ventilation on indoor radon mitigation using advanced CFD simulations. With this in mind, the author's efforts have focused on the development of models and methods of numerical simulation of indoor radon, as well as on the measurement of indoor radon, temperature and relative humidity with advanced equipment.

The author's contribution to the knowledge in the area can be summarized as follows:

- Development of CFD models for analyzing indoor radon concentration and distribution in one-family residences.
- Analysis of IAQ focusing on indoor radon using the aforementioned models. The application of a HRV system was considered in detail because of its capacity for controlling indoor radon concentration as well as indoor temperature, pressure, moisture and ventilation rate. Displacement ventilation was assessed as a likely candidate for ventilation with regard to radon mitigation; the simulation results indicate that the performance of such a system is likely to be dependent on the vertical position of its installation within the occupied zone.

It is important to note that the presented work is supported by three peer-reviewed journal publications and one peer-reviewed conference paper.

2 Literature review

This chapter provides a review of the literature on previous relevant research: energy use and heat recovery ventilation system; ventilation and indoor radon mitigation; radon transport mechanisms and effects of environmental conditions; radon modeling methods.

2.1 Indoor radon levels, energy use and heat recovery ventilation system

The World Health Organization recommends 100 Bqm⁻³ as a new indoor radon action level (WHO, 2009). This value is currently 200 Bqm⁻³ in Sweden. Based on a recent radon survey in Sweden, 35 % of all monitored small houses and 28 % of apartments had radon levels that exceeded 200 Bqm⁻³ (Hjelte, Ronquist, & Ronnqvist, 2010).

Sweden has the second highest indoor radon levels among Scandinavian countries. Based on the radon risk map of a municipality in Sweden, about 70 % of Swedish surface (ground) has normal risk, with radon content of 10,000–50,000 Bqm⁻³ due to bedrocks and soil with low normal Uranium content and average permeability (Dubois, 2005).

Around 300,000 buildings in Sweden include uranium-bearing building materials in the form of lightweight (blue) concrete which is used for internal and external walls and sometimes in floor structures. The radon level in houses in which a substantial proportion of the building material consists of this type of concrete is elevated. Radon exhalation rate (E) from building materials in some Swedish buildings built between 1929 and 1975 is in the range 0.01 to 0.07 Bqm⁻²s⁻¹ (Clavensjö & Åkerblom, 1994).

In a survey of radon measurement in 1,528 dwellings by Västerås municipality produced with such material (Table 3), almost all homes were contaminated with radon levels higher 200 Bqm⁻³, and more than 87 % had radon levels in the range of 200–600 Bqm⁻³, in which the radon level can be lowered using a heat recovery ventilation system. The minimum, maximum and average indoor radon levels found in this survey were 201; 4,650 and 405 Bq/m³ respectively.

These dwellings need mitigation measures in to lower the radon content at least to 100 Bqm⁻³. Increased ventilation is one possible general measure,

and this measure works regardless of whether the source of radon is the ground, building materials and/or domestic water.

*Table 3. Annual radon average concentration in Västerås, Sweden
(Taken from Västerås Municipality, 2009)*

| Indoor radon (Bq/m ³) | Number of dwellings | Percentage (%) |
|--------------------------------------|------------------------|-------------------|
| 200–400 | 954 | 62.4 |
| 400–600 | 385 | 25.2 |
| 600–800 | 127 | 8.3 |
| 800–4650 | 62 | 4.1 |
| Total | 1528 | 100 |

When considering increased ventilation (i.e. a higher outdoor air flow rate) as a measure against radon it is important to be clear about two possible conditions:

- 1) The actual building has a lower total outdoor air flow rate than the requirements, with for example an average outdoor air flow rate lower than the minimum requirement in Sweden of 0.35 l / s m² floor area on average. In this case increased ventilation will have a “double” advantage by both improving the IAQ in general and lowering the radon content. The increased energy demand for space heating as a result of a higher outdoor air flow rate is not primarily the result of a measure against radon, but rather the result of a very general measure to increase the ventilation from a rate that is below minimum requirements.
- 2) The actual building has a total outdoor air flow rate in line with the requirements or higher. In this case increased ventilation will generally cause “over-ventilation”, combined with an “unnecessary” increased energy demand for space heating. At the same time the advantage with respect to lowered radon content still exists, but in this case increased ventilation is not as favorable as in condition 1. In this condition increased ventilation as a measure against radon faces very tough competition from other possible measures.

These two possible conditions are very important as a background to this thesis. However, the contents of this thesis do not focus specifically on separating the two possible conditions, but focus instead on the general influence of increased ventilation as a measure against radon.

With the very simplest assumption of steady-state conditions and complete mixing of the indoor air, it is well known that there is essentially a linear

relation between outdoor air flow rate and indoor radon concentration. This means that a doubling of outdoor air flow will only reduce indoor radon by about 50 %, e.g. from 600 Bq/m³ to 300 Bq/m³. It is important to be clear about this general limitation regarding radon limitation by increased ventilation. This thesis includes simulations of the influence of increased ventilation where complete mixing is not assumed, but rather includes complex air flow patterns and radon transport within a building.

In Sweden, electricity use for domestic purposes (including household lighting, electrical equipment and appliances) increased from about 9.2 to 20.7 TWh over the period of 1970–2010. This is because of the increase in the number of households, domestic appliances and electronic equipment and general increasing industrialization. Residential buildings and commercial premises used a total of 85 TWh for space heating and domestic hot water production in 2010. Of this, 42 % was used in detached houses, 32 % was used in apartment buildings and 26 % was used in commercial premises (Swedish Energy Agency, 2010). In 2005, average domestic electricity use amounted to about 6,200 kWh per year in detached houses, and about 40 kWh per m² per year in apartment buildings, which for a 66 m² apartment means annual electricity use of 2,640 kWh per year (Swedish Energy Agency, 2010).

The level of ventilation heat losses for a building relative to the total heat losses including transmission can vary widely between different buildings. In general, the ventilation heat losses as a fraction of the total will increase with the size of the building and with improved thermal insulation. For a large and very well insulated building, ventilation losses can be completely dominant. In low energy and airtight houses, as much as 50 % of the heat demand is often attributed to ventilation. This heat loss can be significantly reduced by using a heat recovery ventilation system, a good option among several other energy-efficient ventilation strategies for sustainable building concepts (Laverge & Janssens, 2012). This thesis focuses on the use of a heat exchanger to minimize ventilation losses. Other ways to utilize the heat in the exhaust air, e.g. with an exhaust air heat pump, are not investigated in this thesis.

Jokisolao (2003) and Lazzarin (1998) have compared various ventilation systems to show the advantages of heat recovery systems in cold climates (Jokisalo, Kurnitska, & Torkki, 2003; Lazzarin & Gasparella, 1998). Energy-efficiency could be improved by up to 67 % compared to a traditional exhaust ventilation system by using a heat recovery system with a nominal temperature efficiency of 80% (Jokisalo, Kurnitska, & Torkki, 2003).

2.2 Ventilation effect and Indoor Radon Mitigation

The half-life of radon is only 3.82 days. Removing or sealing the radon source therefore greatly reduces the risk within a few weeks. In addition to removing or sealing the source, improving the ventilation rate of residential buildings can significantly reduce the radon level. The full impact of ventilation on radon levels is felt within hours. Generally, indoor radon concentrations can be diluted and reduced by increasing outdoor ventilation rates. The minimum indoor radon level in a sufficiently ventilated room is the same as the outdoor level (William, 1990; ASHRAE, 2001).

Since indoor radon cannot usually be eliminated by source control, ventilation is used to dilute radon to an acceptable level.

Unlike a supply or exhaust fan ventilation system, a heat recovery ventilation system balances the indoor pressure in relation to the soil and the outdoors.

Because of thermal gradients it is usual to have negative pressure indoors at floor level and positive pressure at roof level. This refers to a standard case with a significant temperature difference between indoors and outdoors (in winter) and a normal mechanical supply and exhaust ventilation system. The average pressure difference between indoors and outdoors can still be zero. Such a ventilation system mitigates indoor radon because of diluting and mixing effects (Handel, 2011).

Generally, the remediation techniques depend on the radon source, radon level and building type. Table 4 summarizes and lists remediation techniques with corresponding radon levels.

Table 4. Radon levels and remediation techniques (Radiological Protection Institute of Ireland, 2010)

| Radon levels (Bqm ⁻³) | Remediation techniques |
|-----------------------------------|---|
| C > 1000 | Sub-floor depressurization (Radon sump) |
| C < 600 | Improved indoor ventilation |
| C = 400–500 | Increased under-floor ventilation, sealing of cracks and gaps in the floor using polyethylene sheet and silicon glue (10 % effective) |

2.3 Radon transport mechanisms and environmental conditions effects

As a gas, radon simply diffuses through the soil and other materials around the foundation of a home. Radon gas transportation from the soil into houses

results from physical and meteorological factors. Radon atoms escape through the larger air-filled pores within the soil and building materials, and a fraction reach the building-air interface before decaying and entering indoor air via the air flow. This transport occurs by molecular diffusion and forced flow (pressure induced flow), collectively referred to as diffusion and advection mechanisms. Radon transport into buildings therefore depends on convective flow from the soil pores through cracks in the floor and diffusion from building materials and soil. Convective flow depends on pressure differences across the substructure, and diffusion flow is dependent on the radium content, porosity, moisture, permeability and structure of the soil (Kesikuru, Kokotti, Lammi, & Kalliokoski, 2001).

Theoretical and mathematical relations indicate that diffusion and advection mechanisms lead to radon transport. Both of these mechanisms are functions of physical and environmental conditions such as air flow, ventilation rate, indoor temperature and relative humidity, and pressure difference between indoors and outdoors. In addition houses tend to operate under negative pressure, meaning that the air pressure inside the home is lower than outside. This negative pressure results from the stack effect, the vacuum effect of exhaust fans, and a downwind effect caused by wind around a home (Loureiro, 1987; Spoel, 1998). The stack or chimney effect is due to the increased building temperature, which creates a rising vacuum cleaner effect which sucks out indoor air (Hoffmann, 1997).

Hoffmann (1997) also states that rainfall has negative impact on pressure, and a short time after rainfall indoor radon is increased because of the rising stack effect.

Previous studies have shown that physical and environmental conditions such as indoor and outdoor pressure difference, ventilation rate, temperature, moisture and meteorological factors have impacts on indoor radon. Outdoor temperature variations, storms and rainfalls are the most important factors affecting mean radon levels (Milner, Dimitroulopoulou, & ApSimon, 2004).

Cozmuta (2003) showed that radon surface exhalation rate has a direct correlation with relative humidity in the range 30–70 %. Radon release rates from concrete increase linearly with moisture rates in this range. However, this reaches a maximum at 70 to 80 % humidity, after which transport rates decrease dramatically (Cozmuta, Van der Graff, & de Meiter, 2003).

Properties of radon such as diffusion coefficient, exhalation rate and emanation coefficient are affected by indoor air temperature and moisture. These relations are important when the diffusion mechanism is dominant in radon transport, and are explained in Appendix B.

2.3.1 Radon concentration equation in a ventilated room

In a ventilated room, the radon diffusion coefficient is disregarded and the radon transport equation or radon concentration in a building or room with volume V is described (Petropoulos & Simopoulos, 2001; Clavensjö & Åkerblom, 1994) as the following:

$$C_i(t) = C_0 e^{-\lambda t} + \frac{EA}{V\lambda} (1 - e^{-\lambda t}) \quad (2.3)$$

where C_i is the indoor radon concentration (Bqm^{-3}) at time $t(h)$, C_0 is either the initial radon content at $t = 0$ h or the outdoor radon concentration, λ is the total radon decay rate and ventilation rate ($\lambda = \lambda_{Rn} + \lambda_v$) in h^{-1} , $E(Bqm^{-2}h^{-1})$ is the radon flux or radon exhalation rate from the soil or building material, A is the exhalation surface area (m^2) and V is volume (m^3) of the house or chamber.

At the steady state situation Equation 2.3 is reduced to:

$$C_i = \frac{EA}{V(\lambda_{Rn} + \lambda_v)} + C_0 \quad (2.4)$$

This equation also implies that the minimum value of the indoor radon concentration is equal to the outdoor radon concentration.

When $C_0 = 0$ the indoor radon concentration level can be calculated as (Clavensjö & Åkerblom, 1994):

$$C_i = \frac{EA}{V(\lambda_{Rn} + \lambda_v)} \quad (2.5)$$

where $C(Bqm^{-3})$ is the indoor radon at steady state, $E(Bqm^{-2}h^{-1})$ is the radon exhalation rate, $A(m^2)$ is the radon exhalation surface (in this study the house floor), $V(m^3)$ is the volume of the room, λ_{Rn} is the radon decay constant, and $\lambda_v(h^{-1})$ is the air change rate in the house.

2.3.2 The effects of temperature and humidity on the pressure field

In radon transport the dominant force is the pressure field, which is dependent on the advection mechanism of the indoor radon transport (Wang, F.; Ward, I C., 2002).

The balance between the condensation and the evaporation of water leads to a vapor pressure which depends on the temperature. At high temperatures air can hold more vapor than at low temperature (Sonntag, 1990). The relative humidity of the indoor air changes due to changes in the total pressure, and the pressure field influences the indoor radon concentration as

stated in the radon transport Equation 4.5. This effect is described in greater detail in Section 4.8.

2.4 Radon modeling methods

Numerical modeling using CFD is a powerful tool that can be used to estimate and predict indoor radon. These models can also help to design an improved cost-effective radon mitigation system. Numerical modeling of radon entry into buildings is a valuable and comparatively inexpensive tool for assessing the many factors controlling radon entry (Anderson, 2001).

Zhuo et al. (2000) used CFD to study the concentrations of radon in a ventilated room. They showed that the activity distribution of radon is uniform except near the supply and exhaust locations. However, as the ventilation rate increases, the concentrations of radon fall and its activity distribution becomes more complex due to the effect of turbulent flow. The simulation results of radon activity and distribution were comparable with the experimental results in a test room (Zhuo, Iida, Moriizum, & Takahashi, 2001).

In an experimental work, Marley and Philips (Marley & Paul, 2001) claimed that mitigation of radon gas in buildings is mainly based on reducing the pressure difference between the radon source and the indoor air. This study specifies the influence of mechanical ventilation systems in the control of radon level.

In a study by Wang and Ward, FLUENT, a commercial CFD package, was used to develop a model of multiple radon entry into a house. A grid-independency test, convergence behavior analysis and comparison with analytical solutions were used for model verification. They also used an inter-model validation method to validate the strength of the model, i.e. using the model to run a simulated case by an existing model (Wang, F.; Ward, I C., 2002).

Revzan (2008) developed a 3D steady state finite difference model for radon simulation. In this study, the simulation results were much lower than the measurement results, likely due to errors in the measurement of soil permeability and variations in the permeability of the basement slab having a significant influence on the pressure field (Revzan, 2008).

The previous studies in this field have focused solely on factors affecting radon distribution in soil. These studies do not explain how physical and environmental factors affect indoor radon. *However, the current study aims to consider different indoor temperature and humidity conditions, ventilation rates and other possibly important parameters to determine their effects on indoor radon distribution and concentration.*

3 Materials and Methodology

This chapter describes materials and methods used in this study. Materials include radon detectors, a heat recovery ventilation system, and the case study house. Employed methods are measurement, analytical analysis, dynamic and CFD simulation tools.

The structure of this thesis is organized as follows:

- Analysis of energy use and an air to air heat recovery ventilation unit using dynamic simulation software, IDA ICE, and analytical calculation.
- Economic analysis of using the heat recovery unit.
- CFD modeling and simulation to investigate the influence of some indoor air conditions and characteristics on indoor radon level and distribution.

3.1 Materials

3.1.1 Case study house

The case study house is a detached house in Stockholm that was built in 1970. This house provides suitable conditions for carrying out the objectives of this thesis because of the availability of a heat exchanger unit and radon data for several years, as well as agreement and assistance of the home owner to test the indoor radon. This house is 2-storey structure and the volume of each storey is about 260 m³. The foundation of the building is located on bedrock. The primary radon level was about 4,000 Bqm⁻³ on the first (ground floor) storey, originating from the ground. The final radon level decreased to about 600 Bqm⁻³ after sealing part of the first storey and using a radon sump in this storey (before installing the heat exchanger unit). Figure 1 shows the floor plan of the case study house.

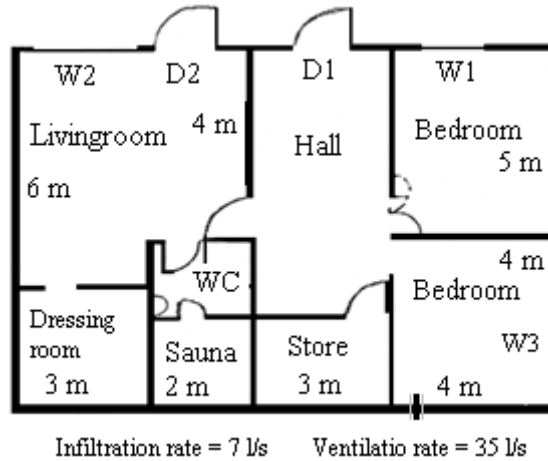


Figure 1. Ground floor plan and zone divisions of the case study house

3.1.2 Heat recovery unit

Several different types of heat exchanger can be used in order to transfer heat from exhaust to supply air, but this study is limited to an application with a rotary heat exchanger. The rotor unit has a high efficiency and recovers up to 80 % of the heat and moisture from the air extracted from the house (Flexit, 2009). For a large majority of buildings, including normal residential buildings, moisture recovery is not needed. Perhaps 80 % of all problems and damage in buildings including sick building symptoms can be related to moisture. Ventilation has a very important function in limiting the accumulation of different pollutants and water vapor. The rotor material is an air permeable and heat conductive material which picks up heat from the exhaust air and transfers it to the supplied air. The heat recovery wheel absorbs and transfers moisture (it is coated with a desiccant), thereby providing both sensible and latent energy recovery. Figure 2 shows the incoming and outgoing air streams at the wheel.

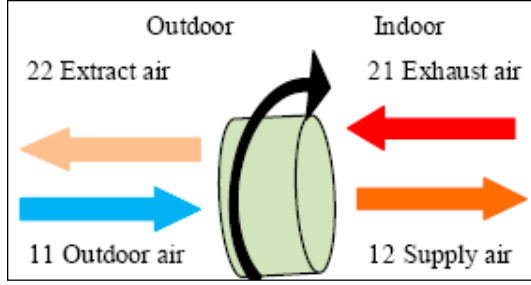


Figure 2. Air flows through the rotary heat exchanger

The key factors when evaluating the performance of a rotary heat exchanger are temperature and humidity efficiency. These factors are usually specified by the manufacturer.

These factors are defined as:

$$\text{Temperature efficiency } \eta_t: \quad \eta_t = \frac{t_{12} - t_{11}}{t_{21} - t_{11}} \quad (3.1)$$

$$\text{Moisture efficiency } \eta_w: \quad \eta_w = \frac{w_{12} - w_{11}}{w_{21} - w_{11}} \quad (3.2)$$

where t = temperature in °C, w = water content of air in g/kg, 11 = fresh air condition before heat exchanger (outdoor), 12 = supply air condition after heat exchanger (indoor), 21 = extracted air condition before heat exchanger (indoor), 22 = exhaust air condition after heat exchanger (outdoor). Using Equation (3.1) and the measured temperatures, $t_{11} = -7.4$, $t_{12} = 14.5$ and $t_{21} = 22$ °C, shows that these values are not always reached, as demonstrated below:

$$\eta_t = (14.5 + 7.4) / (22 + 7.4) = 74.5\%$$

In this study a mechanical ventilation system with an air-to-air heat exchanger unit provides supply air to the building. This unit is a rotary energy recovery system, which recovers energy as both heat (sensible) and humidity (latent). Figure 3 shows the installed heat exchanger system inside the house.



Figure 3. The rotary heat exchanger installed in the building

The operation points of the unit can be determined from the diagram provided by the manufacturer, consisting of a number of curves and axes. Given the ventilation rate, it is possible to find operation ratings of pressure, noise and fan electrical energy consumption (Paper I). These values are shown in Table 5.

Table 5. The operation ratings of the unit

| Specifications | Operating rating |
|----------------------------|------------------|
| 2 Fans power rating | 2×35 W |
| Efficiency | 74.5% |
| Ventilation rate | 0.5 Ach (35 l/s) |
| Noise | 50 dBA |

3.1.3 Radon detectors

In this thesis both an Alpha Track Detector (ATD) and a Continuous Radon Monitor (CRM) are used to measure radon concentration. Unlike an ATD, which is passive and requires laboratory analysis to obtain the results, users can use CRM to detect radon instantly and anywhere with a personal computer.

The R2 CRM is an electronic device which is useful for measuring radon levels in the short and long term. This radon meter is used to identify indoor radon problems and the influence of physical and environmental factors such as ventilation effects and indoor conditions. The device also measures and logs indoor temperature and humidity so that any influence from the measuring environment can be determined. The CRM undergoes control irradiation at the Swedish Radiation Safety Authority (SSM) and gives very reliable

values with 10 % accuracy (Radonelektronik, 2009). Figure 4 shows the R2 CRM used in this study.



Figure 4. The R2 continuous radon meter

3.2 Research methods

Research methods applied in this study include measurement, analytical analysis, economic analysis, and dynamic and numerical simulation. These methods are described in the following sections.

3.2.1 Measurement

Radon concentrations were measured and monitored in the case study house in Stockholm with some interruptions, from February 2008 to December 2012 during the cold seasons. Table 6 shows the time period and type of detectors used for measurement. For quality control and to check the accuracy of the measurement, on the first occasion, two plastic films of CR-39 detectors and R1 and R2 CRM devices were placed in the case study house simultaneously. The R2 CRM was placed at desktop level while CR-39 detectors were hung from the ceiling at the height of the occupied zone.

Since the R2 CRM is able to measure and log radon level, indoor temperature and humidity at the same time (R1 only measures radon levels), it was used to observe the influence of different ventilation rates, indoor temperature and relative humidity on radon levels.

The heat recovery system unit was used to vary the ventilation rate between 0.25, 0.5 and 1 air change rate (Ach), and to vary the indoor temperature.

Table 6. Date and time period of the measurements

| Date | Period | Type of detectors | Ventilation rate (Ach) |
|-------------|----------|-------------------|------------------------|
| Feb, 2008 | 2 weeks | CR-39 | 0.25 |
| Jan, 2010 | 3 months | CR-39 and R1 | 0.25 |
| April, 2010 | 3 weeks | CR-39 and R1 | 0.5 |
| March, 2010 | 12 days | R2 and R1 | 0.5 |
| March, 2010 | 12 days | R2 | 0.5 |
| April, 2010 | 12 days | R2 | 1 |
| Dec, 2011 | 10 days | R2 | 0.5 |
| Dec, 2012 | 20 days | R2 | 0.5 |

3.2.2 Analytical analysis

In the case study house, the radon exhalation rate radon considered was $E = 65 \text{ Bqm}^{-2}\text{h}^{-1}$, and from the data regarding the house, Equation 2.5 was used to calculate indoor radon levels for different ventilation rates. This analysis was used for comparison with the results from the measurements and modeling simulation. In Equation 2.5, the factors that affect indoor radon are radon exhalation rate (E), radon decay rate (λ_{Rn}), ventilation rate (λ_v) and height above the floor (H). These factors are related according to the following equation:

$$C_i = \frac{E}{H(\lambda_{Rn} + \lambda_v)} \quad (3.3)$$

In a ventilated room since $\lambda_{Rn} \ll \lambda_v$ the effect of the radon decay rate can be neglected. Indoor radon concentration at steady state therefore reduces to:

$$C_i = \frac{E}{H \lambda_v} \quad (3.4)$$

where $H = \frac{V}{A} = 2.4 \text{ m}$ is the height of the case study house.

This relation clearly indicates that indoor radon concentration in a given house depends only on the air change rate and the radon exhalation rate. In this thesis this analysis is used to confirm numerical results at four distinct air change rates.

If $\lambda_v \approx 0$, equation (3.3) is reduced to:

$$C_i = \frac{E}{H \lambda_{Rn}} = C_{max} \quad (3.5)$$

For this case study, radon exhalation rate (E) can be calculated using the maximum measured indoor radon, $C_{max} = 3580 \pm 380 \text{ Bqm}^{-3}$, and given $H = 2.4 \text{ m}$ and $\lambda_{Rn} = 2.1 \times 10^{-6} \text{ s}^{-1}$, then $E = 65 \pm 7 \text{ Bqm}^{-2} \text{ h}^{-1} = 18 \pm 2 \text{ mBqm}^{-2} \text{ s}^{-1}$. These values are accepted as input data in the numerical simulations and used to check sensitivity analysis.

3.2.3 Economic analysis

In order to calculate the costs and energy losses imposed by the heat recovery unit as a radon mitigation and ventilation system and the utility costs of the residential building, the ventilation loss, operational energy cost, heat degree days, fan(s) energy use, heat energy cost, indoor air temperature and ventilation rate and initial and installation costs of the heat recovery unit must be known. Some of these factors are calculated in section 3.2.5.

3.2.4 Heating degree days (HDD) calculations

Degree day values are a common and accepted method for determining the potential impact of regional climate modifications on energy demand for space heating and air conditioning. Typically, a linear relationship is assumed between degree days and energy consumption. In industry and academia, heating and cooling degree days are a useful method which has been used for decades (Akander, Alvarez, & Johannesson, 2005). In a cold climate, high heating degree days are very important from the perspective of energy recovery and multipurpose applications such as a radon mitigation ventilation system.

More specifically, heating degree days (degree hours) are a simplified means of calculating the building's energy demand for space heating, and can be useful for example when estimating the energy saving by a heat exchanger. The degree days depend on the location (outdoor temperature), the selected indoor temperature and the passive heat.

Consideration must be given to the contributions of passive heating (household electricity, body heat, solar radiation and heat from hot water), and it is very important that the degree days only refer to the demand for space heating, and not to the total amount of heat required to achieve the indoor temperature. This can be done by estimating the average temperature increase due to passive heating; the mean value of passive heating during the heating season divided by the building's specific ventilation and transmission heat losses per °C temperature difference between indoors and outdoors. For example, if passive heating on average contributes 3 °C of the indoor temperature increase, combined with an assumed indoor temperature of 21 °C, this means that the base temperature (limit temperature) would be $21 - 3 = 18 \text{ °C}$.

For a very well insulated building with a lot of passive heat, the low base temperature and the low degree days value will result in a much lower energy saving as a result of using a heat exchanger. If the building is heated by a heat pump, it is also the case that the saving in purchased energy for active heating from using a heat exchanger will be much lower. However, these phenomena are not addressed specifically within this thesis.

Heating degree day calculations in this study were carried out using a base temperature of 18°C. Heat degree days can be calculated as follows (Mourshed, 2012):

$$HDD = \sum_{m=1}^{12} [D_m \sum \max \{T_b - T_d, (0.0)\}] \quad (3.6)$$

$$HDD = T_b - T_d \text{ if } T_d < T_b$$

$$HDD = 0 \text{ if } T_d \geq T_b$$

where D_m is the number of days in month m , T_d is the daily mean temperature and T_b is the base temperature.

3.2.5 Ventilation loss

This section considers the “theoretical” portion of the space heating that compensates for ventilation losses. It is assumed that the fan-driven supply air flow represents 90 % of the fan-driven exhaust air flow (a normal ratio leading to a small negative average indoor pressure, which is an advantage with regards to humidity), temperature efficiency for the heat exchanger is 74.5 %, and air leakage in addition to fan-driven ventilation is equal to 0.05 Ach.

The heat exchanger only affects the fan-driven supply air (90 % of the exhaust air):

$$0.90\lambda_v \times V = 0.90 \times 0.5 \text{ Ach} \times 259 \text{ m}^3 = 116.55 \text{ m}^3 \text{h}^{-1}$$

where λ_v = air change ventilation rate, V = building effective volume (m^3).

Total infiltration (air leakage) not affected by the heat exchanger is the sum of the fan-driven infiltration (10 % of the exhaust air flow) and the air leakage (0.05 Ach) corresponding to air leakage both in and out in addition to fan-driven ventilation (Oman, 2011; Mourshed, 2012), i.e. $0.10 \times 0.5 \text{ Ach} \times 259 \text{ m}^3 + 0.05 \text{ Ach} \times 259 \text{ m}^3 = 25.9 \text{ m}^3 \text{h}^{-1}$

Specific ventilation loss (Q_v) is defined as:

$$Q_v = \text{Fan - driven supply air} + \text{total infiltration}$$

$$Q_v = \Sigma \dot{m} C_p \quad (3.7)$$

where C_p = air heat capacity ($1,010 \text{ J.kg}^{-1}\text{C}^{-1}$) and \dot{m} = mass flow kg s^{-1} .

$$Q_v = 0.039 \times 1,010 + 0.0086 \times 1,010 = 39.39 + 8.69 = 48.09 \text{ W}^\circ\text{C}^{-1}$$

Ventilation losses (E_v), which is defined as the sum of fan-driven supply air (E_s) and total infiltration (E_l) losses, is calculated from the basic equation

$$Q = \dot{m} C \Delta T : E_v = E_s + E_l = Q_v \times 24 \times HDD \quad (3.8)$$

where E_s = the specific portion of the space heating in Wh/year required to compensate for the heat losses caused by the fan-driven supply air, E_l = the specific portion of the space heating in Wh/year required to compensate for the heat losses caused by the total infiltration (air leakage) not affected by the heat exchanger, and $24 \times HDD$ = heat degree hours per year.

Based on monthly long-term mean temperatures in Stockholm, the heating degree days are estimated to be about 4,500 degree days (108,000 heat degree hours per year (Wunderground, 2010).

The heat exchanger reduces the heat demand by a factor $(1-\eta_t)$. The energy demand of heating using heat exchanger (E_{Hex}) is:

$$E_{Hex} = E_s (1 - \eta_t) \quad (3.9)$$

Recovered heat loss (E_{rec} in Wh/year) comes directly from the following expression:

$$E_{rec} = E_s - E_{Hex} = \eta_t E_s \quad (3.10)$$

If we consider the normal ranges of variation of each variable as

$$0.5 \leq \lambda_v \leq 1; 4,000 \leq HDD \leq 6,000; \text{ and } 0.7 \leq \eta_t \leq 0.85,$$

the annual energy recovery can be determined.

3.2.6 The life cycle cost analysis of heat recovery ventilation system

The net present value (NPV) method is a method used to evaluate the cost-effectiveness of an investment in the future. According to this method, an

investment is profitable if the net present value (B_0) of all savings is larger than the capital initial cost (A_0), as shown in Equation 3.11 (Nilsson, 2006).

$$B_0 > A_0 \quad (3.11)$$

where A_0 = initial investment and B_0 = NPV of all savings, which is defined as:

$$B_0 = I b \quad (3.12)$$

where b = Annual savings in monetary unit, and I = NPV factor which is expressed as:

$$I = \frac{1-(1+i)^{-n}}{i} \quad (3.13)$$

where i = interest rate, and n = time in years.

Taking into account the annual increases in the energy price, a new NPV factor I_q can be calculated (Nilsson, 2006):

$$I_q = \frac{1-\left(\frac{1+q}{1+i}\right)^n}{\frac{1+i}{1+q}-1} \quad (3.14)$$

where q = annual energy cost escalation rate = 2 % and i = annual interest rate = 4 % (Nilsson, 2006).

In the present study, NPV analysis is used to show whether the investment to install a heat recovery system is cost-effective or not. This analysis, presented in section 5.4 and Paper I, shows that installing an air handling unit is useful and cost-effective because it both reduces energy costs and mitigates indoor radon levels.

3.3 Energy dynamic simulation

For a long term assessment of the heat recovery ventilation efficiency, a complete time series of outdoor temperature and all building losses and gains during the heating period should be considered. The variations of outdoor temperature and ventilation rate may change the heat recovery temperature and humidity efficiencies. All these time dependent effects are taken into account using energy dynamic programs. The IDA Indoor Climate and Energy (IDA ICE) energy dynamic program used in this study is a multi-zone dynamic simulation software package used to study thermal indoor climate

and predict energy consumption of the whole building, heat recovery of the rotary heat exchanger unit analysis, simulate thermal comfort and IAQ.

The case study house is considered as a building with 8 zones. Energy and heat are provided by a primary source and a balanced heat recovery unit. Weather data is taken from a database of the Stockholm climate. Boundary conditions and input data used in this simulation are listed in Appendix A.

3.4 Computational fluid dynamics (CFD)

CFD analysis is used to investigate the effects of indoor air parameters on indoor radon treatment numerically. CFD can be easily used for indoor air flow analysis, and reduces the mathematical limitations. It is also more cost-effective than full-scale laboratory and tracer gas methods. CFD programs are designed to solve the governing equations in the form of partial differential equations (PDE), and are employed to solve equations involving velocity, temperature and species transport numerically. In a room with ventilation, CFD programs are able to describe the processes in the room, including the conservation of mass, energy, momentum and species such as radon. The reasons for using CFD and the finite volume method (FVM) are described in greater detail in the next chapter.

4 Numerical Modeling Procedure

In order to visualize the progress of the behavior of fluid flow and indoor radon and air conditions effects, the conservation of mass, energy, momentum and species transport in the flow field must be defined. The resulting governing equations are PDE which include several independent variables and their partial derivatives.

There are different approaches for solving PDE. One such approach is numerical solution using CFD. CFD code is designed to solve PDE numerically. The CFD codes convert PDE from continuous equations to discrete equations (algebraic equations) based on different discretization methods.

4.1 Discretization methods

In fluid dynamics, the major discretization methods are Finite Volume Method (FVM), Finite Difference Method (FDM) and Finite Element Method (FEM).

Unlike the analytical solution, which solves the equations for all points in the domain, the numerical methods support only discrete points (nodes) and values are calculated at discrete locations on a meshed geometry. The creation of the geometry and mesh is the first pre-processing step in numerical modeling. The shape of these cells in 3-D is usually polyhedral (tetrahedral, hexahedral, prism, etc.).

The FDM uses the differential forms of the governing equations and applies the local Taylor series expansion to approximate differential equations, whereas the FVM and FEM use the integral form of the governing equations. The FEM divides complicated equations into small elements that can be solved in relation to each other. Solving the problems with the FEM method typically needs more computer memory compared to the FVM (Motaman, 2013). The main advantage of FVM is that it can be used with unstructured grids. In this method the computational domain is divided into small volumes, and variables of a problem such as velocity, temperature, and species, etc. are placed at the centroid of the control volume rather than at nodal points. The values of field variables at vertices are obtained by interpolation. Volume integrals are then converted to surface integrals using the divergence theorem. These terms are then calculated as fluxes across volume sur-

faces of each finite volume, because the flux entering a given volume is identical to that leaving the adjacent volume. These methods are called conservative (Abd Alnasser Almate A., 2014).

FLUENT is a powerful commercial CFD code which uses FVM to solve partial differential equations and has been widely used for indoor air flow problems. FLUENT is thus used in this study.

4.1.1 Finite control volume analysis

The conservation law is used in FVM to solve numerical equations. The general conservation form of fluid flow for a small control volume of a dependent variable (C) may be written as:

$$\frac{\partial(\rho C)}{\partial t} + \text{div}(\rho CV) = \text{div}(\rho D \text{grad} C) + S_C \quad (4.1)$$

This equation has 4 terms. From the left: the first term states the time rate change of the fluid element of the variable(C), this is the so-called unsteady effect; the second term is the net rate of flow (C) out of the fluid element, this is because of the advection (motion) effect; the third term is the change rate of C due to the diffusion effect; and the final term is the source term, which is the change rate of fluid flow due to generation. In this study the governing equations are presented in the form of Equation 4.1.

In the FVM, the conservation law is applied to each finite element at which the computation of the flux across the boundary is required. The following steps are undertaken for solving PDE in this method. The first step is conversion of each volume integral of the PDE to a surface integral using the divergence theorem. The second step is integration of the differential form of the PDE over each volume. The conservation equations for each volume may be solved simultaneously. In the third step, surface integrals are converted to algebraic equations using mean value theorem. In the final step the algebraic equations are converted to matrices, which can then be solved by the iteration method.

4.2 Governing equations used

The governing equations for this study are conservation of mass (continuity), momentum (Navier-Stokes equations), and energy, and concentration of species equations are generally referred to as transport equations. To find all unknown variables (pressure, velocity components, temperature), another equation called the state equation is needed.

Air flow in a room is incompressible due to the low indoor air velocity, which is in the order of less than 1 meter per second. For an incompressible

air flow, the transport equations are of the following forms in a Cartesian coordinate system. These equations generally describe indoor air flow, heat transfer and radon transport.

The mass conservation equation:

$$\frac{D(\rho)}{Dt} = \frac{\partial \rho}{\partial t} + \nabla \cdot (\rho V) = \frac{\partial \rho}{\partial t} + \frac{\partial}{\partial x}(\rho u) + \frac{\partial}{\partial y}(\rho v) + \frac{\partial}{\partial z}(\rho w) = 0 \quad (4.2)$$

where ρ is density and u, v and w are the velocity components of the velocity vector V in the x, y , and z directions respectively (White, 2011).

The flow is considered as incompressible, thus the reduced form of Equation (4.2) in the steady state condition is as follows:

$$\nabla \cdot (V) = \frac{\partial}{\partial x}(u) + \frac{\partial}{\partial y}(v) + \frac{\partial}{\partial z}(w) = 0$$

The momentum conservation equation:

For incompressible flow the general form of the momentum equation is as follows:

$$\frac{\rho D(V)}{Dt} = -\nabla P + \mu \nabla^2 V + F_B \quad (4.3)$$

where P is static pressure vector, μ is air viscosity and F_B is body force vector.

Equation 4.3 can be expanded in x, y, z directions. There is no body force in x and y directions, but in the z direction the body force is equal to the weight ρg . The simplified forms of the momentum equations used in this study are as follows:

In the x direction:

$$\frac{\rho D(u)}{Dt} = \frac{\partial(\rho u)}{\partial t} + \nabla \cdot (\rho u V) = -\frac{\partial P}{\partial x} + \mu \left(\frac{\partial^2 u}{\partial x^2} + \frac{\partial^2 u}{\partial y^2} + \frac{\partial^2 u}{\partial z^2} \right) \quad (4.3a)$$

in the y direction:

$$\frac{\rho D(v)}{Dt} = \frac{\partial(\rho v)}{\partial t} + \nabla \cdot (\rho v V) = -\frac{\partial P}{\partial y} + \mu \left(\frac{\partial^2 v}{\partial x^2} + \frac{\partial^2 v}{\partial y^2} + \frac{\partial^2 v}{\partial z^2} \right) \quad (4.3b)$$

and in the z direction:

$$\frac{\rho D(w)}{Dt} = \frac{\partial(\rho w)}{\partial t} + \nabla \cdot (\rho w \mathbf{V}) = -\frac{\partial p}{\partial z} + \mu \left(\frac{\partial^2 w}{\partial x^2} + \frac{\partial^2 w}{\partial y^2} + \frac{\partial^2 w}{\partial z^2} \right) + \rho g \quad (4.3c)$$

where p is the static pressure, μ is the viscosity of the air, i.e. $1.83 \times 10^{-5} \text{ kgm}^{-1}\text{s}^{-1}$ at $T = 293 \text{ K}$, and g is acceleration due to gravity (White, 2011).

The energy conservation equation:

The general form of the energy conservation equation of indoor incompressible air is:

$$\frac{\partial(\rho C_p T)}{\partial t} + \nabla \cdot (\rho C_p T \mathbf{V}) = \nabla \cdot (k \nabla T) + S_e \quad (4.4)$$

In this study the following reduced form is used:

$$\nabla \cdot (\rho C_p T \mathbf{V}) = \nabla \cdot (k \nabla T)$$

where C_p is the specific heat capacity of the air, k is the thermal conductivity, and S_e is energy source, which is zero in this case (White, 2011).

Radon transport equation:

Theoretical and mathematical relations indicate that diffusion and advection mechanisms² lead to radon transport (Spoel, 1998). Advection mechanisms are more related to physical and environmental conditions such as air flow, ventilation rate, indoor temperature, relative humidity and pressure differences between indoors, the ground and the outdoors.

The general form of the radon mass transfer equation, like Equation (4.1) referred to as the total radon transport equation, integrates radon diffusion transport, advection transport, radon generation and radon decay rate. In steady state and incompressible flow it is written as the following conservation equation (Wang & Ward, 2000):

$$\frac{dC}{dt} = \nabla \cdot (D \nabla C) + \nabla \cdot C \mathbf{V} - \lambda_{Rn} C + G = 0 \quad (4.5)$$

where D = Radon diffusion coefficient in air ($\text{m}^2 \text{s}^{-1}$), and C = Radon activity concentration in air (Bq m^{-3}).

G = Radon generation rate ($\text{Bq m}^{-3} \text{s}^{-1}$), \mathbf{V} is the velocity vector and $\lambda_{Rn} = 2.1 \times 10^{-6} \text{ s}^{-1}$.

² Diffusion is driven by concentration gradient and advection is due to pressure difference caused by mechanical ventilation. Note that advection is fluid motion due to fluid stream, but convection used for heat transfer includes both diffusion and advection.

In a room air flow, the dominant driving force is the advection force caused by physical and environmental conditions such as wind, rainfall, stack effect, temperature, relative humidity and mechanical ventilation systems or combinations of these. If the dominant source is diffusion, such as during migration in soil, a different transport equation would apply. This equation and some points related to this issue are explained in Appendix B.

As mentioned for Equation 4.1, the radon transport equation can be written in a general form as:

$$\frac{\partial(\rho C)}{\partial t} + \text{div}(\rho CV) = \text{div}(\rho D \text{grad}(C)) + S_C \quad (4.6)$$

In the above expression, S_C is the source term and V is the velocity vector, ρ is the density of the radon and D is the diffusion coefficient. Here, since radon is transported to the air and there is no radon generation and decay in the air, $S_C = 0$ and the equation reduces to:

$$\frac{\partial(\rho C)}{\partial t} + \text{div}(\rho CV) = \text{div}(\rho D \text{grad}(C)) \quad (4.7)$$

For steady state conditions and constant radon density, Equation 4.7 reduces to

$$\text{div}(CV) = \text{div}(D \text{grad}(C)) \quad (4.8)$$

In two dimensions, the differential form of this equation becomes

$$\frac{\partial(Cu)}{\partial x} + \frac{\partial(Cv)}{\partial y} = \frac{\partial}{\partial x} \left(D \frac{\partial C}{\partial x} \right) + \frac{\partial}{\partial y} \left(D \frac{\partial C}{\partial y} \right) \quad (4.9)$$

Integration of Equation 4.8 over a three dimensional control volume CV yields

$$\int_{CV} \text{div}(CV) dV = \int_{CV} \text{div}(D \text{grad}(C)) dV \quad (4.10)$$

The left hand term (the convective term) and the right hand term (the diffusion term) are re-written as integrals over the entire bounding surface of the control volume by using divergence theorem (Versteeg & Malalasekera, 2007).

The complete description and discretization form of the indoor radon transport equation lies outside of the scope of this thesis. The interested reader is referred to (Bakker, 2010) for more information on the subject.

In addition to these governing equations, because the turbulence model is used in this study, two additional transport equations of turbulent energy

must be solved using FLUENT. These are k , a variable describing the energy in the turbulence fluid; epsilon (ϵ), the turbulent dissipation rate; and omega (ω), the specific dissipation. Because the near wall treatment is used, the transition shear stress transport (SST) model is preferred instead of the k - ϵ model. The model considered for this study is steady state, species and turbulent flow (as opposed to unsteady, two-phase or laminar flow).

4.3 Turbulence model

There are a variety of turbulence models in FLUENT. The selection of the turbulence model depends on the accuracy, computational cost and flow characteristics of the specific problem. In this work the modeling is of low Reynolds number flow in an enclosed environment containing either the regions near the wall (requiring shear stresses near the wall, and where viscous forces dominate inertial forces) or the regions far from the wall and free shear (where inertial forces dominate viscous forces). Different turbulent models have been developed for low Reynolds number flows and high Reynolds number flows. The low Reynolds number means that the model can be used throughout the computational domain (both near and far from the walls). A model for high Reynolds number flows requires additional wall functions in order to manage near walls treatment.

In this study, the transition SST model, also called the shear-stress transport (SST) k - ω model is used. This model is a combination of k - ϵ and k - ω models which is used to overcome the viscous effects near solid boundaries (walls) as well as to manage layers far from the solid boundaries. Because it captures recirculation regions and its stability, this model is better than other models for turbulence modeling in the air flow for this study (Langtry, 2006; Menter, 2006). In addition, the transition SST model consists of 4 transport equations: one equation for the turbulent kinetic energy k , one equation for the energy dissipation rate ω , one equation for the intermittency γ , and one equation for the transported transition momentum thickness Reynolds number $Re_{\theta t}$.

The SST model is a turbulence model in which the turbulent viscosity is modified to account for the transport of the principal turbulent shear stress. This feature enables the SST k - ω model to outperform both the standard k - ω model and the standard k - ϵ model in this context. Other modifications include the addition of a cross-diffusion term in the ω equation and a blending function to ensure that the model equations behave appropriately in both the near-wall and far-field zones (ANSYS Inc, 2011; Langtry, 2006).

4.4 Boundary conditions and input data

Since simulations are performed for Sweden – and specifically for a detached house located in Stockholm – values and constants are set specifically for this geographical location. These values vary with the time of year. For example, the maximum radon exhalation rate occurs in July due to the environmental conditions. Since measurements were taken from December through March, the average radon exhalation rate through these months is used. Some values, such as wind speed and indoor/outdoor temperature, are taken from the data included in IDA ICE.

The radon exhalation rate in the case study house is based on measured data and calculation with Equation (3.5): $E = 0.018 \text{ Bqm}^2\text{s}^{-1}$.

The following sub-sections explain the boundary conditions and input data which have been used in the model.

4.4.1 Inlet Vent

The supply air terminal device in the room is the fresh air supplier. This boundary is defined as “Velocity Inlet” in the model. Specifications which must be defined for this boundary are “Velocity magnitude and hydraulic diameter”, turbulence specifications including “Intermittency”, “Turbulent intensity”, “Static temperature”, and species mass fractions including “Mass fraction of radon” and “Mass fraction of water vapor”.

1. Velocity magnitude and hydraulic diameter:

The supply air terminal device size is $20 \text{ cm} \times 30 \text{ cm}$. The hydraulic diameter of the supply air terminal device can be calculated as follows

$$D_{h,Vent} = \frac{4A}{P} = \frac{4 \times 30 \times 20}{2(20+30)} = 24 \text{ cm} \quad \text{or} \quad 0.24 \text{ m}$$

In all cases, supply air terminal device size and therefore hydraulic diameter is constant.

Calculations are carried out for several air change rates which are listed in Table 9. For each air change rate, the velocity at the supply air terminal device is calculated from the following expression:

$$V_{Vent} = \frac{Ach \times Volume_{Room}}{Area_{Vent}}$$

For example for $Ach = 0.5 \text{ hr}^{-1}$, velocity at supply air terminal device (vent) is

$$V_{Vent} = \frac{0.5 \frac{1}{hr} \times 70.8 \text{ m}^3 \times \frac{1 \text{ hr}}{3600 \text{ s}}}{0.2 \times 0.3 \text{ m}^2} = 0.164 \frac{\text{m}}{\text{s}}$$

2. Intermittency:

For all cases the flow pattern is turbulent and since the transition SST model is used, the intermittency must be defined for these cases. Intermittency is a probability index which shows whether a given point is located inside a turbulent region. This index starts at zero upstream of the transition region and ramps up to one between the start of the transition region and the fully turbulent region. Therefore for all cases with the turbulent flow regime determined in Table 9, intermittency at the supply air terminal device (vent) is equal to one.

3. Turbulence intensity:

Turbulence intensity is defined as:

$$I = \frac{u'}{u_{avg}}$$

where u' is the root-mean-square of the velocity fluctuations and u_{avg} is the mean flow velocity.

This specification at the inlet boundary is calculated from external measured data. For internal flows, this specification is dependent on the upstream data of the fluid flow. If the flow is under-developed, low turbulence intensity can be used. The turbulence intensity at the core of fully-developed duct is estimated as follows (ANSYS Inc, 2011):

$$I = 0.16(Re_D)^{-\frac{1}{8}} \quad (4.11)$$

For example, for $Ach = 0.5 \text{ hr}^{-1}$ turbulence intensity can be calculated as follows:

$$Re_{D,0.5 \text{ hr}^{-1}} = \frac{\rho V_{Vent} D_{h,Vent}}{\mu} = \frac{1.225 \frac{\text{kg}}{\text{m}^3} \times 0.164 \frac{\text{m}}{\text{s}} \times 0.24 \text{ m}}{1.7894 \times 10^{-5} \frac{\text{kg}}{\text{ms}}} = 2,692.7$$

$$I_{0.5 \text{ hr}^{-1}} = 0.16(Re_{D,0.5 \text{ hr}^{-1}})^{-\frac{1}{8}} = 0.16(2692.7)^{-\frac{1}{8}} = 0.0596 \text{ or } 5.96\%$$

For other ventilation rates and different temperatures at the vent, the results are shown in Table 7.

Table 7. Velocity and turbulence intensity for different ventilation rates

| Ach (hr^{-1}) | V_{Vent} (ms^{-1}) | Re_D | I (%) |
|---------------------|--------------------------|---------|---------|
| 0.05 | 0.017 | - | - |
| 0.25 | 0.082 | 1,346.4 | 6.50 |
| 0.5 | 0.164 | 2,692.7 | 5.96 |
| 1.0 | 0.328 | 5,385.4 | 5.46 |

4. Species mass fractions:

Mass fraction of each species must also be determined at this boundary (the inlet vent). Since a supply air terminal device is used as fresh air supplier, the mass fraction of radon at this boundary is zero. The mass fraction of water vapor must be determined according to relative humidity and temperature. Calculations for determining mass fraction of water vapor have been carried out and are presented in section 4.8. These same calculations can be used here. The sum of the mass fractions of all species must be equal to one. Therefore the mass fraction of air is obtained by subtracting the mass fractions of radon and water vapor from 1.0.

4.4.2 Outlet

All supply air from the rooms leaves the house through the unique outlet. Due to the geometrical conditions (Figure 5), supply air from Room 1 exits this room through the air holes of internal Door 1 (all internal doors are supposed to be closed). Therefore, the outlet for Room 1 is located on internal Door 1 (Figure 6).

Since there is one outlet, this boundary is defined as an outflow and consequently its flow rate weighting is one. Considering outflow also helps the model achieve quick convergence.

4.4.3 Outer Surfaces

Outer surfaces are exposed to the outdoor air conditions. These surfaces include the outer lateral walls, the roof, the window and the main door. The same boundary conditions are used for each of these surfaces (however according to Section 4.7, the appropriate material and thickness must be used for each component). Wall with convection heat transfer was shown empirically to model these boundaries appropriately. Therefore outdoor air temperature and convective heat transfer coefficient ($CHTC$) must be defined.

According to results from IDA ICE (Appendix A), average outdoor air temperature and wind speed in Stockholm from December to March are $-2\text{ }^{\circ}C$ and $2.5\text{ }ms^{-1}$ respectively.

Flow around buildings is highly complicated, since it is defined by impinging flow, separating flow, reattaching flow, circulating flow, vortexes,

etc. It is therefore difficult to calculate $CHTC$ using simple equations. However, several correlations have been presented for calculating $CHTC$.

In this study the following expression is used for $CHTC$ (Shao, 2010):

$$CHTC \left(\frac{W}{m^2 K} \right) = 4.2 V \left(\frac{m}{s} \right) + 6.01 \quad (4.12)$$

where V is the wind speed of outdoor air.

Using this equation gives:

$$CHTC = 4.2 \times 2.5 + 6.01 = 16.5 \left(\frac{W}{m^2 K} \right)$$

4.4.4 Internal Surfaces

Internal surfaces include the internal walls and the internal doors (Door 1, Door 2 and Door 3). Since indoor temperature is considered as uniform, heat transfer through these surfaces can be neglected, thus these boundaries are considered as wall with zero heat flux.

4.4.5 Floor Zone

This study investigates effective parameters (including ventilation rate, temperature and relative humidity) for controlling indoor radon concentration in a specific range. Soil is therefore not modeled, and radon exhalation rate from the measurements from this specific geographical location and time period are used to determine radon entry rate into the room. Radon entry into the room is modeled through generation of radon in the floor. Therefore, the floor is modeled as a porous zone with a specific radon generation rate. Porous zone features of the floor do not have any bearing on the results. Radon generation rate (G_{Radon}) in the floor for Room 1 can be obtained as follows:

$$\dot{m}_{Radon} = E \times Area_{Floor} = 0.018 \frac{Bq}{m^2 s} \times 29.5 m^2 = 0.53 \frac{Bq}{s}$$

$$G_{Radon} = \frac{\dot{m}_{Radon}}{Volume_{Floor}} = \frac{0.53 \frac{Bq}{s} \times (1.75 \times 10^{-19} \frac{kg}{Bq})}{0.295 m^3} = 3.2 \times 10^{-19} \frac{kg}{m^3 s}$$

Radon generation rate must be converted to SI units for use in FLUENT. Conversion is done by multiplication based on the following conversion factor (Wang & Ward, 2000):

$$1 Bq = 1.75 \times 10^{-19} kg \quad (4.13)$$

4.5 The House Plan Geometry

The house plan geometry is shown in Figure 5. The house plan consists of 8 rooms. Each room has its own vent. Radon enters the house through the floor. The radon entry rate into the house is determined based on the radon exhalation rate for the geographical location. A heat exchanger unit is placed in Room 4. Here the effect of the heat exchanger is ignored and it is replaced by an outlet vent located in Room 4 to play the role of the heat exchanger. The air change rate in each room corresponds to the volume of that room, and all inlet air from the rooms passes through the unique outlet.

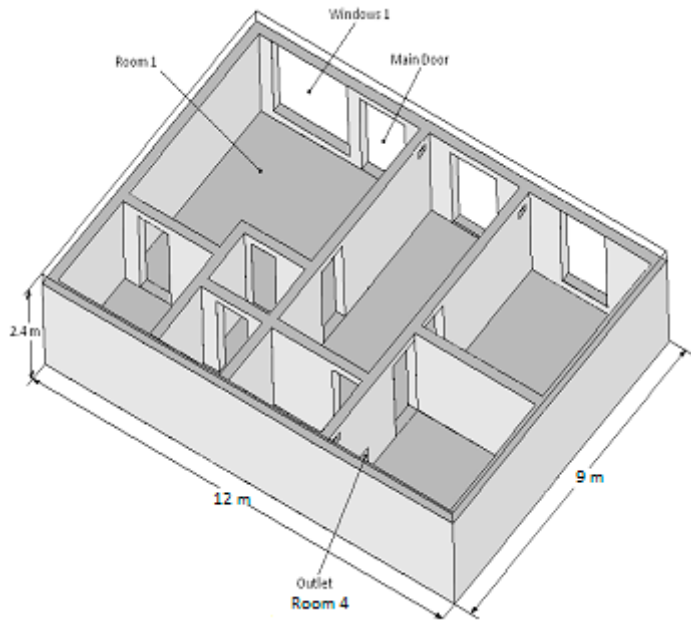


Figure 5. The house plan geometry

Room 1 is the sitting room and is therefore very important from the view point of radon concentration. This room is thus considered for analysis and conclusion. The Geometry of Room 1 is shown in Figure 6. In this geometry all internal doors (Door 1, Door 2 and Door 3) are closed. The Main Door and Window are also closed and are exposed to the outdoor air. The supply air leaves the room through the air holes. Figure 6 show that all supply air from the rooms leaves the house through the unique outlet. Therefore supply air from Room 1 exits from this room through the air holes of internal Door 1. In other words, Room 1 is considered to have one outlet located on internal Door 1 (Figure 6).

Radon enters Room 1 through the floor. Radon entry rate into the room is determined from the radon exhalation rate.

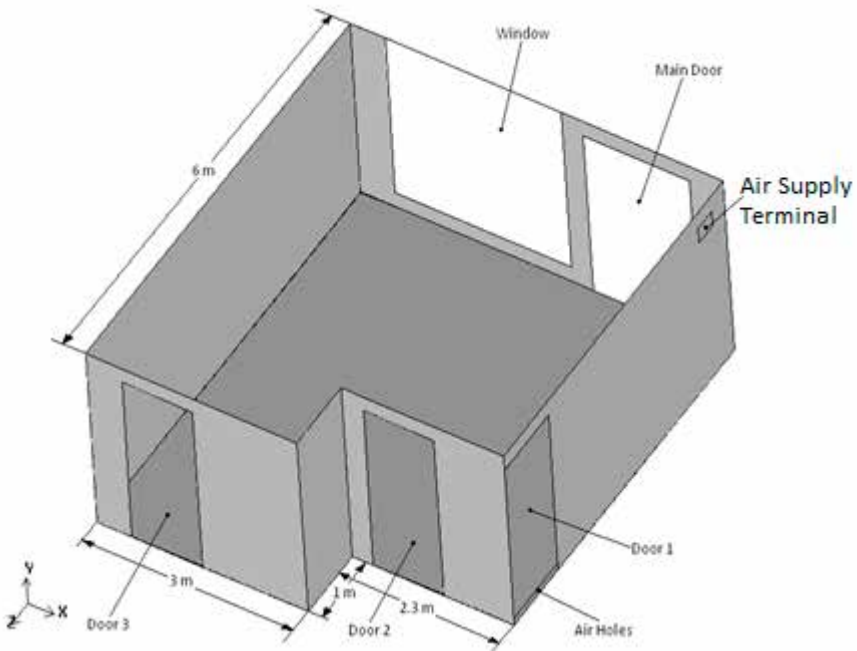


Figure 6. Room1 geometry

The Floor area is 29.5 m² and the supply air terminal device area is 0.06 m². The height of the room is 2.4 m and the volume 70.8 m³.

The dimensions of the house elements are summarized in Table 8.

Table 8. Sizes of the building elements

| Elements | Size (m) | Thickness (m) |
|----------------|----------|---------------|
| Window | 2.5×2.2 | 0.025 |
| Main Door | 1.5×2.2 | 0.05 |
| Internal Doors | 1×2.2 | 0.02 |
| External walls | - | 0.03 |
| Roof | - | 0.03 |

4.6 Parameters Variation Range

This study considers variations in three parameters, and examines the effects of changes in these parameters on indoor radon content. The parameters are

air change rate, temperature and relative humidity. Considered values of air change rate are 0.05, 0.25, 0.5 and 1.0 hr^{-1} ; the temperature ranges from 15 °C to 25°C; and relative humidity ranges are between 30 % and 80 % (Paper III, IV). 13 cases within these ranges are defined the studies as shown in Table 9.

Table 9. *Different cases studied in this work*

| Temperature changes | | Relative humidity changes | | Ventilation rate changes | |
|---------------------|---|---------------------------|---|--------------------------|--|
| Case No. | Parameters | Case No. | Parameters | Case No. | Parameters |
| N1 | Ach=0.5 hr^{-1} , T=15 °C, RH=40% | N6 | Ach=0.5 hr^{-1} , T=21 °C, RH=30% | N11 | Ach=1.0 hr^{-1} , T=21 °C, RH=40% |
| N2 | Ach=0.5 hr^{-1} , T=18 °C, RH=40% | N3 | Ach=0.5 hr^{-1} , T=21 °C, RH=40% | N3 | Ach=0.5 hr^{-1} , T=21 °C, RH=40% |
| N3 | Ach=0.5 hr^{-1} , T=21 °C, RH=40% | N7 | Ach=0.5 hr^{-1} , T=21 °C, RH=50% | N12 | Ach=0.25 hr^{-1} , T=21 °C, RH=40% |
| N4 | Ach=0.5 hr^{-1} , T=23 °C, RH=40% | N8 | Ach=0.5 hr^{-1} , T=21 °C, RH=60% | N13 | Ach=0.05 hr^{-1} , T=21 °C, RH=40% |
| N5 | Ach=0.5 hr^{-1} , T=25 °C, RH=40% | N9 | Ach=0.5 hr^{-1} , T=21 °C, RH=70% | - | - |
| - | - | N10 | Ach=0.5 hr^{-1} , T=21 °C, RH=80% | - | - |

4.7 Materials Properties

Materials used in the model are air, water vapor and radon as fluids; light concrete for the floor, dense concrete for the walls and the roof, window material, main door material and internal door material as solids. Properties of these materials are shown in Tables 10 and 11 for fluids and solids respectively.

Table 10. Properties of the fluids (Lide, 2004)

| Property | Radon | Water vapor | Air |
|--|------------------------|-----------------------|------------------------|
| Density (kgm^{-3}) | 9.73 | 0.554 | 1.225 |
| Heat capacity ($Jkg^{-1}K^{-1}$) | 93.55 | 2,014 | 1,006.43 |
| Thermal conductivity ($Wm^{-1}K^{-1}$) | 0.0036 | 0.026 | 0.024 |
| Viscosity ($kgm^{-1}s^{-1}$) | 2.445×10^{-5} | 1.34×10^{-5} | 1.789×10^{-5} |
| Molecular weight ($kgmol^{-1}$) | 222 | 18.015 | 28.966 |

Table 11. Properties of the solids (Lide, 2004)

| Material | Density (kgm^{-3}) | Heat capacity ($Jkg^{-1}K^{-1}$) | Thermal Conductivity ($Wm^{-1}K^{-1}$) |
|--------------------------------|------------------------|------------------------------------|--|
| Light concrete, Floor | 1,200 | 1,000 | 0.4 |
| Dense concrete, Walls and Roof | 2,100 | 840 | 1.4 |
| Window | 2,700 | 880 | 0.8 |
| Main door and Internal doors | 720 | 1,250 | 0.16 |

Diffusion coefficients are defined for fluid species in the model. Diffusion coefficients of air and radon are $2.88 \times 10^{-5} m^2s^{-1}$ and $1.1 \times 10^{-5} m^2s^{-1}$ respectively and they are approximately constant with temperature changes in the modeled range. The diffusion coefficient of water vapor varies with temperature and is $2.5 \times 10^{-5} m^2s^{-1}$ at 22 °C and $2.39 \times 10^{-5} m^2s^{-1}$ at 8 °C (Lide, 2004; Cussler, 1997).

The temperature range in this study lies between these two points. The diffusion coefficient of water vapor is therefore estimated by linear interpolation between these two points according to the following equation:

$$D \left(\frac{m^2}{s} \right) = 7.857 \times 10^{-8} T \text{ (}^\circ\text{C)} + 1.821 \times 10^{-6} \quad (4.14)$$

4.8 Relative Humidity

Relative humidity is one of the parameters whose effects on indoor radon content are examined in this study. The relative humidity range studied ranges from 30 % to 80 %. Relative humidity is defined in the model by

determining the mass fraction of water vapor. Mass fraction of water vapor is defined as the ratio of mass of water vapor to the total mass in a specific volume. Any specific volume contains radon, water vapor and air. Therefore the total mass is the sum of the all these species masses.

Relative humidity is defined as the ratio of partial pressure of water vapor to the saturated vapor pressure of water at a given temperature (Sonntag, 1990).

$$RH = \frac{p_{H_2O}}{p^*_{H_2O}} \times 100 \quad (4.15)$$

where RH is the relative humidity of the mixture, p_{H_2O} is the partial pressure of water vapor in the mixture, and $p^*_{H_2O}$ is the saturation vapor pressure of water at the temperature of the mixture.

Since saturated vapor pressure of water changes with temperature, for a specific value of relative humidity, the partial pressure of water vapor will also vary with temperature changes. This means that the mass fraction of water vapor at a specific relative humidity will vary with temperature.

Saturated vapor pressure of water at a given temperature can be obtained from the Antoine equation (Sonntag, 1990):

$$p^* = 10^{(A - \frac{B}{C+T})} \quad (4.16)$$

where p^* is saturated vapor pressure in $mmHg$, T is temperature in Celsius and A , B and C are constants.

For water at between $1^\circ C$ and $100^\circ C$, A , B and C are 8.071, 1730.63 and 233.426 respectively.

$mmHg$ can be converted to Pascal as follows:

$$p (Pa) = \frac{p (mmHg)}{13.595 \times 9.807} = \frac{p (mmHg)}{133.322}$$

Therefore saturated vapor pressure of water between $1^\circ C$ and $100^\circ C$ can be obtained from the following expression:

$$p^* (Pa) = \frac{10^{(8.071 - \frac{1730.63}{233.426+T(^{\circ}C)})}}{133.322}$$

The mass fraction of water vapor in the mixture for $T = 15^\circ C$ and $RH = 30\%$ is calculated using the Antoine equation:

$$T = 15^\circ C \quad \xrightarrow{\text{yields}} \quad p^*_{H_2O} = \frac{10^{(8.071 - \frac{1730.63}{233.426+15})}}{133.322} = 1,697.65 Pa$$

Thus, using the definition of partial pressure of water vapor yields

$$p_{H_2O} = p_{H_2O}^* \times RH \times 0.01 = 1697.65 \times 30 \times 0.01 = 509.30 \text{ Pa}$$

Radon content is negligible in comparison to water vapor and air and therefore partial pressure of radon is approximately zero.

Partial pressure of air can be calculated using Dalton's law of partial pressures. According to this law:

$$p_{Total} = p_{H_2O} + p_{Air} + \overbrace{p_{Radon}}^{\approx 0} = p_{H_2O} + p_{Air} \quad (4.17)$$

The calculations are carried out at atmospheric pressure, therefore total pressure is approximately 101.3 kPa. Partial pressure of air becomes:

$$p_{Air} = p_{Total} - p_{H_2O} = 101300.0 - 509.30 = 100,790.70 \text{ Pa}$$

At atmospheric pressure and indoor temperature, air and water vapor behave approximately as an ideal gas. For any volume of V , the mass of each species can be obtained from the ideal gas law as follows:

$$m = \frac{pV}{RT} \quad (4.18)$$

where p is the absolute pressure in Pa, V is the volume in m^3 , R is the gas constant in $Jkg^{-1}K^{-1}$, T is absolute temperature in K and m is the mass of gas in kg.

The gas constants for water vapor and air are approximately $461.5 Jkg^{-1}K^{-1}$ and $287 Jkg^{-1}K^{-1}$ respectively (Lide, 2004).

Mass fraction of water vapor can be calculated as follows:

$$MF_{H_2O} = \frac{m_{H_2O}}{m_{Total}} = \frac{m_{H_2O}}{m_{H_2O} + m_{Air} + \underbrace{m_{Radon}}_{\approx 0}} = \frac{m_{H_2O}}{m_{H_2O} + m_{Air}} = \frac{1}{1 + \frac{m_{Air}}{m_{H_2O}}} \quad (4.19)$$

where MF is mass fraction.

Using the ideal gas law:

$$MF_{H_2O} = \frac{1}{1 + \frac{(\frac{pV}{RT})_{Air}}{(\frac{pV}{RT})_{H_2O}}} = \frac{1}{1 + \frac{(\frac{p}{R})_{Air}}{(\frac{p}{R})_{H_2O}}} = \frac{1}{1 + \frac{(\frac{100790.7}{287})}{(\frac{509.3}{461.5})}} = 0.00313 \text{ or } 0.31\%$$

For the other cases, calculations are carried out in a similar way. The results are shown in Table 12.

Table 12. Mass fraction of water vapor for different relative humidity and temperatures

| RH (%) | T (°C) | p* _{H2O} (Pa) | p _{H2O} (Pa) | p _{Air} (Pa) | MF _{H2O} |
|--------|--------|------------------------|-----------------------|-----------------------|-------------------|
| 30 | 15 | 1,697.65 | 509.30 | 100,790.70 | 0.00313 |
| | 18 | 2,055.75 | 616.73 | 100,683.27 | 0.00379 |
| | 21 | 2,478.18 | 743.45 | 100,556.55 | 0.00458 |
| | 23 | 2,800.18 | 840.05 | 100,459.95 | 0.00517 |
| | 25 | 3,158.04 | 947.41 | 100,352.59 | 0.00584 |
| 40 | 15 | 1,697.65 | 679.06 | 100,620.94 | 0.00418 |
| | 18 | 2,055.75 | 822.30 | 100,477.70 | 0.00506 |
| | 21 | 2,478.18 | 991.27 | 100,308.73 | 0.00611 |
| | 23 | 2,800.18 | 1,120.07 | 100,179.93 | 0.00690 |
| | 25 | 3,158.04 | 1,263.22 | 100,036.78 | 0.00779 |
| | | | | | |
| 80 | 15 | 1,697.65 | 1,358.12 | 99,941.88 | 0.00838 |
| | 18 | 2,055.75 | 1,644.60 | 99,655.40 | 0.01016 |
| | 21 | 2,478.18 | 1,982.54 | 99,317.46 | 0.01226 |
| | 23 | 2,800.18 | 2,240.14 | 99,059.86 | 0.01387 |
| | 25 | 3,158.04 | 2,526.43 | 98,773.57 | 0.01566 |

4.9 Defined Functions

Radon concentration is measured in Bqm^{-3} , while FLUENT gives this value in molar concentration or $kmolm^{-3}$.

Therefore a custom field function is defined in order to calculate radon concentration in Bqm^{-3} as follows:

$$C_{Radon} \left(\frac{Bq}{m^{-3}} \right) = \frac{C_{Radon,Molar} \left(\frac{kmol}{m^{-3}} \right) \times M_{Radon} \left(\frac{kg}{kmol} \right)}{1.75 \times 10^{-19} \left(\frac{kg}{Bq} \right)} \quad (4.20)$$

where, M_{Radon} is the molecular weight of ^{222}Rn .

4.10 Convergence Criteria

The radon distribution field in the indoor environment is obtained by solving the governing conservation equations, i.e. continuity equation, momentum equations in three dimensions, energy equation, turbulence equations and species transport equations including radon and water vapor. These equations are commonly solved through an iterative process. To stop the iterative process and obtain a solution for the governing equations, several criteria must be defined depending on the problem conditions such as geometry, boundary conditions, initial conditions, etc.

In this work, six convergence criteria are considered for stopping the iterative process, and these must be met simultaneously. It should be noted that convergence is in principle achieved by minimizing the numerical residuals that represent the physical condition that is sought to be attained. Residuals in the order of 10^{-3} or better are considered as sufficient, and the respective convergence criterion represented by the residual in question is then considered to have been met.

The first convergence criterion is that the radon concentration at the outlet is equal to the average radon concentration generated in the room. Second, the average static temperature must also no longer vary at the moment of convergence. Third, since the model is solved as steady-state and there is a unique outlet, at the convergence situation the radon flow rate in outlet must exactly be equal to the radon entry rate into the room, namely 0.53 Bqs^{-1} , and it must not vary over time. Fourth, residuals must also be considered through the iterative process. Residuals are a measure of imbalances in each conservation equation. These must not change drastically (i.e., the rate of change of the residuals) through the iterative process, yet residuals alone cannot imply the convergence of an iterative process. Fifth, mass balance must be met in the model. Mass enters through the supply air terminal device (input mass through the radon generation in the floor can be neglected and is considered as a separate criterion) and leaves the model through the outlet. Both must be equal in the convergence situation since the model is solved in the steady state. Sixth, energy balance must also be met. In other words, since the model is solved as steady-state, incoming energy flows must be equal to outgoing energy flows. Incoming energy flows include the energy which enters through the supply air terminal device (input energy through the generated radon in the floor can be neglected). Outgoing energy flows include the energy which leaves the model through the outlet in addition to energy loss to the outdoor environment.

4.11 Near-wall treatment

The shear stress transport (SST) $k-\omega$ turbulence model used in this study requires meshing of the model environment.

Flow near the wall can be divided into regions designated viscous, buffer and fully turbulent sub-layers.

In the laminar (viscous) sub-layer region ($y^+ < 5$, y^+ refers to the dimensionless distance of the first node from the wall) inertial forces are less dominant and the flow exhibits laminar characteristics. This is known as the low-Re region. The SST turbulent model is a low-Re turbulent model which aims to resolve this area, and therefore requires an appropriate mesh resolution to do this accurately. In the log law (fully turbulent) region, convective forces

dominate over viscous forces and create high turbulent stresses; this is known as the high-Re composite region. In the SST turbulent model the entire turbulent boundary layer is resolved, including the log law region. However, it is possible to use semi-empirical expressions known as wall functions to bridge the viscosity-affected region between the wall and the fully turbulent region.

When using low-Re models such as the SST turbulent model, the average y^+ value (the first node dimensionless distance from the wall) should be in the order of ~ 1 to ensure that the laminar sub-layer is being captured (Gerasimov, 2006). High quality numerical results for the boundary layer will only be obtained if the overall resolution of the boundary layer is sufficient. The minimum number of cells to cover a boundary layer accurately is around 10, but values of 20 are desirable. The total thickness should be implemented such that around 15 or more nodes cover the boundary layer (ANSYS Inc, 2011).

Going by the above, since in this study the SST turbulent model is used, $y^+=1$ is chosen for calculation of the distance of the first node from the wall, and the resolution of the boundary layer is set to 12 with a specific growth factor between the nodes to accurately capture the boundary layer.

Calculations to obtain the first node distance from the wall and the ratio between the cells (growth factor) are shown below for $Ach = 0.5 \text{ hr}^{-1}$.

Wall shear stress, according to the definition, can be calculated from the following expression:

$$\tau_w = \frac{1}{2} C_f \rho V_{Vent}^2 \quad (4.21)$$

where, C_f is the skin friction, V_{Vent} is the flow velocity at the supply air terminal device and ρ is the density of air. C_f is obtained from the following approximation formula:

$$C_f = [2\text{Log}_{10}(Re_{Room}) - 0.65]^{-2.3} \quad \text{for} \quad Re_{Room} < 10^9$$

In this case ($Ach=0.5 \text{ hr}^{-1}$), thus

$$C_f = [2\text{Log}_{10}(2692.7) - 0.65]^{-2.3} = 0.015$$

$$\tau_w = \frac{1}{2} \times 0.015 \times 1.225 \times (0.164)^2 = 2.47 \times 10^{-4} \frac{\text{kg}}{\text{ms}^2}$$

According to the definition, first node distance (y) from the wall can be obtained from the following expression:

$$y = \frac{y^+ \mu}{\rho u_\tau} \quad (4.22)$$

where ρ and μ are the density and the dynamic viscosity of air respectively and u_τ is the friction velocity. Dimensional analysis shows that friction velocity (which is a characteristic velocity at the wall) can be defined in the following way:

$$u_\tau = \sqrt{\frac{\tau_w}{\rho}} \quad (4.23)$$

where ρ is the density of air and τ_w is wall shear stress.

In this case ($Ach=0.5 \text{ hr}^{-1}$), and thus for $y^+ = u^+ = 1$ this gives:

$$u_\tau = \sqrt{\frac{2.466 \times 10^{-4}}{1.225}} = 0.014 \frac{m}{s}$$

The first node distance (y) can be calculated from Equation 4.22 as follows:

$$y = \frac{1 \times 1.7894 \times 10^{-5}}{1.225 \times 0.014} = 1.04 \text{ mm}$$

12 cells in the boundary layer with a specific ratio between the cells are used in order to accurately capture the boundary layer. In order to determine this ratio, the boundary layer thickness must be provided. At the boundary layer edge, the velocity is equal to the free stream velocity. Dimensionless velocity for a wall-bounded flow is defined as follows:

$$u^+ = \frac{V}{u_\tau} \quad (4.24)$$

where V is the local velocity and u_τ is the friction velocity.

According to the law of the wall, u^+ and y^+ are correlated in the log-layer region as follows:

$$u^+ = \frac{1}{0.41} \ln(y^+) + 5.1 \quad (4.25)$$

And in the laminar sub-layer region ($y^+ < 15$):

$$u^+ = y^+$$

In this case ($Ach=0.5 \text{ hr}^{-1}$) the maximum u^+ (at the boundary layer edge) can be calculated as follows:

$$u_{Edge}^+ = \frac{V_{vent}}{u_t} = \frac{0.164 \frac{m}{s}}{0.014 \frac{m}{s}} = 11.7$$

By using the law of the wall in the log-layer region (see Equation 4.25), the corresponding y^+ for the above u^+ can be calculated as the following:

$$y_{Edge}^+ = e^{(0.41u^+ - 5.1)} = e^{(0.41 \times 11.55 - 5.1)} = 14.08$$

and therefore boundary layer thickness, which is the corresponding y for the y_{Edge}^+ , can be calculated as follows:

$$\delta \equiv y_{Edge} = \frac{y_{Edge}^+ \mu}{\rho u_t} = \frac{14.08 \times 1.7894 \times 10^{-5}}{1.225 \times 0.014} = 14.7 \text{ mm}$$

where δ is the boundary layer thickness.

The nodes are placed within the boundary layer with a specific growth factor. Therefore, boundary layer thickness can also be obtained from the following expression as the sum of the geometric series of cells sizes within the boundary layer:

$$\delta = \frac{y(r^n - 1)}{r - 1} \quad (4.26)$$

where y is the first node distance from the wall, r is the ratio between the cells (growth factor) and n is the number of cells within the boundary layer.

For the calculated values of y and δ for this case ($Ach = 0.5 \text{ hr}^{-1}$) and considering 12 cells within the boundary layer ($n=12$), $r = 1.03$. For other ventilation rates, calculations can be carried out in a similar way.

A sample of the meshed model from the isometric view is shown in Figure 7. In the figure, boundary layer cells can be easily seen.

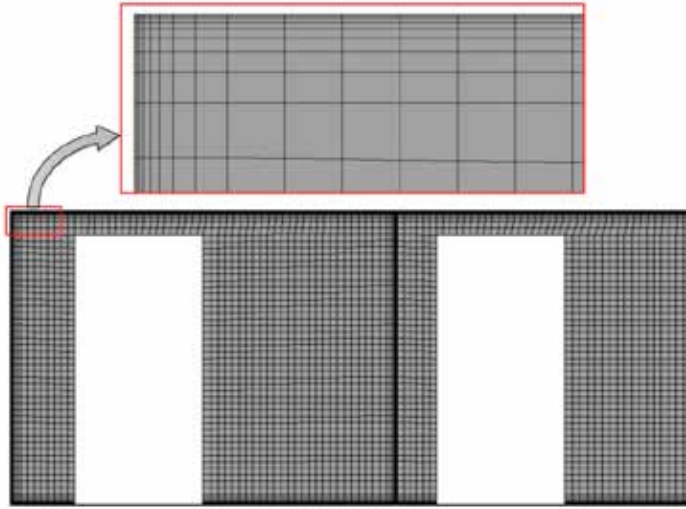


Figure 7. A sample of the meshed model (front view)

4.12 Mesh Independence Study

Grid refinement is necessary when the simulation grid cannot resolve attributes accurately and is done to minimize numerical diffusion. Grid refinement must be performed until the solution is reasonably grid independent. In order to achieve grid independency two aspects need to be considered: grid distribution and the total number of grid cells in the computational domain. An acceptable grid with rational respect and aspect ratios makes for fast convergence, and residual errors decrease as the cell number increases. However, increasing grid refinement increases computing capacity requirements and costs (Wang & Ward, 2000). A necessary part of any research that is based on numerical simulation is a mesh independence test to establish the accuracy of the results. Numerical simulations are computationally expensive and the size of the computational grid is considered among the significant factors influencing the computation time. In order to identify the minimum mesh density to ensure that the converged solution obtained from CFD is independent of the mesh resolution, a mesh sensitivity analysis should be carried out in the development and analysis of the CFD model.

In the present study, three meshes are investigated. The mesh sizes are: 2,000,000; 2,700,000 and 3,300,000 cells. The same ventilation rate, temperature and relative humidity are considered for these mesh sizes, i.e. 0.5 hr^{-1} , 15°C and 30 % respectively. The model is solved for each mesh to compare their performance. Several parameters can be considered for comparing the

performance of different mesh sizes. In this work, four parameters are considered for this purpose, average radon concentration, average static temperature, radon flow rate in the outlet and radon concentration along a vertical line in the middle of the room.

The results after convergence for each mesh for the first three parameters are presented in Table 13.

Table 13. Average radon concentration, average static temperature and radon flow rate in the outlet for different mesh sizes

| Mesh size (Cells) | Average radon concentration | | Radon flow rate in the outlet | |
|----------------------|-----------------------------|-----------|-------------------------------|-----------|
| | C Radon (Bqm-3) | Error (%) | m Radon (Bqs-1) | Error (%) |
| 2,000,000 | 37.004 | - | 0.5473 | - |
| 2,700,000 | 37.124 | 0.33 | 0.5766 | 3.40 |
| 3,300,000 | 37.188 | 0.17 | 0.5842 | 1.30 |

Percentage errors in each row in Table 13 have been calculated relative to the preceding row. Therefore, the first row does not have a percentage error.

Table 13 clearly shows that between the results of 2,000,000 cells and 2,700,000 cells there is a jump in the values of interest, especially in the average radon concentration, which is very important to this work. However, between the results of 2,700,000 cells and 3,300,000 cells, differences are negligible, especially the difference between the values of average radon concentration, which is less than 0.2%.

For better visualization, average radon concentration, average static temperature and radon flow rate in the outlet for different meshes sizes have been plotted in Figures 8 to 10. These figures clearly show that the differences between the results from 2,700,000 cells and 3,300,000 cells are negligible, and that there is a larger difference between the results with 2,000,000 cells and other mesh densities, especially in average radon concentration.

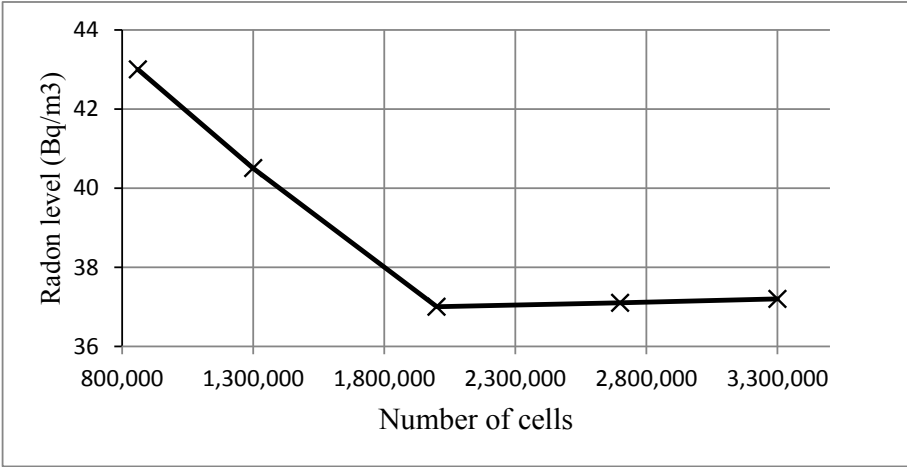


Figure 8. Average radon concentration for different mesh sizes

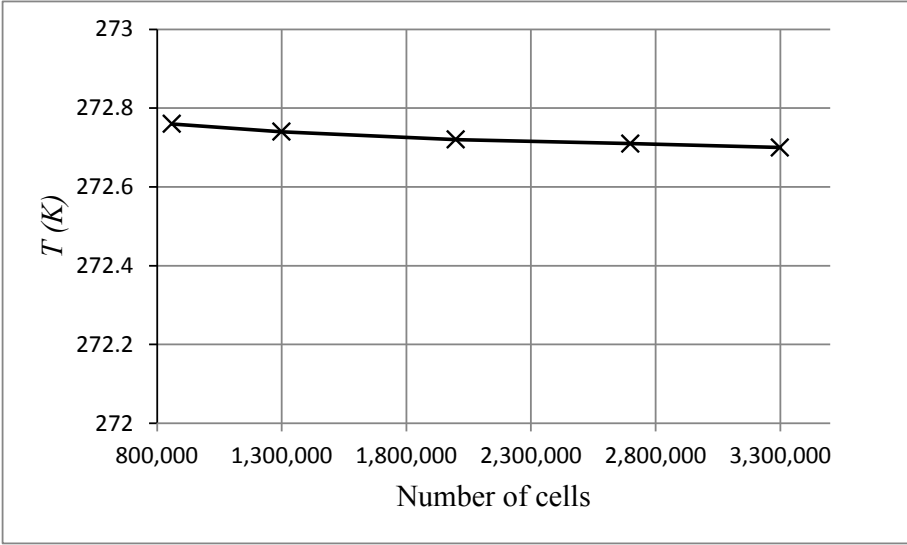


Figure 9. Average static temperature for different mesh sizes

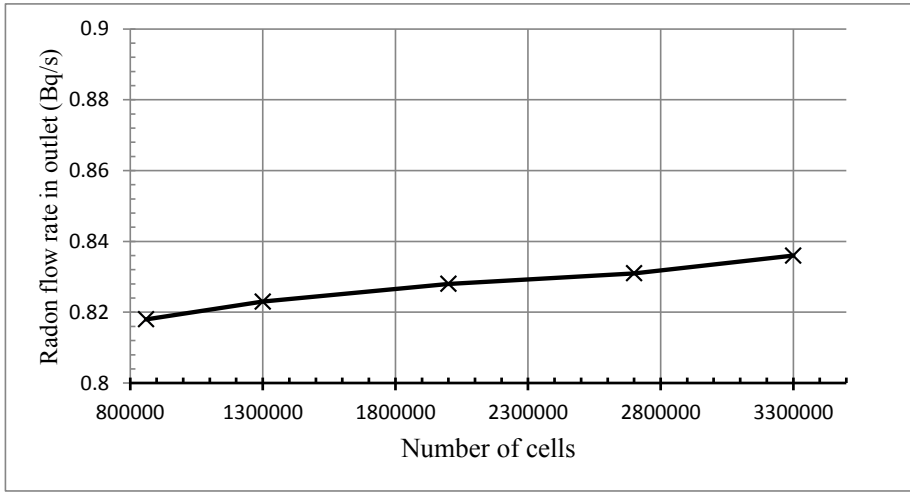


Figure 10. Radon flow rate in the outlet for different mesh sizes

The fourth parameter which is considered in this study for comparing performance of different mesh sizes is the radon concentration profile along a vertical line in the middle of the room. Figure 11 shows this parameter for the different mesh sizes.

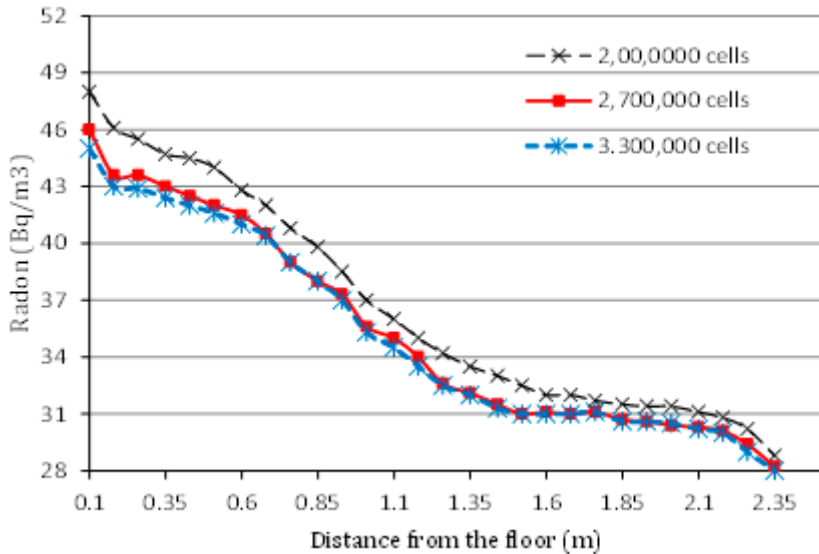


Figure 11. Radon concentration profile along a vertical line in the middle of the room for different mesh sizes

Figure 11 shows that the radon concentration profile also has the same shape for all the different mesh densities tested. It is evident that as the number of

cells in the mesh is increased, the variation in the radon concentration profile decreases. Thus the change in radon concentration profile between meshes with 2,700,000 and 3,300,000 cells is negligible.

Based on the above, we can be confident that a mesh with 2,700,000 cells is sufficient to carry out the simulations, as it gives a mesh-independent result at the minimum possible computational cost. Therefore this number of cells is selected for the simulations in this study.

4.13 Examination of convergence criteria

Simulations were carried out for the different cases indicated in Table 9. Within each simulation, all convergence criteria must be met to obtain a solution for the case. In this section, convergence criteria are examined for the case designated N11 in Table 9 ($Ach = 1.0 \text{ hr}^{-1}$, $T = 23 \text{ }^{\circ}\text{C}$, $RH = 40\%$). A similar procedure is used for the other cases.

As mentioned before, six convergence criteria are considered for determining the convergence of the iterative process to obtain a solution.

The first convergence criterion is the average radon concentration in the room. At convergence, average radon concentration must no longer change. Figure 12 shows plot average radon concentration against iterations, showing that average radon concentration approaches a specific value after which it does not change with increasing iterations. The first convergence criterion is therefore satisfied.

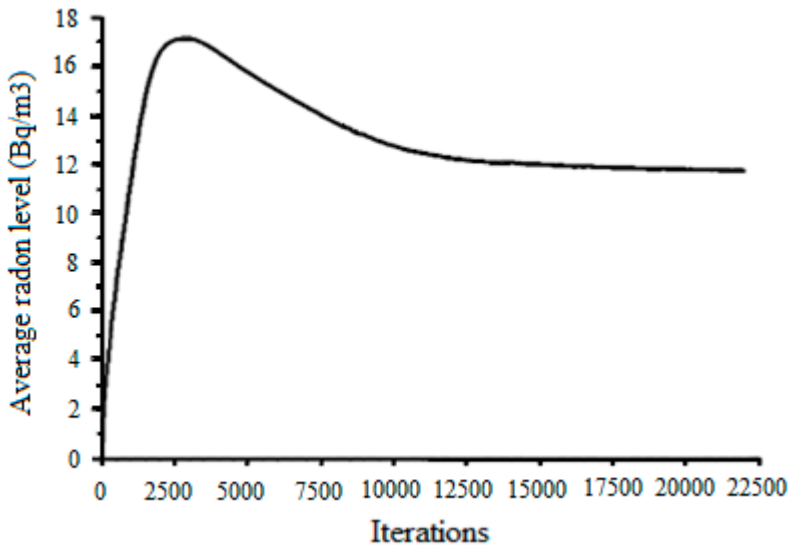


Figure 12. Average radon concentration versus iterations for the case N11

The second convergence criterion is the average static temperature inside the room. At convergence, this parameter must no longer change. Figure 13 plots the average static temperature against iterations, showing that average indoor static temperature no longer changes, thus satisfying the second criterion.

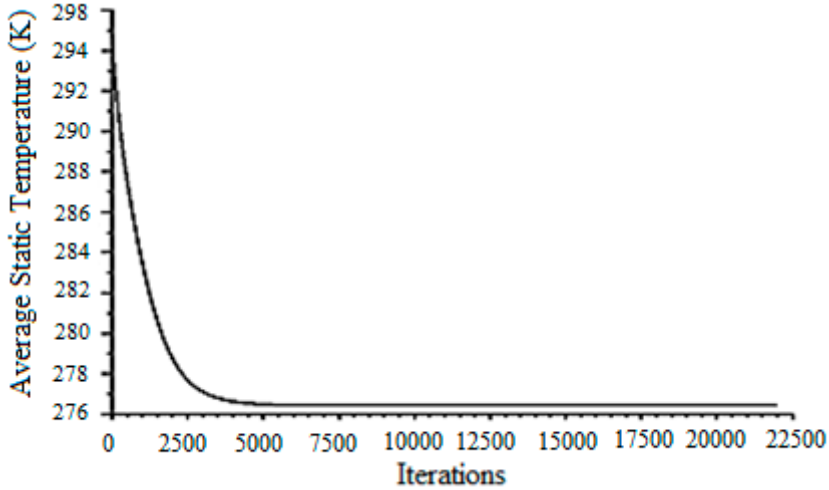


Figure 13. Average indoor static temperature versus iterations for the case indicated with N11

The third convergence criterion is the radon flow rate in the outlet. After convergence, as previously mentioned, the radon flow rate in the outlet must be exactly 0.826 Bqs^{-1} , i.e. equal to the radon entry rate into the room. This can be easily checked and it has been confirmed. Furthermore, the radon flow rate in outlet must not change after convergence. Figure 14 plots the radon flow rate in the outlet against iterations, showing that it approaches 0.826 Bqs^{-1} and no longer changes once it has reached this value, indicating that the third convergence criterion has satisfied.

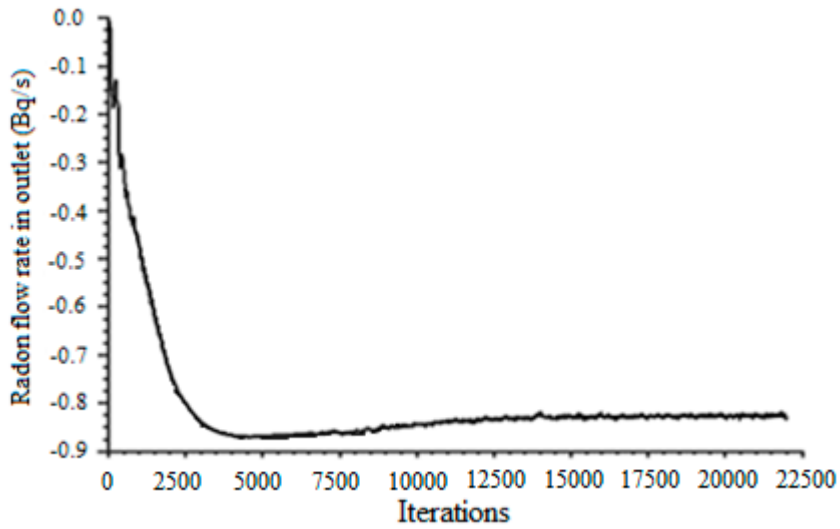


Figure 14. Radon flow rate in the outlet versus iterations for the case indicated with N11

The fourth convergence criterion concerns the residuals. Figure 15 plots the residuals versus iterations. The residuals do not change drastically and their variations are moderate with increasing iterations. Therefore, the fourth convergence criterion has also been satisfied.

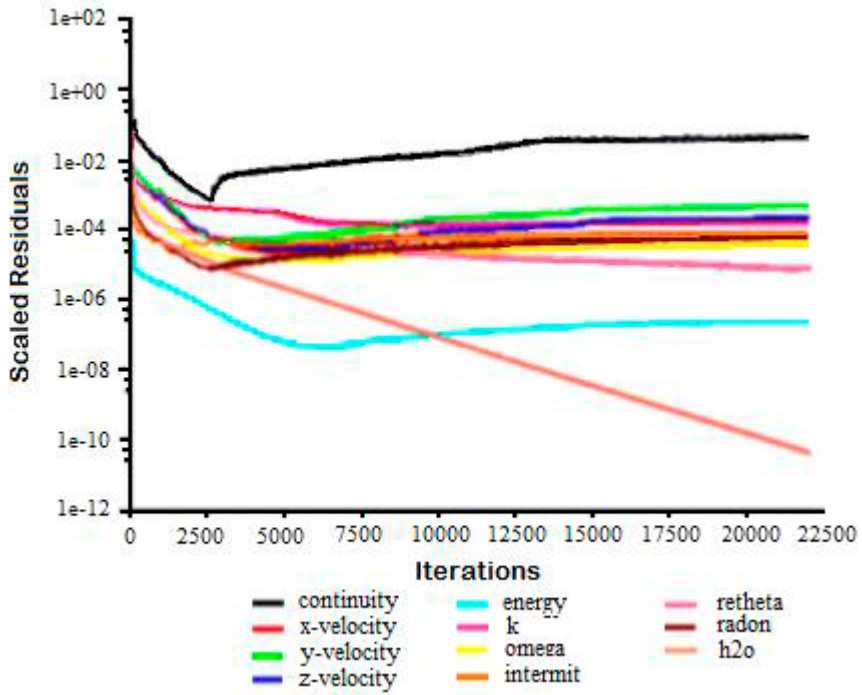


Figure 15. Residuals versus iterations for the case indicated with N11

The fifth convergence criterion is the mass balance. In order to calculate the mass balance, the input mass flow rate at the vent is first calculated as follows. Input flow contains three species; radon, water vapor and air. Mass fraction of radon at the vent is zero. Mass fraction of water vapor for case N11 is obtained from Table 12, and from this the mass fraction of air can be determined.

$$MF_{H_2O} = 0.0069$$

Mass flow rate can be calculated from the following equation:

$$\dot{m} = \rho V_{vent} A_{vent}$$

where A_{vent} is the area of the vent which is 0.06 m^2 . V_{vent} is the velocity at the vent, and according to Table 7 for case N11 it is 0.328 ms^{-1} . ρ is the density of the mixture, which can be calculated from the ideal gas law as follows:

$$PV = \frac{m}{M_{Mixture}} \bar{R}T \quad (4.27)$$

where m is the mass of the mixture and $M_{Mixture}$ is the molar mass of the mixture. P is the absolute pressure (101,300.0 Pa), V is the volume of the mixture, n is the number of moles in the mixture and the universal gas constant \bar{R} is 8.31446 $Jmol^{-1}K^{-1}$ (Lide, 2004). T is the absolute temperature, in this case (N11) it is $23 + 273 = 296 K$.

Density of the mixture $\rho = \frac{m}{V}$, which using the ideal gas law, gives

$$\rho = \frac{PM_{Mixture}}{\bar{R}T}$$

Therefore, for the density of mixture calculation, the molar mass of the mixture should be calculated. The molar mass of the mixture is calculated as follows:

$$M_{Mixture} = \frac{m}{n_{Total}} \quad (4.28)$$

where m is the total mass of the mixture and n_{Total} is the total number of moles within the mixture.

As mentioned before, there is no radon at the inlet (vent). Therefore, the total number of moles at the inlet only includes the number of moles of water vapor and air.

$$M_{Mixture} = \frac{m}{n_{H_2O} + n_{Air}}$$

Number of moles of water vapor and air can be calculated as follows:

$$n_{H_2O} = \frac{m_{H_2O}}{M_{H_2O}}$$

$$n_{Air} = \frac{m_{Air}}{M_{Air}}$$

where M_{H_2O} and M_{Air} are the molar mass of water vapor and air respectively. Using the mass fraction of water vapor, gives

$$n_{H_2O} = \frac{m_{H_2O}}{M_{H_2O}} = \frac{m \times MF_{H_2O}}{M_{H_2O}}$$

Since the mass fraction of radon at the supply air terminal device (vent) is zero, the mass fraction of air can be obtained from the following expression:

$$MF_{Air} = 1 - MF_{H_2O}$$

Therefore, the number of moles of air is:

$$n_{Air} = \frac{m_{Air}}{M_{Air}} = \frac{m \times MF_{Air}}{M_{Air}} = \frac{m \times (1 - MF_{H_2O})}{M_{Air}}$$

Substituting the expressions for the number of moles of water vapor and air in the molar mass expression for the mixture gives

$$M_{Mixture} = \frac{m}{n_{H_2O} + n_{Air}} = \frac{m}{\frac{m \times MF_{H_2O}}{M_{H_2O}} + \frac{m \times (1 - MF_{H_2O})}{M_{Air}}} = \frac{1}{\frac{MF_{H_2O}}{M_{H_2O}} + \frac{(1 - MF_{H_2O})}{M_{Air}}}$$

Using the value of MF_{H_2O} for case N11 and the data in Table 9, the molar mass of the mixture can be calculated as follows:

$$M_{Mixture} = \frac{1}{\frac{MF_{H_2O}}{M_{H_2O}} + \frac{(1 - MF_{H_2O})}{M_{Air}}} = \frac{1}{\frac{0.0069}{18.015 \left(\frac{kg}{kmol}\right)} + \frac{(1 - 0.0069)}{28.966 \left(\frac{kg}{kmol}\right)}} = 28.845 \frac{kg}{kmol}$$

Therefore, density of the mixture can be calculated as follows:

$$\rho = \frac{PM_{Mixture}}{RT} = \frac{101300.0 \text{ Pa} \times 28.845 \frac{kg}{kmol} \times \frac{1 \text{ kmol}}{1000 \text{ mol}}}{8.31446 \frac{J}{molK} \times 296 \text{ K}} = 1.187 \frac{kg}{m^3}$$

and the mass flow rate at the supply air terminal device (input mass) is:

$$\dot{m} = \rho V_{Vent} A_{Vent} = 1.187 \frac{kg}{m^3} \times 0.328 \frac{m}{s} \times 0.06 \text{ m}^2 = 0.023 \frac{kg}{s}$$

In order to verify the mass balance we must also examine the mass flow rate at the outlet. There is only one outlet in the model. FLUENT gives a value of $0.023 \text{ (kg s}^{-1}\text{)}$ for the radon flow rate at the outlet. Therefore the mass balance is met and thus the fifth convergence criterion has also been satisfied.

The sixth convergence criterion is the energy balance. Input energies include the input energy through the vent and the input energy from radon. The radon flow rate through the floor is negligible in comparison with the flow rate at the supply air terminal device. The input energy from radon can therefore be ignored. There is thus only one source of input energy, namely the supply air terminal device (inlet). Output energies include the output energy through the outlet and heat rejection to the outdoor environment through the outer surfaces (including outside walls, roof, window and main door). First, the difference between the input energy through the supply air terminal device and the output energy through the outlet is calculated. The

obtained value must be equal to the heat rejection to the outdoor environment through the outer surfaces to achieve energy balance.

The difference between the input energy through the supply air terminal device and the output energy through the outlet can be calculated as follows³:

$$Q_1 = Q_{Air} + Q_{Water} = \dot{m}_{Air}c_{p,Air}(T_{Vent} - T_{Outlet}) + \dot{m}_{H_2O}c_{p,H_2O}(T_{Vent} - T_{Outlet})$$

where Q_1 is the difference between the input energy through the supply air terminal device and the output energy through the outlet, \dot{m}_{Air} and \dot{m}_{H_2O} are the mass flow rate of air and water vapor respectively in the model, $c_{p,Air}$ and c_{p,H_2O} are the heat capacity of air and water vapor respectively and can be obtained from Table 11, T_{Vent} and T_{Outlet} are the average static temperature of the mixture at the supply air terminal device and at the outlet respectively. T_{Vent} in the case under consideration (N11) is 23 °C and T_{Outlet} is obtained using FLUENT, and is 1.357 °C.

Using the mass fraction of water vapor, the above equation can be rewritten as follows:

$$Q_1 = [\dot{m}(1 - MF_{H_2O})c_{p,Air} + \dot{m}MF_{H_2O}c_{p,H_2O}](T_{Vent} - T_{Outlet}) \text{ or}$$

$$Q_1 = \dot{m}(T_{Vent} - T_{Outlet})[(1 - MF_{H_2O})c_{p,Air} + MF_{H_2O}c_{p,H_2O}]$$

where \dot{m} is the total mass flow rate in the model and MF_{H_2O} is the mass fraction of water vapor.

For case N11, Q_1 is

$$Q_1 = 0.023(23 - 1.357)[(1 - 0.007)1006.43 + 0.007 \times 2014.0] = 504.50 \text{ J}$$

The heat rejection to the outdoor environment through each outer surface is obtained from FLUENT and presented in Table 14.

Table 14. The heat rejection to outdoor environment through each outer surface, case N11

| Outer surface | Heat rejection (J) |
|---------------|--------------------|
| Outside walls | 125.99 |
| Roof | 302.30 |
| Main door | 18.65 |
| Window | 58.60 |

³ There is no internal source in Room 1.

From the data in Table 14, the total heat rejection to outdoor environment, Q_2 , can be calculated as follows:

$$Q_2 = 125.99 + 302.30 + 18.65 + 58.6 = 505.54 \text{ J}$$

Comparison between Q_1 and Q_2 implies that the sixth convergence criterion has been satisfied.

Thus all convergence criteria for the considered case (N11) have been satisfied, implying that the model has been converged and the solution has been obtained.

5 Results and discussion

Results and discussion are presented as the following: radon measurements, energy dynamics simulation and economic analysis, and numerical simulation.

5.1 Radon measurement

As previously mentioned, radon concentrations were measured through ATDs and CRMs. Radon levels are measured by ATD which are sent to a nuclear laboratory for processing. Data measured by the continuous radon meter are directly accessible by a computer.

Measurements of the indoor radon content in this one-family house were recorded between 2008 and 2010. During this period the building had an exhaust air ventilation system. In 2010 a heat recovery ventilation system was installed alongside some remediation actions such as floor sealing and creation of a radon sump. These actions significantly improved IAQ and reduced the indoor radon level. Indoor radon concentration in this house at the normal ventilation rate, 0.5 Ach, is currently below 100 Bqm^{-3} . Air leakage is not included in the air change rate in these measurements. Table 15 shows the results of indoor radon measurements in the case study house.

Table 15. Measured indoor radon levels (Bqm^{-3})

| Date and period | ATD ¹ (Bqm^{-3}) | CRM ² (Bqm^{-3}) | Ventilation rate (Ach) | Ventilation Type | Remedial action |
|----------------------|------------------------------------|------------------------------------|------------------------|--------------------|-------------------------|
| 2008-2 (2weeks) | 3,580±380 | ----- | 0.05 ⁴ | Exhaust fan off | No action |
| 2010-1 (3months) | 1,280±160 | 1,580±158 | 0.25 | HRV ³ | Radon sump & sealing |
| 2010-04 (3 weeks) | 100±20 | ----- | 0.25 | HRV | 3 connected sumps |
| 2010-3 (12days) | ----- | 97±10 | 0.25 | HRV | 3 connected sumps |
| 2010-3 (12days) | ----- | 45±4 | 0.5 | HRV | 3 connected sumps |
| 2010-4 (12 days) | ----- | 25±2 | 1.0 | HRV | 3 connected sumps |
| 2011-11 (10 days) | ----- | 39±4 ⁵ | 0.5 | HRV | 3 connected sumps |
| 2012-11 | ----- | 34±3 ⁶ | 0.5 | HRV | 3 connected sumps |

¹Alpha track detector, ²Continuous radon monitor, ³Heat recovery ventilation

In order to show the impact of ventilation rate on radon level, radon concentrations were measured with three different ventilation rates. Figure 16 shows the effects of these different air change rates on radon levels measured with a CRM. The measurement study confirmed that varying ventilation rates resulted in different radon levels. These results are also published in papers II and IV.

⁴ It is assumed that when there is no mechanical ventilation, the air leakage is at least 0.05 Ach.

⁵This is a sample of measurements at different changes of indoor temperature and humidity.

⁶ This is a sample of measurements at different distances from the floor.

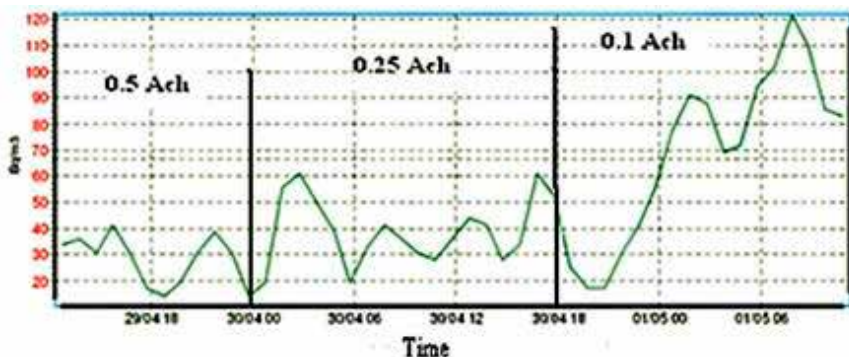


Figure 16. Radon level measurements versus ventilation rate

In order to show the influence of indoor temperature and relative humidity on indoor radon level, several measurements were carried out. Continuous radon measuring results do not show strong correlations between indoor radon levels and indoor RH and temperature in the tested ranges.

Figure 17 shows a sample result from the R2 CRM. Radon and temperature were monitored simultaneously. Green and purple curves show fluctuations of radon and temperature levels in the case study house respectively. These curves indicate instantaneous changes of indoor radon and temperature.

In the case of temperature it was observed that indoor radon fluctuations correlate with indoor temperature (see Figure 17). Since indoor radon level is dependent on many factors such as outdoor conditions, this relation is not strong. One possible physical interpretation could be that a higher indoor temperature increases the influence of thermals (stack effect), given its tendency to increase the magnitude of the negative indoor pressure at floor level. This increased negative pressure would increase the infiltration of air, including radon gas, from the ground (advection effect), and for this reason we would expect to see a correlation between higher indoor temperature and higher radon content. However, this relation should be relatively weak, unless the indoor temperature is varied more dramatically.

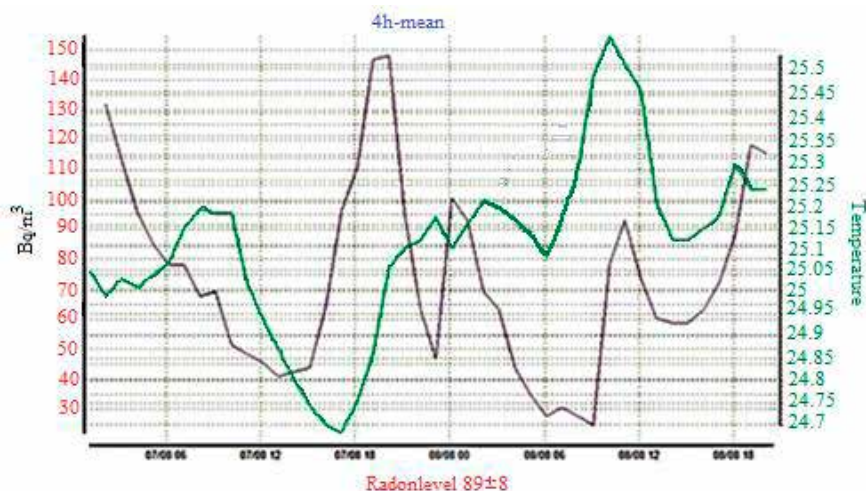


Figure 17. Radon level (green curve) and temperature (purple curve).
Radon is on the red axis (Bq/m^3), temperature is on the green axis, and the horizontal axis represents time in hours from 21-24 December.

Several measurements were carried out to investigate the relationship between indoor radon level and the height above the floor. To measure radon level, a R2 CRM device was placed at different heights (0, 50, 90 and 200 cm) from the floor at 0.5 Ach. Figure 18 shows this relationship between the average radon level and height, which reflects the theoretical relation Equation 3.3.

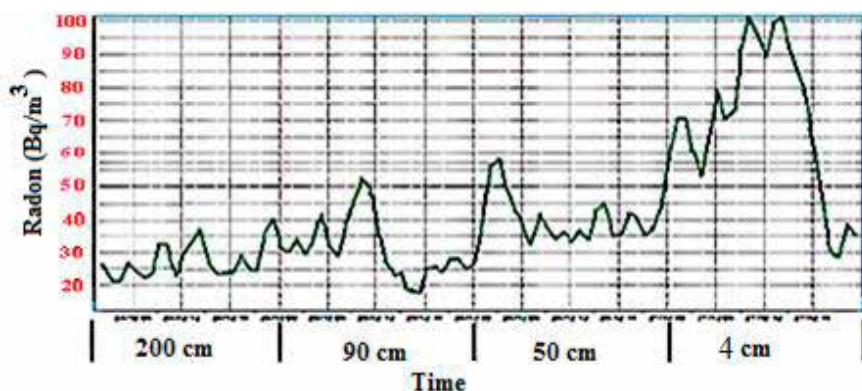


Figure 18. Radon level changes versus measurement height above the room floor

The horizontal axis indicates the measurement time periods for the different height set ups. The results indicate an inverse relationship between radon level and height (H).

To further verify the relation between indoor radon level and height above the floor several measurements were taken at different locations. These measurements, shown in Figures 19 and 20 supported the relationship between radon level and height above the floor.

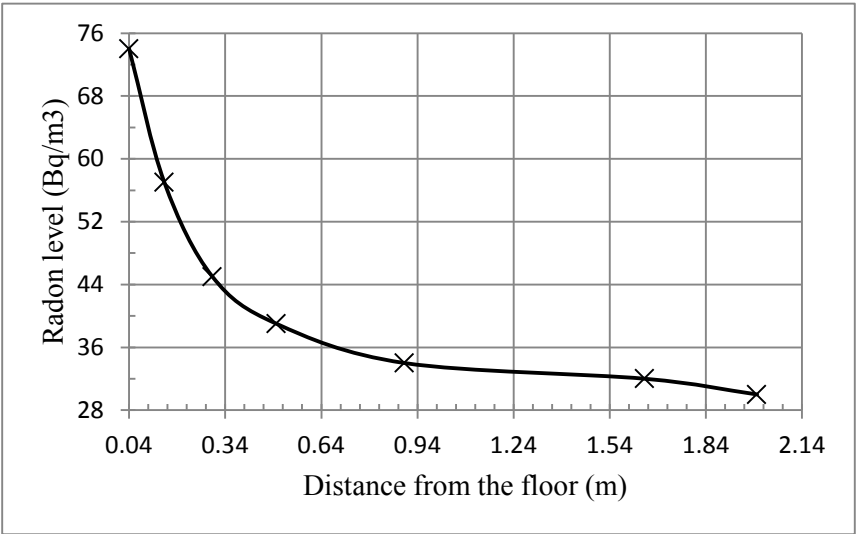


Figure 19. Average radon levels versus height (0-200 cm from the floor)

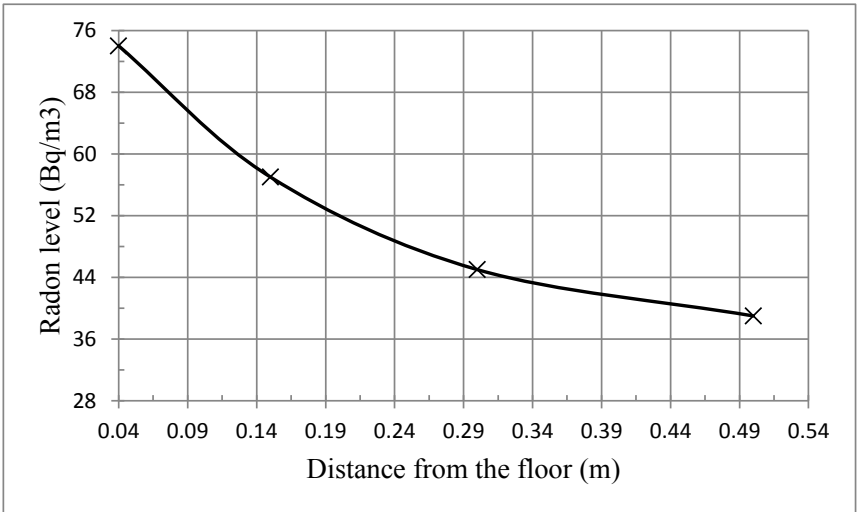


Figure 20. Average radon levels versus height (0-50 cm from the floor)

5.2 Analytical analysis of radon level in the case study house

Analytic calculations from Equations (3.3) and (3.5) give indoor radon levels for different ventilation rates (0.0 to 1.0 Ach) and $E = 0.018 \text{ Bqm}^{-2}\text{s}^{-1}$. The calculation results are as follows: $C_{0.0} = 3,582$, $C_{0.25} = 108$, $C_{0.5} = 54$, and $C_1 = 22 \text{ Bqm}^{-3}$.

These results from analytic calculations were compared with the measured data listed in Table 15. The comparison is shown in Table 16.

Table 16. Radon level versus ventilation rate by measurement and analytic methods

| Air change rate (Ach) | Measurement(Bqm^{-3}) | Analytic(Bqm^{-3}) |
|--------------------------|----------------------------------|-------------------------------|
| $\cong 0.0$ | $3,580 \pm 380$ | 3,582 |
| 0.25 | 97 ± 10 | 108 |
| 0.5 | 45 ± 4 | 54 |
| 1.0 | 25 ± 2 | 22 |

The comparison in Table 16 shows that indoor radon levels resulting from analytical calculations corresponded closely with the measured data, with a maximum difference of 14%.

5.3 Dynamic energy simulation and calculation

The annual recoverable energy with constant room temperature can be easily determined by energy calculation and dynamic energy with IDA ICE. The annual energy saving is generally varied by changing the ventilation rate and heating degree days (HDD). Several dynamic simulations were carried out for different ventilation rates and heat exchanger unit efficiencies. IDA ICE uses its own database to estimate HDD. The Stockholm, Bromma climate profile in the database was selected for this study. The energy data is based on available data for the heat exchanger unit produced by the FLEXIT Company, and the energy calculation for the case study house is based on Equation 3.11. The results of the dynamic simulation are shown in Table 17.

Table 17. Dynamic simulation and energy calculation results

| Ventilation rate (Ach) | Heat recovery (kWh) simulation | Heat recovery (kWh) calculation |
|---------------------------|-----------------------------------|------------------------------------|
| 0.5 | 3,380 | 3,200 |
| 1.0 | 6,759 | 6,400 |

Comparison of these simulation and calculation results shows good agreement between the data with an error of about 6 % at 0.5 Ach. This discrepancy results from the different values of the heat recovery unit efficiency and heating degree days used in these methods.

The normal range of the ventilation rate and HDD in similar cold climates is typically 0.5–1 Ach and 4,000–6,000 degree days respectively. The annual heat recovery through this type of ventilation system would be in the range of 20 to 90 kWh per m^2 per floor area. For this case study the annual heat recovery is about 30 kWh per m^2 per floor area.

5.3.1 Economic analysis of the heat recovery ventilation unit

The net present value (NPV) method was used to evaluate the cost-effectiveness of a future investment as discussed in Paper I.

The initial capital investment and installation cost of the rotary heat exchanger unit is about 25,000 SEK, with 25 years lifetime. The energy consumption of the 2 DC fans is 350 kWh per year and the cost of replacing the 2 filters is 500 SEK per year. Energy costs in Sweden are roughly 1 SEK/kWh including tax and VAT. It should be noted that the 25,000 SEK only covers the heat exchanger unit itself. If the assessment included installation of an exhaust air ventilation system with a supply air and exhaust air system, the total (higher) cost for the supply air system with ducting etc. should be included. In this case the assumption is that the supply air system is already in place, and thus only the additional investment for the heat exchanger unit is considered.

A comparison against all possible exhaust air ventilation systems has been deemed to lie outside the scope of this thesis. It is worth mentioning that exhaust air heat pumps are very commonly used in Swedish one-family houses. The economic study in this thesis does not include any comparison with heat pumps. This choice is not expected to affect the overall conclusions drawn from the research.

NPV can be calculated based on Equations 3.14–3.17.

Annual savings: $b = \text{Costs of recovered energy per year} - \text{Annual maintenance cost}$ ($3,168 - 350 - 500 = 2,318$ SEK), and therefore $B_0 = 36,207$ SEK and $A_0 = 25,000$ SEK, which means that $B_0 > A_0$. Table 18 shows the details of these values.

Table 18. Values used for life cycle cost analysis

| Variables | Abbreviations | Values |
|------------------------|---------------|--------------|
| HRV capital investment | A_0 | 25,000 (SEK) |
| Interest rate | i | 4% |
| Annual savings | b | 2,318 (SEK) |
| NPV factor | I | 15.62 |
| All savings | B_0 | 36,207 (SEK) |

Since the net present value of all the savings is larger than the initial capital cost, the enterprise is cost-effective and this investment is profitable.

Equation 3.15, taking into account an increasing energy price with annual energy cost escalation rate $q = 2\%$, results in a new NPV factor $I_q = 19.61 > I$, and then $B_0 = 45,456$ SEK. Therefore, taking into account a rising energy price, this investment would have payback about 12 years.

Based on analytical relations, the NPV of this HRV was calculated and the results of the life cycle cost analysis are shown in Table 19. They show that the use of a HRV system is cost-effective, and taking into account the annual increase of the energy cost, the investment will have a payback period of about 12 years.

Table 19. Ventilation system life cycle cost analysis

| Ventilation system | Capital cost (SEK) | Annual costs (SEK) | | Life-cycle costs (SEK) |
|--------------------|-----------------------|--------------------|-------------|---------------------------|
| | | Energy | Maintenance | |
| Traditional fan | 625 | 4,387 | ----- | 86,000 |
| HRV with AC fan | 25,000 | 613 | 500 | 44,830 |
| HRV with DC fan | 25,000 | 350 | 500 | 39,674 |

The NPV analysis shows that installing an air handling unit is beneficial from the perspective of reducing energy cost as well as for mitigation of indoor radon level.

Heat recovery units are manufactured in Europe and the small sizes suitable for single family buildings cost in the range of 17,000-30,000 SEK (Flexit, 2009).

The economic evaluation of the heat exchanger for the exhaust air depends on the volume and duration of the ventilation. The payback time decreases when the annual utilization hours increase. This means that heat recovery ventilation systems are more advantageous in climates with long and severe winters like Sweden, or those with hot summers.

5.4 Results and discussion of numerical modelling

Papers II and IV discuss the results of two different modeling approaches. In the first approach the house and soil are modeled, but the whole house is considered as a single room, i.e. without internal partitions. The soil as a porous media is considered as the radon source. In Paper IV the whole house is modeled and partitions are assumed for the individual rooms

This section presents the results of simulations of Room 1 from Paper IV for different cases listed in Table 9. The simulations have been further improved relative to what was presented in Paper IV by means of a significantly refined mesh. These refined results show the effects of different indoor air parameters (including ventilation rate, temperature and relative humidity) on indoor radon concentration.

5.4.1 Air Change Rate Effects on Indoor Radon Content

In order to investigate the air change rate effects on indoor radon content, four cases have been considered. The cases are listed in Table 9 as N11, N3, N12 and N13. The model has been solved as described in previous sections and the results are shown in Table 20 and Figure 21.

Table 20. Average radon content for different air change rates at $T = 21$ °C and $RH = 40\%$

| Case No. | Ventilation rate (hr^{-1}) | Average radon concentration (Bqm^{-3}) |
|----------|-----------------------------------|---|
| N11 | 1.0 | 17 |
| N3 | 0.5 | 40 |
| N12 | 0.25 | 82 |
| N13 | 0.05 | 2,828 |

These results indicate that increasing ventilation rate reduces average radon concentration. This is a reasonable result, since increasing ventilation rate dilutes indoor air and moves the radon out of the room thereby reducing average radon concentration within the room.

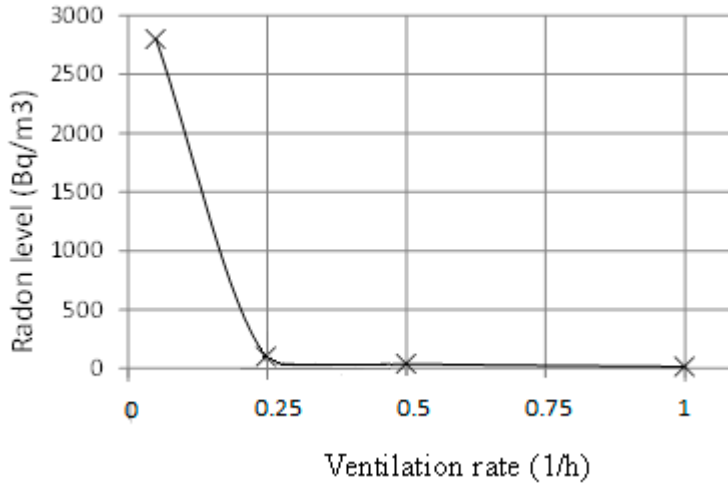


Figure 21. Average radon content for different air change rates at $T = 21^{\circ}\text{C}$ and $\text{RH} = 40\%$

Radon concentrations along a vertical line in the middle of room are plotted in Figures 22 and 23. They indicate that the radon concentration profile is changed by ventilation rate changes. In other words, ventilation rate affects both radon concentration and radon distribution.

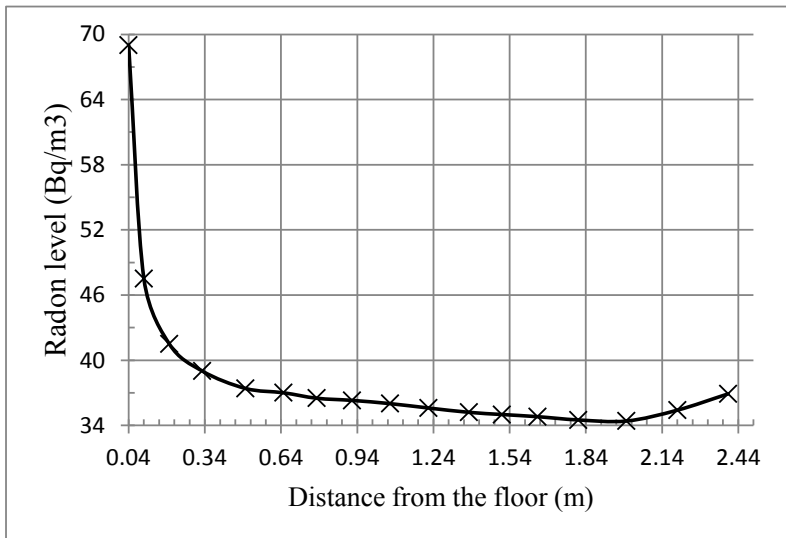


Figure 22. Radon concentration along a vertical line in the middle of the room for N3 ($\text{Ach} = 0.5\text{hr}$, $T = 21^{\circ}\text{C}$, $\text{RH} = 40\%$)

These results show that indoor radon concentration decreases as the distance from the floor is increased.

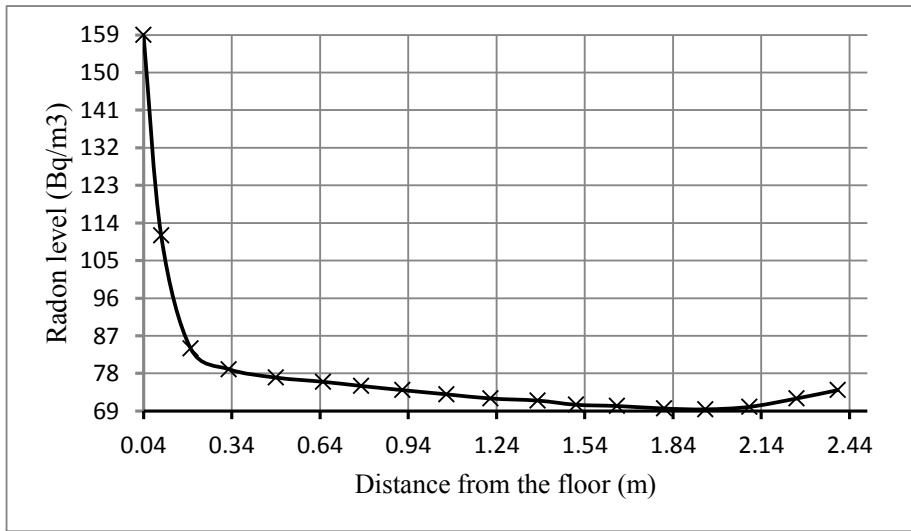


Figure 23. Radon content along a vertical line in the middle of the room for N12 ($Ach = 0.25 \text{ hr}^{-1}$, $T = 21 \text{ }^{\circ}\text{C}$, $RH = 40\%$)

Contours of radon concentration and air velocity for different ventilation rates in two vertical planes in the middle of room (Figure 24) are shown in Figures 25 to 30.

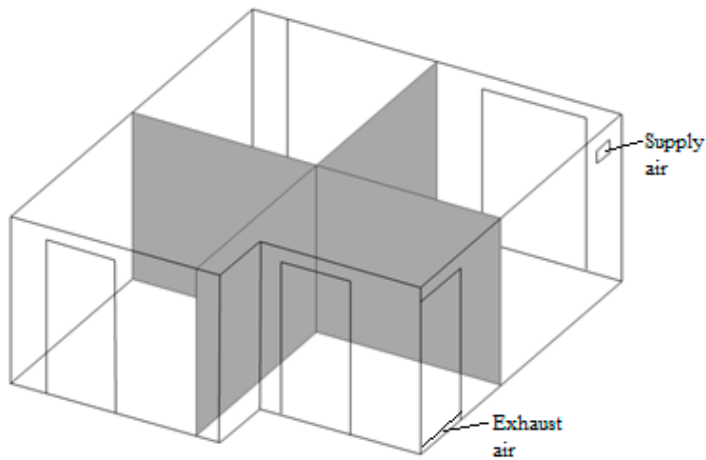


Figure 24. Position of two vertical planes in the middle of room for showing distribution of different quantities within the room

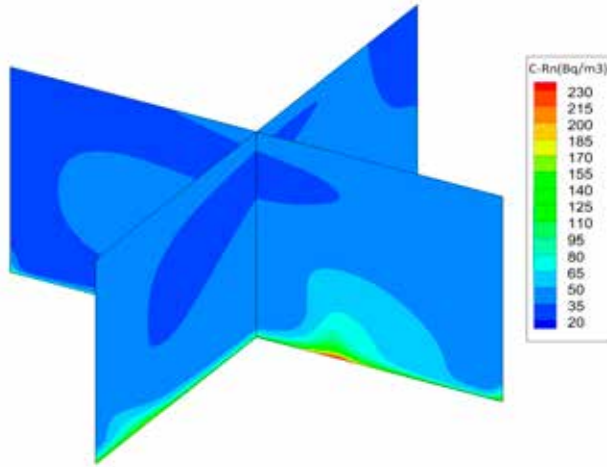


Figure 25. Contours of radon concentration (Bq m^{-3}) in two vertical planes in the middle of room for N3 ($\text{Ach}=0.5 \text{ hr}^{-1}$, $T=21 \text{ }^{\circ}\text{C}$, $\text{RH}=40\%$)

Figure 25 visualizes radon concentration in the room. It shows that radon is at a maximum at floor level and at a minimum near the air terminal device and ceiling. Due to its distance from the vent, the occupied zone has a relatively high radon concentration.

Figure 26 shows contours of air velocity in the room. Air velocity is highest near the supply air terminal device. These areas have better air mixing and therefore lower radon concentration.

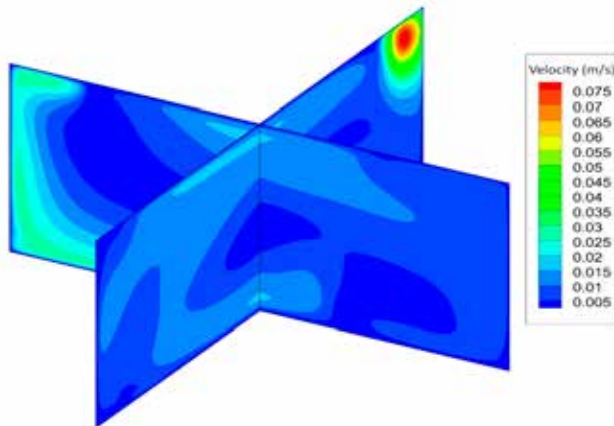


Figure 26. Contours of air velocity (ms^{-1}) in two vertical planes in the middle of room for N3 ($\text{Ach} = 0.5 \text{ hr}^{-1}$, $T = 21 \text{ }^{\circ}\text{C}$, $\text{RH} = 40\%$)

Figure 27 shows radon concentration with 0.25 Ach. Comparison with Figure 25 shows that the maximum level is nearly doubled with the lower ventilation rate.

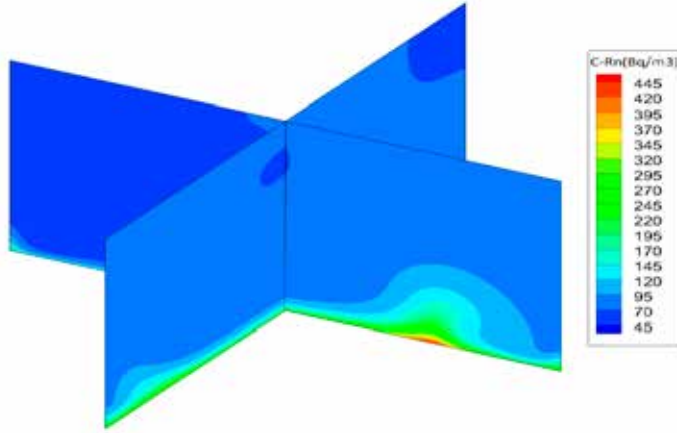


Figure 27. Contours of radon concentration (Bq m^{-3}) in two vertical planes in the middle of room for N12 ($\text{Ach} = 0.25 \text{ hr}^{-1}$, $T = 21^\circ\text{C}$, $\text{RH} = 40\%$)

Figure 28 shows that air velocity is stagnated in most parts of the room with the lower ventilation rate, including in the occupied zone.

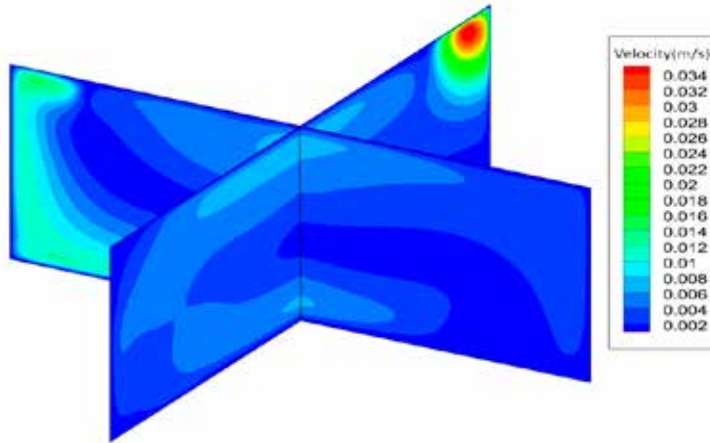


Figure 28. Contours of air velocity (ms^{-1}) in two vertical planes in the middle of room for N12 ($\text{Ach} = 0.25 \text{ hr}^{-1}$, $T = 21^\circ\text{C}$, $\text{RH} = 40\%$)

5.4.2 Temperature Changes Effects on Indoor Radon Concentration

Five cases have been considered in order to investigate the effects of temperature changes on indoor radon content. In these cases, ventilation rate and relative humidity have been fixed at 0.5 hr^{-1} and 40 % respectively. Temperature is varied from 15 °C to 25 °C. These cases correspond to N1, N2, N3, N4 and N5 in Table 9. The model has been solved for these cases as described in previous sections and the results are shown in Table 21 and plotted in Figure 30.

Table 21. Average radon concentration in the room for different temperatures at Ach=0.5 hr⁻¹ and RH=40%

| Case No. | Temperature (°C) | Average radon concentration (Bqm ⁻³) |
|----------|------------------|--|
| N1 | 15 | 32.84 |
| N2 | 18 | 36.04 |
| N3 | 21 | 38.29 |
| N4 | 23 | 39.22 |
| N5 | 25 | 40.20 |

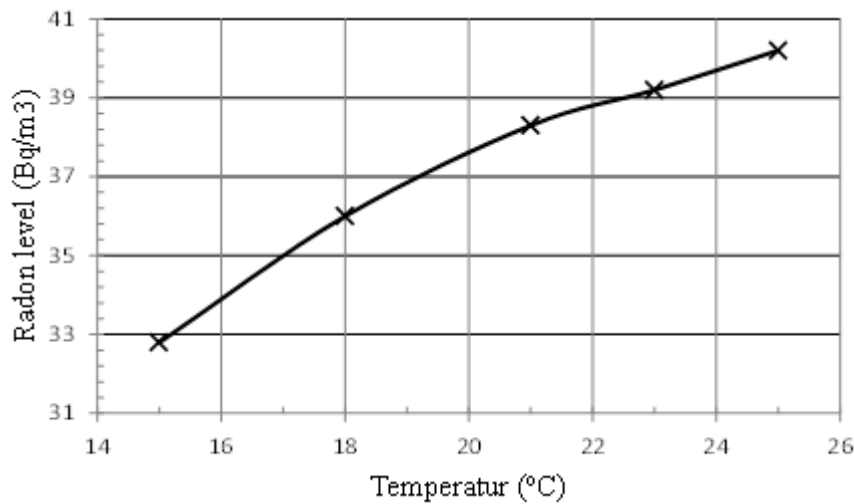


Figure 29. Average radon concentration in the room for different temperatures at Ach = 0.5 hr⁻¹ and RH = 40%

This behavior may be due to the increase in diffusion coefficient with increasing temperature (as discussed in Paper III) and the resulting increase in movement of air molecules. However the effect is not very strong.

The effect of temperature on radon concentration along a vertical line in the middle of the room is shown in Figure 31. These results show that increasing temperature does not affect the indoor radon distribution, and the radon concentration profile has the same shape at all temperatures in the tested range for specific values of ventilation rate and relative humidity. Increasing temperature increases radon concentration and shifts the radon concentration profile upwards.

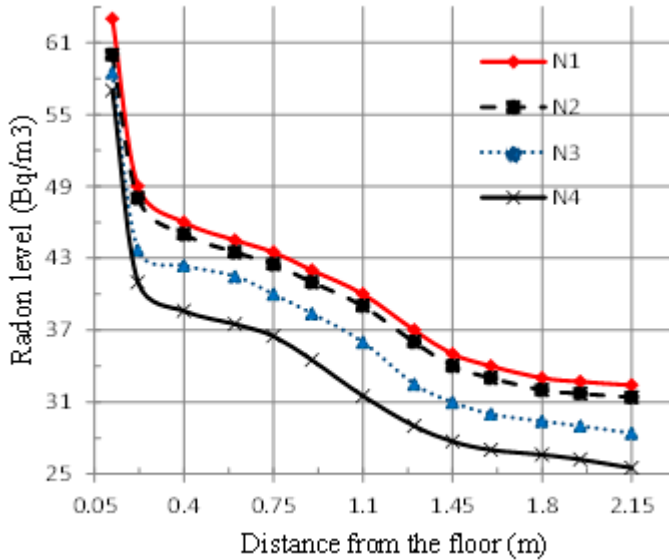


Figure 30. Radon concentration along a vertical line in the middle of room for different temperatures (15 to 23°C) at $Ach = 0.5 \text{ hr}^{-1}$ and $RH = 40\%$

Contours of radon concentration are plotted in Figures 31 and 32. Changes of radon level and its distribution can be seen by comparing these figures, taking into account the changes shown in Figure 29.

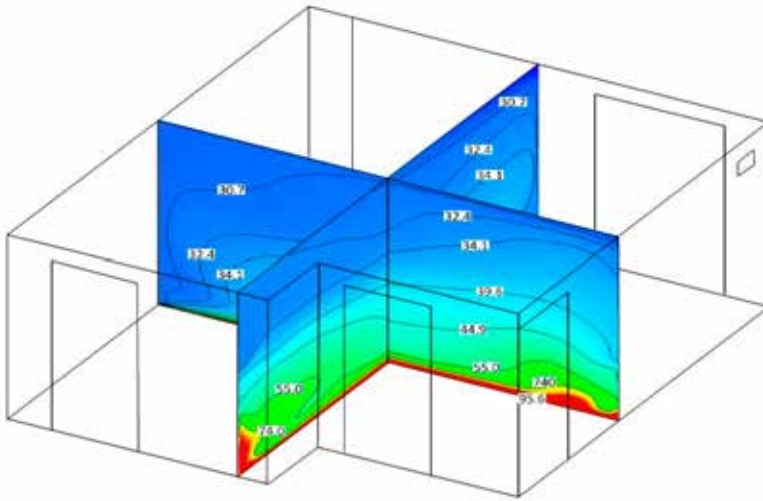


Figure 31. Contours of radon concentration (Bqm^{-3}) in two vertical planes in the middle of room for N3 ($\text{Ach} = 0.5 \text{ hr}^{-1}$, $T = 21 \text{ }^{\circ}\text{C}$, $\text{RH} = 40\%$)

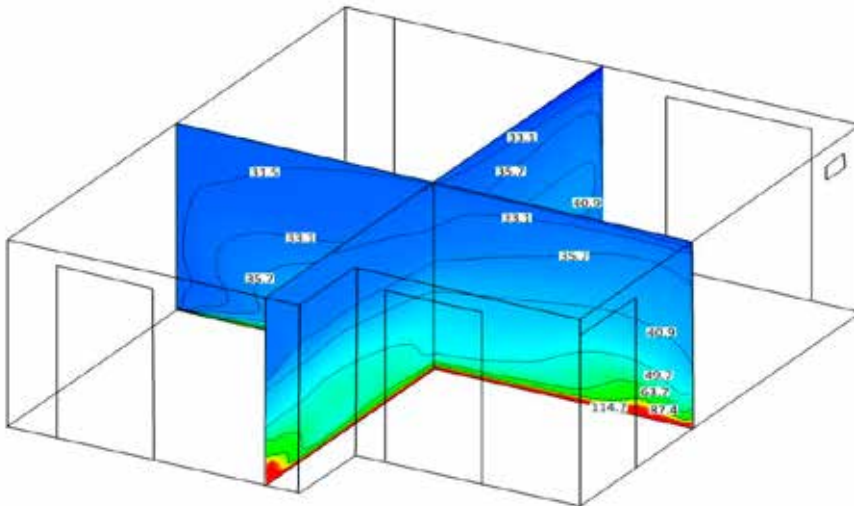


Figure 32. Contours of radon concentration (Bqm^{-3}) in two vertical planes in the middle of room for N4 ($\text{Ach} = 0.5 \text{ hr}^{-1}$, $T = 23 \text{ }^{\circ}\text{C}$, $\text{RH} = 40\%$)

5.4.3 Effects of Relative Humidity Changes on Indoor Radon Concentration

In order to investigate the effects of relative humidity changes on indoor radon concentration, six cases have been considered: N6, N4, N7, N8, N9 and N10, as listed in Table 9. Ventilation rate and temperature are fixed at 0.5 hr^{-1} and $21 \text{ }^{\circ}\text{C}$ respectively. Relative humidity is varied between 30 % and 80%. The model is solved for these cases as described in previous sections and the results are shown in Table 22.

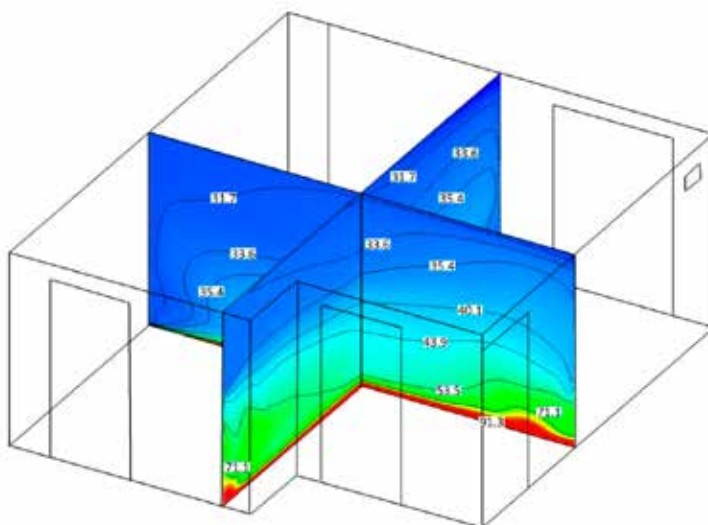
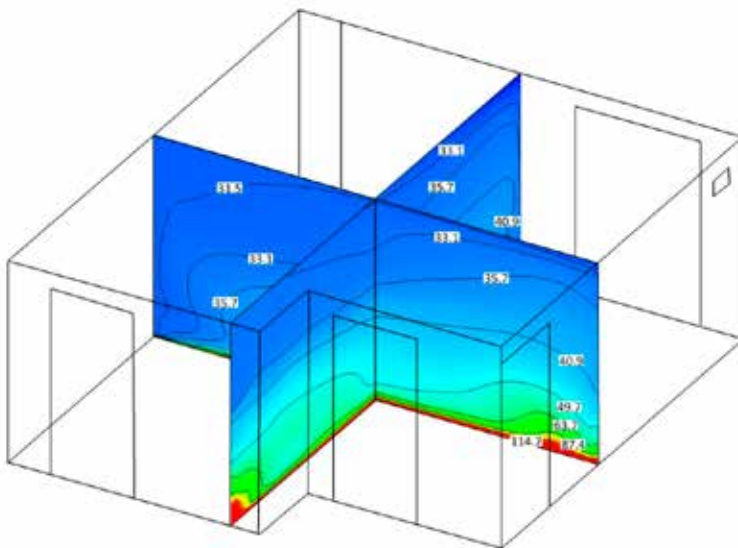
Table 22. Average radon concentration for different relative humidity at $Ach = 0.5 \text{ hr}^{-1}$ and $T = 21 \text{ }^{\circ}\text{C}$

| Case No. | Relative humidity (%) | Average radon concentration (Bqm^{-3}) |
|----------|-----------------------|---|
| N6 | 30 | 39.17 |
| N4 | 40 | 39.22 |
| N7 | 50 | 39.25 |
| N8 | 60 | 39.08 |
| N9 | 70 | 39.82 |
| N10 | 80 | 39.07 |

Table 22 shows that relative humidity does not have a large effect on average indoor radon concentration. The negligible differences observed are due to numerical approximations and rounding.

This simulation is more accurate than the previous simulation presented for $Ach = 0.25 \text{ hr}^{-1}$ and $T = 18 \text{ }^{\circ}\text{C}$ in Paper III because of the increase in mesh size (number of cells).

Contours of radon concentration at different relative humidity are plotted in Figures 33 and 34. These figures indicate that relative humidity changes between 30 % and 80 % have considerable impacts on indoor distribution. Even though the overall average radon level does not change with RH, these figures indicate that a change in relative humidity from 40% to 50% has an effect on indoor radon distribution, i.e. humidity variations can affect radon distribution in the occupied zone.



5.5 Model validation and result comparison

Model validation is performed by inter-model validation (Paper II) and comparison with analytical solutions and measurements.

In a ventilated room, the radon diffusion coefficient is disregarded and radon concentration in a chamber (room) with volume V is described as per Equations (3.3) to (3.5).

In this study, the average radon concentration in Room 1 is calculated for the four considered air change rates using the analytical solution. For instance, at 0.5 Ach Equation (3.4) gives:

$$C_{0.5 \text{ hr}^{-1}} = \frac{0.018 \frac{\text{Bq}}{\text{m}^2 \text{s}}}{2.4 \text{ m} \times 0.5 \frac{1}{\text{hr}} \times \frac{1 \text{ hr}}{3600 \text{ s}}} = 54 \frac{\text{Bq}}{\text{m}^3}$$

Table 23 shows a comparison of average concentrations in Room 1 at different air change rates using measurements, analytical calculation and numerical simulation techniques. The measurement data are not sufficiently accurate for these comparisons, because the measuring time was too short to obtain an acceptable average radon level and the measurement devices have at least 10 percent uncertainty.

For quantitative comparisons, the percentage difference between the FLUENT estimation results and the analytical calculations was computed at each ventilation rate. The maximum difference was found to be less than 10%.

In spite of the errors in each technique, such as the 10 % uncertainty in the measurements by the CRM, the results show good agreement, thus verifying the model.

Table 23. Indoor radon levels obtained by different methods

| Ventilation rate (hr ⁻¹) | Measurement (Bqm ⁻³) | Analytic (Bqm ⁻³) | Numeric (Bqm ⁻³) |
|--------------------------------------|----------------------------------|-------------------------------|------------------------------|
| 1.0 | 25±2 | 22 | 20.57 |
| 0.5 | 45±4 | 54 | 40.06 |
| 0.25 | 97±10 | 108 | 82.08 |
| 0.05 | 3,580±380 | 3,378 | 2,828.55 |

Measurements and numerical methods were both used to examine radon variation with height (Figures 19 and 22). These results can also be used to validate the CFD model.

Table 24 shows indoor radon at different heights for both methods. Comparing the results shows good agreement between them, with a maximum difference of 7%.

Table 24. Indoor radon for different heights above the floor

| H(m) | Measurement (Bqm⁻³) | Numeric (Bqm⁻³) |
|-------------|---|---------------------------------------|
| 0.04 | 74 | 69 |
| 0.5 | 39 | 37 |
| 0.9 | 34 | 36 |
| 2.0 | 30 | 34 |

6 Conclusions and future work

This thesis describes an investigation of two important topics. The first topic considers the effect of heat energy recovery ventilation systems on radon distribution and energy savings. The second topic includes quantifying the influence of indoor air conditions and ventilation parameters on radon concentration by means of numerical methods.

Based on the main objective of this study, it is concluded that a heat recovery ventilation system can influence indoor radon level by controlling air ventilation rate, the pressure difference between indoors and outdoors, indoor temperature and relative humidity. In response to the research question, most of the investigated factors affect indoor radon concentration and distribution and there is a strong correlation between these factors and indoor radon distribution. It is worth noting that indoor radon level can be influenced by concurrent outdoor conditions such as wind, rainfall, pressure and geological conditions as well as the examined indoor factors. For this reason CFD is a useful and applicable tool for investigating these factors individually, and in this study it is used as a standalone and available tool to simulate and predict radon level and distribution in residential buildings. The conclusions of this study are described below.

6.1 Dynamic simulation and heat recovery analysis

The first set of conclusions considers the use of a balanced HRV system and its effect on IAQ with respect to radon concentration. Providing a balance between supply air and exhaust air and maintaining indoor air temperature and relative humidity by means of a HRV unit helps to control indoor radon. The dynamic simulations and theoretical analysis carried out here confirms that the use of a heat exchanger enhances the energy performance of a residential ventilation system.

From an IAQ point of view, increased ventilation is one possible action to mitigate high radon levels. HRV systems can recover energy that would otherwise be lost through increased ventilation and reduce investment pay-back time. Nevertheless, increased ventilation is not recommended as the primary cost-effective mitigation measure, but rather as a complementary

one. Remediation actions such as floor sealing and creation of a radon sump deliver superior performance, as shown in the main body of this thesis.

6.2 Numerical Simulation

Numerical simulation is a valuable, powerful and inexpensive tool for assessing the behavior of harmful contaminants like radon, and for predicting indoor air flow at low cost and relatively quickly in comparison with other methods such as gas tracer and full-scale laboratory methods.

Three dimensional models developed in FLUENT were used to simulate radon entry and exit in a one-family house. The verification of the model and its performance reinforce the idea that radon transport in the house and ventilation effects have been well defined physically and numerically. The performance and sensitivity of the model were confirmed by varying some of the internal and boundary conditions. The results indicate that the considered conditions and assumptions provide a reliable illustration of the actual conditions. This model is therefore likely to be useful and applicable for other similar indoor radon problems with a similar range of conditions.

This study demonstrates that indoor radon level and distribution can generally be affected by indoor air conditions such as temperature, relative humidity, ventilation rate and location. The impacts of these parameters on indoor radon level and distribution are summarized in Table 25.

Table 25. The impacts of parameters on indoor radon level and distribution

| Parameters | Indoor radon level | Indoor radon distribution |
|-------------------------------------|--|--|
| Ventilation rate | High impact, the more ventilation rate the lower the radon level | High impact |
| Supply air terminal device location | High impact, the closer to vent the lower the radon level | High impact |
| Room height | High impact, the closer to the floor, the higher the radon level | High impact |
| Indoor temperature | Low impact, with direct correlation | Low impact, considerable for occupied zone |
| Indoor relative humidity | No impact | Low impact, considerable for occupied zone |

Overall, the results indicate that indoor radon concentrations and dispersion are dependent on radon production rate, ventilation specifications and indoor temperature and humidity conditions. In addition, height above the floor, air infiltration through the main door and windows as well as location of the supply air terminal devices all impact indoor radon level.

Locating supply air terminal devices near the occupied zone in a new building could be a good means of controlling radon level.

Numerical results show that outdoor ventilation rate is the most influential, indoor temperature is less influential and humidity is the least influential factor on indoor radon.

It should be emphasized that this work represents the first step in the field with regard to using CFD to study the sensitivity of indoor radon level and its distribution in small residential buildings. It is hoped that the present study will serve as a stepping stone for further work in the field by other researchers.

6.3 Future work

This thesis focuses on the study of ventilation effects of indoor temperature and humidity on indoor radon mitigation in a residential building, with emphases on IAQ and energy saving approaches. The work could be extended in the future with more detailed three dimensional modeling of the building, which may increase the accuracy of the results.

Some further suggestions for future work include:

1. Modeling of novel energy recovery ventilation systems.
2. External coupling between CFD and BES (Building Energy Simulation) software is likely to be a suitable approach for improving both the simulation results and the calculation of energy balance.
3. Considering outdoor air conditions such as pressure, temperature, and precipitation on indoor radon.
4. Consideration of air leakage from the building, internal heat sources, furniture and residents in models of indoor radon.
5. Investigation of the effectiveness of alternative supply air locations from a radon mitigation viewpoint.
6. Further comprehensive and systematic radon measurements in residential buildings including tight control (where possible) of all factors that affect the measurement results. Such measurements are paramount for validating detailed CFD simulations and confirming new engineering findings.
7. There is a strong demand for comprehensive and systematic radon measurements in buildings including detailed control of all factors regarding the building, etc. that also represent important input data for cal-

culations. CFD with its many possibilities can be useful for finding the best and most economical measure against radon in specific cases, i.e. optimization. However, there is a fundamental limitation when the calculation results cannot be compared with, and thus confirmed by detailed measurement results.

8. Derivation of simplified/analytical correlations or models for indoor temperature and relative humidity using CFD results.

References

- Abd Alnasser Almate, A. A. (2014). Use of Computational Fluid Dynamics. *American Journal of Engineering and Applied Sciences*, 7, pp. 171–184.
- Akander, J., Alvarez, S., & Johannesson, G. (2005). *Energy Normalization Techniques in Energy Performance of residential buildings: a practical guide for energy rating and efficiency*. London ; Sterling, VA : Earthscan.
- Anderson, C. E. (2001). Numerical modeling of radon-222 entry into houses: an outline of techniques and results. *The science of total environment*, 272, pp. 33–42.
- ANSYS Inc. (2011). *ANSYS FLUENT 14.0 Theory Guide*. Canonsburg: ANSYS Inc.
- ASHRAE. (2001). *Ventilation for Acceptable Indoor Air Quality*. Atlanta: ASHRAE.
- Bakker, A. (2010). *Computational Fluid Dynamics*. Retrieved 25.2.2012, from Bakker: www.bakker.org/dartmouth06/engs150/05-solv.pdf
- Chauhan, N., Joshi, M., & Agarwal, T. (2014). Study of indoor radon distribution using measurements and CFD modeling. *Journal of Environmental Radioactivity*, 136, pp. 105–111.
- Clavensjö, B., & Åkerblom, G. (1994). *The Radon Book*. Stockholm: The Swedish Council for Building Research.
- Cozmuta, I., Van der Graff, E., & de Meiter, R. (2003). Moisture dependence of radon transport in concrete: Measurements and modeling. *Health Physics*, 85 (4), pp. 438–56.
- Cussler, E. (1997). *Diffusion: Mass Transfer in Fluid System*. New York: Cambridge University Press.
- Dainius, J., & Aloyzas, K. (2007). Hourly Measurement Method For Radon Progeny. *Journal of Environmental Engineering*, 15 (3), pp. 158–165.
- Dubois, G. (2005). *An overview of radon survey in Europe*. Luxembourg: European Communitis. Retrieved 10.4.2013, from <http://www.academia.edu>
- EPA. (2008). *citizensguide*. Retrieved 28.6.2011, from [epa: www.epa.gov/radon/pdfs/citizensguide.pdf](http://www.epa.gov/radon/pdfs/citizensguide.pdf)
- Flexit. (2009). *products/air-handling-units/*. Retrieved 5.7.2013, from Flexit: <http://www.flexit.no/en/products/air-handling-units/Old-models/>
- Fournier, F., Groetz, J., & Jacob, F. (2005). Simulation of Radon Transport through Building Materials. *Trans Porous Med* (59), pp. 197–214.
- Gerasimov, A. (2006). *Modeling Turbulent Flows with FLUENT*. London: Europe, ANSYS Inc.
- Handel, C. (2011). Ventilation with heat recovery is a necessity in “nearly zero” energy buildings. *REHVA European HVAC Journal*(3), pp. 18–22.
- Hjelte, I., Ronquist, B., & Ronqvist, T. (2010). *The radon situation in Swedish dwellings based on recent measurements*. Helsinki: European IRPA Congress.
- Jokisalo, J., Kurnitska, J., & Torkki, A. (2003). Performance of balanced ventilation with heat recovery in residential buildings in cold climate. *International Journal of Ventilation*, 2, pp. 223–236.

- Keith S, D. J. (2012). *Toxicological Profile for Radon*. Atlanta (GA): Agency for Toxic Substances and Disease Registry (US).
- Keskikuru, T., Kokkoti, H., Lammi, S., & Kalliokoski, P. (2001). Effect of various factors on the rate of radon entry into two different types of houses. *Building and Environment*, 36 (10), pp. 1091–1098.
- Kumar, A., Chauhan, R., & Sahoo, B. (2014). Modeling of indoor radon concentration from radon exhalation rates of building materials and validation through measurements. *Journal of Environmental Radioactivity*, 127, pp. 50–55.
- Langtry, R. G. (2006). Predicting 2D airfoil and 3D wind turbine rotor performance using a transition model for general CFD codes. *44th AIAA Aerospace Sciences Meeting and Exhibit*. Reno: AIAA.
- Laverge, J., & Janssens, A. (2012). Heat recovery ventilation operation traded off against natural and simple exhaust ventilation in Europe by primary energy factor. *Energy and Buildings*, (50), pp. 315–323.
- Lazzarin, R. M., & Gasparella, A. (1998). Thechnical and economical analysis of heat recovery in building ventilation systems. *Applied thermal engineering*, 18, pp. 47–67.
- Lide, D. (2004). *CRC Handbook of chemistry and physics*. Florida: CRC press.
- Loureiro, C. (1987). *Simulation of the steady-state transport of radon from soil into houses with basement under constant negative pressure*. Berkeley, CA.: Lawrence Berkeley Laboratory.
- Malanca, A., Cassoni, F., Dallara, G., & Pessina, V. (1992). Radon in dwellings: the importance of ventilation. *AEROBIOLOGIA*, 8, pp. 57–61.
- Marley, F., & Paul, S. (2001). Investigation of the potential for radon mitigation by operation of mechanical systems affecting indoor air. *Environmental Radioactivity*, 54, pp. 205–219.
- Menter, F. R. (2006). Transition Modelling for General Purpose CFD Codes. *Flow, Turbulence and Combustion*, 77,1, pp. 277–303.
- Milner, J., Dimitroulopoulou, C., & ApSimon, H. (2004). *Indoor concentrations in buildings from sources*. London: UK Atmospheric Dispersion Modelling Liaison Committee.
- Motaman, S. (2013). High-speed imaging and computational modelling of close-coupled gas atomization. *Journal of Computers & Fluids*, 88, pp. 1-10. Retrieved 9.8.2014, from <http://etheses.whiterose.ac.uk/6430/>
- Mourshed, M. (2012). Relationship between annual mean temperature and degree-days. *Energy and Buildings*, 45, pp. 418–425.
- Narula, A. K., Saini, R., Goyal, S. K., & Chauhan, R. P. (2009). Indoor Radiation Levels Enhanced by Underground Radon Diffusion. *Asian Journal of Chemistry*, 21 (10), pp. 275–278.
- Nilsson, P. E. (2006). *Achieving the desired indoor climate*. Lund: Commtech Group.
- Oman, R. (2011). *Energy and Buildings*. Vasteras: Malardalen University.
- Petropoulos, N. P., & Simopoulos, S. E. (2001). Building materials radon exhalation rate. *The Science of the Total Environment*, 272, pp. 109–118.
- Radiological Protection Institute of Ireland. (2010). *RPII*. Retrieved 12.7.2012, from www.epa.ie/pubs/reports/radiation/RPII_Guide_Radon_Remediation_Householders.pdf
- Radonelektronik. (2009, 4 7). *programvara*. Retrieved 2 12, 2010, from Radonelektronik: <http://www.radonelektronik.se/programvara.htm>
- Revzan, K. (2008). *Modeling Radon Entry into Houses with Basements: Model Description and Verification*. Lawrence Berkeley: Lawrence Berkeley National Laboratory, LBNL .

- Shao, J. L. (2010). Field Measurement of the Convective Heat Transfer Coefficient on Vertical External Building Surfaces Using Naphthalene Sublimation Method. *Journal of Building Physics*, 33 (4), pp. 307–326.
- Sonntag, D. (1990). *Important new values of physical constants of 1986, vapour pressure formulations based on the ITS-90 and PsychrometerFormulae*. Viena: Zeitschrift für Meteorologie.
- Spoel, W. V. (1998). *Radon transport in sand: A laboratory study*. Eindhoven, Netherland: Eindhoven University of technology.
- Sundal, A., Henriksen, H., Lauritzen, S., & Soldal, O. (2004). Geological and geochemical factors affecting radon concentrations in dwellings located on permeable glacial sediments — a case study from Kinsarvik, Norway. *Environ Geol*, 45, pp. 843–858.
- Swedish Energy Agency. (2010, 1 31). *Energy in Sweden*. Retrieved 4 10, 2013, from www.energymyndigheten.se.
- Wang, F., & Ward, I. C. (2000). The development of a radon entry model for a house with a cellar. *Building and Environment*, 35, pp. 615–631.
- Wang, F.; Ward, I C. (2002). Radon entry, migration and reduction in houses with cellars. *Building and Environment*, 37, pp. 1153 – 1165.
- Versteeg, H., & Malalasekera, W. (2007). *An introduction to Computational Fluid Dynamics: The Finite Volume Method*. Glasgow: Pearson.
- White, F. M. (2011). *Fluid Mechanics*. New York: McGraw-Hill.
- WHO. (2009). *WHO handbook on indoor radon: a public health perspective*. Geneva: WHO. Retrieved from <http://www.who.int/mediacentre/factsheets/fs291/en/index.html>.
- William, L. R. (1990). *Toxicological profile for radon*. New York: U.S. Public Health Service, in collaboration with U.S. Environmental Protection Agency. Retrieved 12.4.2010, from <http://www.bvsde.paho.org/bvstox/i/fulltext/toxprofiles/radon.pdf>
- Wunderground. (2010). *MonthlyHistory*. Retrieved 30.6.2014, from [wunderground: http://www.wunderground.com/history/airport/ESSA/2010/12/1/MonthlyHistory.html](http://www.wunderground.com/history/airport/ESSA/2010/12/1/MonthlyHistory.html)
- Zhang, F., & Cooke, P. (2010). *Green-building-review*. Retrieved 27.3. 2013, from Dime: <http://www.dime-eu.org/files/active/0/Cooke-2010-Fang-Green-building-review.pdf>
- Zhang, Y. (2004). *Indoor air quality engineering*. Illinois, Urbana: CRC press.
- Zhuo, W., Iida, T., Moriizum, J., & Takahashi, I. (2001). Simulation of the concentrations and distributions of indoor radon and thoron. *Radiation Protection Dosimetry*, 93 (4), pp. 357–368 .

Appendices

Appendix A: IDA, Boundary conditions and input data

This appendix shows the results of dynamic simulation carried out by IDA Indoor Climate and Energy software program.

Table A1 shows project data and case study house specifications.

IDA Indoor Climate and Energy Version: 4.51 License:
IDA40:ED152/R4N4Q (educational license)


| | | | |
|---|---|--|---------------------------------------|
|  | | Energy report for "Air Handling Unit" | |
| Project | | Building | |
| | | Model floor area | 108.0 m ² |
| Customer | H. Afshar | Model volume | 259.3 m ³ |
| Created by | K. Akbari | Model ground area | 0.0 m ² |
| Location | Stockholm/Bromma | Model envelope area | 208.8 m ² |
| Climate file | Stockholm, Bromma-1977 | Window/Envelope | 2.6 % |
| Case | 0.5 ach hex unit SL4, 0.74 etta supply air 16degree | Average U-value | 0.4071 W/(K·m ²) |
| Simulated | 8/3/2014 23:28:14 | Envelope area per Volume | 0.8055 m ² /m ³ |

Table A1. Project data and case study house specifications.

Table A2 shows data base of climate data which is used for energy simulation and calculation.

Climate file

| | Dry-bulb temperature, Deg-C | Rel humidity of air, % | Direction of wind, Deg | Speed of meteorological wind, m/s |
|---------------|-----------------------------|------------------------|------------------------|-----------------------------------|
| January | -2.0 | 88.4 | 163.4 | 3.3 |
| February | -4.7 | 83.8 | 177.9 | 3.1 |
| March | 0.9 | 76.1 | 181.2 | 3.5 |
| April | 2.7 | 73.5 | 181.8 | 3.7 |
| May | 10.3 | 64.5 | 151.8 | 3.5 |
| June | 15.5 | 64.3 | 154.0 | 3.2 |
| July | 14.8 | 76.4 | 174.4 | 3.2 |
| August | 15.2 | 74.5 | 149.1 | 2.4 |
| September | 9.7 | 74.5 | 210.2 | 3.3 |
| October | 7.7 | 83.9 | 198.5 | 3.3 |
| November | 3.6 | 87.4 | 204.5 | 3.8 |
| December | -0.1 | 86.0 | 192.8 | 4.0 |
| mean | 6.2 | 77.8 | 178.2 | 3.3 |
| mean*8760.0 h | 54291.5 | 681313.2 | 1561105.0 | 29345.5 |
| min | -4.7 | 64.3 | 149.1 | 2.4 |
| max | 15.5 | 88.4 | 210.2 | 4.0 |

Table A2. Climate data in IDA data base

The geometry of the case study house is as follows.

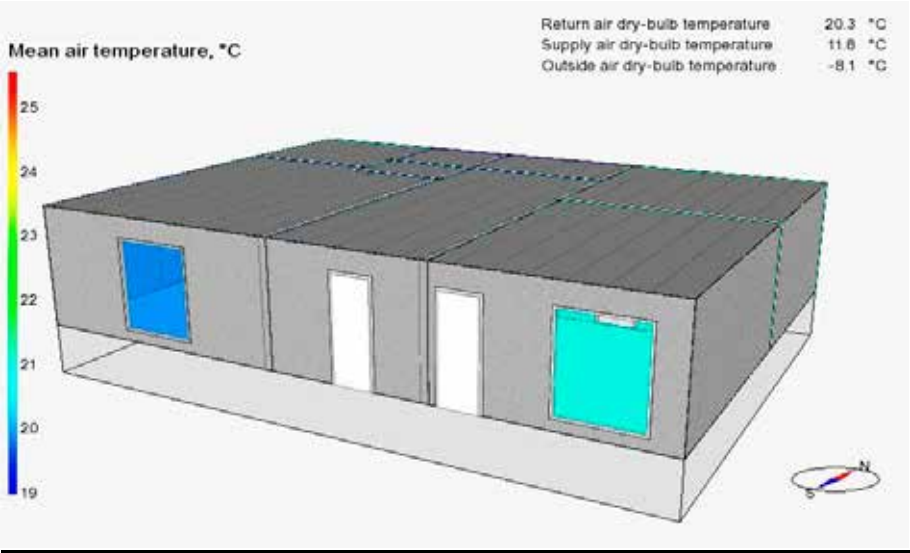


Figure A1: Building geometry

Air handling unit (AHU) temperature for the year 2010 is as follows.

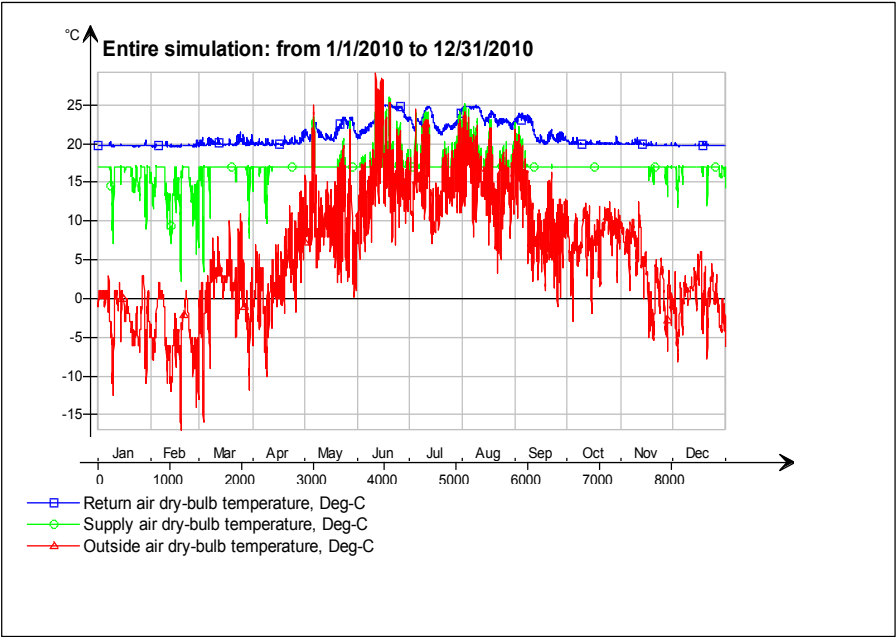


Figure A2. Air handling unit temperature

Energy report for "Air Handling Unit" including heat recovery and fans energy use at 0.5 Ach is as follows.

kWh (sensible and latent)

| Month | Heating | Cooling | AHU heat re-covery | AHU cold re-covery | Humidi-fication | Fans |
|-------|-------------|-------------|--------------------|--------------------|-----------------|-------------|
| | <div></div> | <div></div> | <div></div> | <div></div> | <div></div> | <div></div> |
| Total | 0.0 | 0.0 | 3380.6 | 22.7 | 0.0 | 613.5 |

Table A3. Energy report for "Air Handling Unit"

Appendix B: Radon Transport Equations and Indoor Conditions

1. Radon transport equation in the soil (when diffusion mechanism is dominant)

In a one dimensional problem under certain conditions, such as in the area infinitely distant from the pressure disturbance, the radon transport equation, Equation 4.5, has an analytical solution for diffusion term. Using z as a spatial variable ($0 \leq z \leq \infty$) and $V = 0$, this equation is reduced to:

$$D \frac{d^2 C}{dz^2} - \lambda_{Rn} C + G = 0 \quad (B1)$$

This boundary condition is known as the infinite distant boundary. The results of the differential equation solution can be compared with the solution using the numerical results at this boundary to assess the validity of the model.

To solve this equation, assuming that $X = G - \lambda_{Rn} C$, gives the following equation:

$$D \frac{d^2 X}{dz^2} - \frac{\lambda_{Rn}}{D} X = 0 \quad (B2)$$

Therefore the solution of this differential equation is:

$$X = \alpha_1 \exp\left(\sqrt{\frac{\lambda_{Rn}}{D}} z\right) + \alpha_2 \exp\left(-\sqrt{\frac{\lambda_{Rn}}{D}} z\right),$$

$$\text{and } C(z) = \frac{\alpha_1}{\lambda_{Rn}} \exp\left(\sqrt{\frac{\lambda_{Rn}}{D}} z\right) + \frac{\alpha_2}{\lambda_{Rn}} \exp\left(-\sqrt{\frac{\lambda_{Rn}}{D}} z\right) + \frac{G}{\lambda_{Rn}} \quad (B3)$$

To solve this differential equation, considering boundary condition (at $z = 0$ and $z = \infty$) results:

$$C(z) = \frac{G}{\lambda_{Rn}} (1 - \exp\left(-\sqrt{\frac{\lambda_{Rn}}{D}} z\right)) \quad (B4)$$

where

$$C(0) = 0 \text{ and } C(\infty) = \frac{G}{\lambda_{Rn}} = C_{\text{maximum}}.$$

Radon generation rate (G) is a function of radium activity (A_{Ra}), soil porosity (ϵ), soil density (ρ) and emanation factor (f) which is expressed as follows:

$$G = A_{Ra} \rho f \frac{1-\epsilon}{\epsilon} \quad (B5)$$

This solution shows that if the pressure disturbance is zero, the radon concentration along the boundary depends only on the diffusion coefficient and the radon decay constant.

2. Diffusion length

One of the variables in radon transport is radon diffusion length, which depends on soil and materials structure.

For a one dimensional problem, using z as the spatial variable ($0 \leq z \leq \infty$), radon diffusion length can be derived from Equation B4:

$$C(z) = \frac{G}{\lambda_{Rn}} \left(1 - e^{\left(\frac{-z}{l}\right)} \right) \quad (B6)$$

$$l = \sqrt{D/\lambda_{Rn}} \quad (B7)$$

where l is radon diffusion length (m), D is radon diffusion coefficient (m^2s^{-1}) and λ_{Rn} is radon decay constant ($2.1 \times 10^{-6}\text{s}^{-1}$). The diffusion length is defined as the characteristic distance travelled by radon atoms during one half life.

Papers

Paper I



MEQ
24,5

682

Impacts of heat recovery ventilators on energy savings and indoor radon level

Keramatollah Akbari

*School of Sustainable Development of Society and Technology,
Mälardalen University, Västerås,
Sweden and Technology Development Institute, ACECR, Tehran, Iran, and*

Robert Oman

*Sustainable Development of Society and Technology,
Mälardalen University, Västerås, Sweden*

Abstract

Purpose – This paper aims to investigate the impact of heat recovery ventilators (HRVs) on the energy use and indoor radon in a one family detached house. Heat recovery ventilation systems, because of reducing ventilation loss through recovered exhaust air, can play a good role in the effectiveness of ventilation to reduce energy use. In addition HRVs can maintain pressure balance and outdoor ventilation rate at a required level to mitigate indoor radon level.

Design/methodology/approach – In this study, a multizone model of a detached house is developed in IDA Indoor Climate and Energy (IDA ICE 4.0). The model is validated using measurements regarding use of energy for heating, ventilation and whole energy use. The performance of the heat recovery ventilation system is examined with respect to radon mitigation and energy saving by measuring the radon concentration and analyzing the life cycle cost of a heat exchanger unit.

Findings – The results of the measurements and dynamic simulation showed that the heat recovery ventilation system could lead to 74 per cent energy savings of the ventilation loss, amounting to about 30 kWh m⁻² per year. Life cycle cost analysis used for assessing total costs and the result showed that using this system is quite cost-effective and investment would payback during 12 years.

Research limitations/implications – Limitations of this study generally refer to radon measurement and simulation because of radon complex behavior and its high fluctuations even during short periods of time.

Practical implications – Heat recovery ventilation systems with reducing radon concentration improve indoor air quality and decrease environmental problems with energy savings.

Social implications – Using balanced heat recovery ventilation can have benefits from the viewpoint of environmental impacts and household economy.

Originality/value – Employment of a heat recovery unit to control indoor radon level is a new usage of this technology which along with energy savings can improve sustainable development.

Keywords Heat recovery, Ventilation, Energy saving, Radon, Indoor Climate and Energy (IDA 4.0)

Paper type Case study



Nomenclature

| | |
|-----------|---|
| A_0 | initial investment |
| B_0 | all savings in net present value method |
| B | annual savings in monetary unit |
| c_p | heat capacity (KJ kg ⁻¹ °C ⁻¹) |
| E_{Hex} | ventilation loss with heat exchanger |
| E_{rec} | recovered energy (kWh) |
| E_v | ventilation loss (kWh) |
| G_t | heat degree hours |

| | |
|--------------------|---|
| i | interest rate |
| M_{water} | water mass (kg) |
| \dot{m} | mass flow (kg s^{-1}) |
| n | time in year unit |
| Q_v | specific ventilation loss ($\text{W } ^\circ\text{C}^{-1}$) |
| q | annual energy cost escalation rate |
| t | temperature ($^\circ\text{C}$) |
| V | volume (m^3) |
| η | temperature efficiency |
| λ | radon decay rate (h^{-1}) |
| λ_v | ventilation rate (h^{-1}) |
| ρ | air density |

1. Introduction

Energy consumption in the building sector continues to grow steadily, and makes up around 40 percent of total energy consumption in many countries (Kåberger *et al.*, 2009). Therefore measures of reduction building energy use are a major concern.

In 2007, Swedish Energy Agency reported that electricity use between households, varying from 2000 to 7000 kWh per year for a detached house, and about 61 percent of energy use in this sector is used for space heating and domestic hot water (Kåberger *et al.*, 2009; Swedish Energy Agency, 2009). In Sweden, heat recovery from exhaust ventilation in existing buildings is an approach to reduce total energy use per heated area up to 20 percent below 1995 levels by 2020 (Ministry of Sustainable Development, 2006).

Energy in buildings is used to overcome the heat losses due to the ventilation, infiltration and transmission through the buildings envelope. The energy performance of buildings is significantly affected by ventilation and generally accounts for 30-60 percent of the buildings energy use (Awbi, 1998).

The prevalence of heat recovery ventilators (HRVs) systems in residential buildings in Sweden has increased over the last few decades. The increase in energy efficiency through heat recovery systems such as these contributes to a more sustainable society.

A heat recovery unit because of saving energy and reducing radon level has two different useful performances. The aim of this study is to show the effectiveness of HRV systems for reducing energy consumption and controlling indoor radon level due to balances between incoming and outgoing air streams.

Using HRV systems can help many of the more than 500,000 dwellings in Sweden which suffer from elevated radon concentrations in the range 200-800 Bq m⁻³, and the 1,000,000 dwellings that have radon concentrations of 100-200 Bq m⁻³ (Swedjmark and Mjones, 1987), which need increased ventilation to reduce indoor radon concentrations. Besides of energy use concerns in building sector, more than 30 percent of Swedish residents live in dwellings which have radon levels above safe level, i.e. 100 Bq m⁻³, which requires remedial actions (Zeeb and Shannoun, 2009).

Since large volumes of Swedish bedrock consist of uranium-rich granite and pegmatite, radon level is much higher than an action level (Swedjmark and Mjones, 1987). Radon gas decays into metal ions which produce α -particles. Breathing these particles are harmful for human body air ways and lead to lung cancer (Zeeb and Shannoun, 2009).

Several studies have compared various ventilation systems to show the advantages of heat recovery systems in cold climates (Jokisalo *et al.*, 2003). One of these studies

showed that energy efficiency could be improved by up to 67 percent compared to a traditional exhaust ventilation system by using a heat recovery system with a nominal temperature efficiency of 80 percent (Jokisalo *et al.*, 2003; Turiel *et al.*, 1983).

The best currently available system for reducing ventilation losses and controlling indoor radon is the recovery ventilator. A heat recovery unit with effectiveness at least 50 percent can save large amount of energy and it can be economically very advantageous (Lazzarin and Gasparella, 1998).

Comparison between an exhaust fan and a heat recovery ventilation system in a cold climate showed that a heat exchanger air-to-air ventilation system can save up to 2710 kWh per year compared to a traditional ventilation system and space heating (Hekmat *et al.*, 1986). This amounts to an increase in energy efficiency of around 30 percent in an insulated house. This is the best current technology for reducing radon levels (Hekmat *et al.*, 1986; Hubbard *et al.*, 1996).

2. Methodology

2.1 Materials and methods

The investigation was conducted in a single-family detached house, where radon levels were measured in conjunction with remedial changes to reduce these levels. A rotary heat exchanger unit and radon detectors were employed to measure heat recovery and radon level, respectively.

The radon measurement tools included a continuous radon monitor (CRM, R2) produced by Radonelektronik Company (Radonelektronik, 2009) which is an electronic device with 10 percent error and α -track detectors. Passive α -track detectors contain a plastic sheet of film onto which the α -particles produced from radon and radon progeny etch lines as they pass through the monitor. These etched lines are then analyzed in a laboratory and the radon concentration is quantified with 10 percent accuracy. The heat recovery unit (Flexit SL4 R) is an air handling unit with rotor technology produced by Flexit Company (FLEXIT, 2009) with 80 percent nominal efficiency.

IDA indoor climate and energy (ICE) was used as a multizone dynamic simulation tool to predict energy consumption, heat recovery of the rotary heat exchanger unit analysis, simulation of thermal comfort and indoor air quality in buildings. Research methods applied in this study include analytical analysis, measurement, dynamic simulation and life cycle cost analysis.

2.2 Case study description

The building selected for case study is a detached one family house in Stockholm built in 1975. This house is a two-storey structure with a volume of about 259 m³ on each level. This corresponds to a floor area of about 108 m², windows (W1, W2 and W3) area 8.8 m², main door (D1) area 3.3 m² and internal door(s) area 2.2 m². Some parts of this house was renovated and sealed in order to energy conservation and radon reduction. This house is situated on bedrock and major radon gas originates from the floor.

Total energy purchased were 25,860 and 22,920 kWh per year before and after using heat recovery ventilation system, respectively. Figure 1 shows the floor plan of this house.

3. The heat recovery ventilation system

A mechanical ventilation system with an air-to-air heat exchanger unit provides the air supply to the first floor. Figure 2 illustrates incoming and the outgoing air streams the installed heat exchanger system inside the first storey.

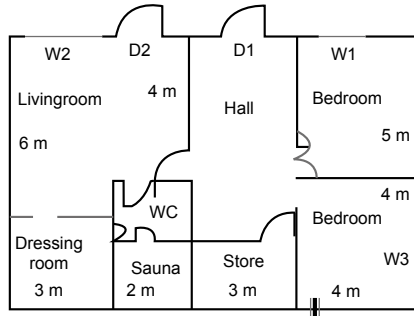


Figure 1.
Ground floor plan
and zone divisions of
the case study house

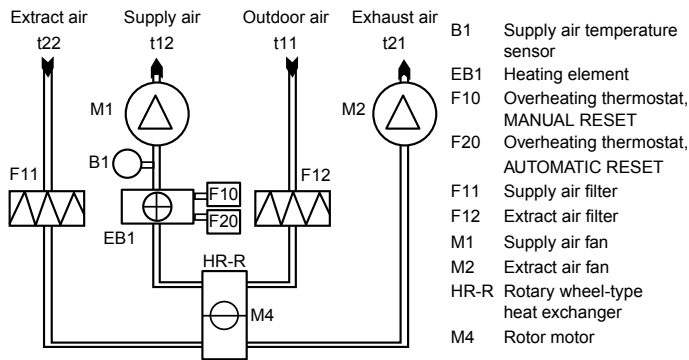


Figure 2.
Schematic diagram
of the rotary heat
exchanger installed
in the building

Source: Taken from FLEXIT Company

The operating points of the unit can be determined from the diagram shown in Figure 3. The operating points at 0.5 and 1.0 Ach are shown with the orange dashed and continuous lines, respectively in Figure 3.

Given the ventilation rates and Figure 3, it is possible to find the operating rates such as pressure, noise and fan(s) electrical energy consumption. The unit efficiency was derived from Equation (1) as shown below, and the determined values are shown in Table I.

Temperature efficiency η (Taniplan, 2009):

$$\eta = (t_{12} - t_{11}) / (t_{21} - t_{11}) \quad (1)$$

This unit provides the outdoor air at three levels, i.e. 0.25, 0.5 and 1 Ach. At a particular instance, the outdoor and the indoor conditions ($t_{11}, t_{21}, RH_{\text{Outdoor}}, RH_{\text{Indoor}}$) were measured through Equation (1).

According to the manufacturer, the maximum temperature and relative humidity (RH) efficiencies of this rotary heat exchanger unit are 80 percent (FLEXIT, 2009).

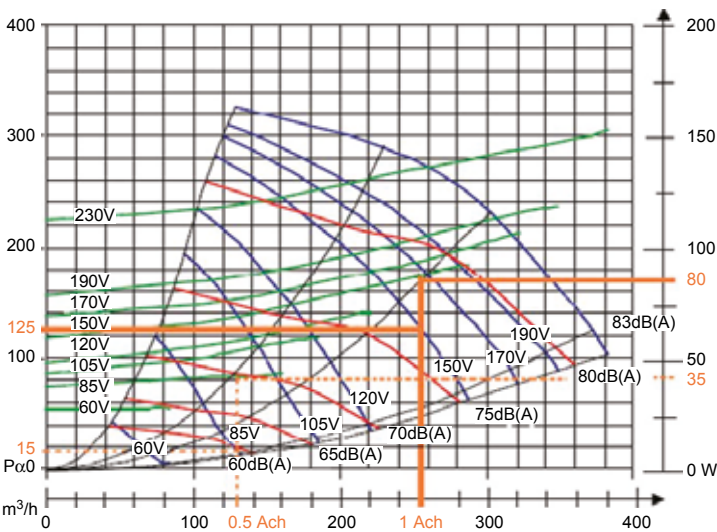


Figure 3.
Characteristics curves of
air supply AC fan

Notes: 1, Capacity curves (blue); 2, operation curves (black); 3, power consumption curves (green); 4, sound curves (red); 5, operation points (orange)
Source: (From FLEXIT Company; FLEXIT (2009))

Table I.
The operating rates
of the unit

| Specifications | Operating rates |
|-------------------------------|---------------------------------|
| 2 Fans power (max. 2 × 165 W) | 70 W |
| Temperature efficiency | 74.5% |
| Ventilation rate | 0.5 Ach (35 l s ⁻¹) |
| Noise | 50 dBA |

These values are not always reached, as demonstrated below:

$$\eta_t = (14.5 + 7.4) / (22 + 7.4) = 74.5\%$$

This unit can use two types of fans, alternative current (AC) and direct current (DC). The fans mechanical efficiency or specific fan power (SFP) for AC and DC fans are calculated 9.7 and 5.5 kW per cubic meter per second at 0.5 Ach, respectively. This means that mechanical efficiency of an AC fan is about 0.56 percent lower than of a DC fan.

As shown in Figure 3, the AC fan power at 0.5 Ach is about 35 W and the annual energy use of two fans (supply and exhaust fans) would be 613 and 350 kWh for AC fans and DC fans, respectively.

4. Heat losses of the house

Thermal losses in buildings are generally attributable to ventilation losses, transmission losses of the envelope and losses of domestic hot water. Ventilation losses are increasing due to the new indoor air quality standards and the focus on reducing indoor radon concentration in cold climates. Reducing losses due to ventilation are therefore expected to have a large impact on energy use. Calculations of the ventilation losses for this case study are as the following.

Ventilation losses are investigated using exhaust fan and heat recovery as a ventilation system.

4.1 Using exhaust fan

It is assumed that the fan-driven supply air flow represents 90 percent of the fan-driven exhaust air flow (a normal ratio leading to a low negative pressure indoors on average, which is an advantage when humidity is taken into account), temperature efficiency for the heat exchanger 74 percent and air leakage in addition to fan-driven ventilation equal to 0.05 Ach:

$$0.9 \times 0.5 \text{ Ach} \times 259 \text{ m}^3 = 116.55 \text{ m}^3 \text{ h}^{-1} = 0.04 \text{ kg s}^{-1} = 32.4 \text{ l.s}^{-1}$$

Total infiltration (air leakage) not affected by the heat exchanger is the sum of fan-driven infiltration (10 percent of the exhaust air flow) (Oman, 2011), and the air leakage at 0.05 Ach corresponding to air leakage both in and out in addition to fan-driven ventilation:

$$0.1 \times 0.5 \text{ Ach} \times 259 \text{ m}^3 + 0.05 \text{ Ach} \times 259 \text{ m}^3 = 25.9 \text{ m}^3 \cdot \text{h}^{-1} = 7.21 \text{ s}^{-1}$$

Specific ventilation loss (Q_v) is the sum of fan-driven supply air loss (Q_s), and the total infiltration loss (Q_l):

$$Q_v = Q_s + Q_l = \Sigma \dot{m} c_p \quad (2)$$

where c_p is the air heat capacity ($1.01 \text{ kJ kg}^{-1} \text{ }^\circ\text{C}^{-1}$) and \dot{m} is the mass flow (kg s^{-1})

$$Q_v = 39.4 + 8.7 = 48 \text{ W} \cdot \text{ }^\circ\text{C}^{-1}$$

Based on monthly long mean temperature in Stockholm (Worldclimate, 2009) and fixing room temperature at 20°C , the heating degree days (HDDs) give 4,500 degree days corresponding to 108,000 heat degree hours per year:

$$E_v = Q_v \times G_t \quad (3)$$

where g_t is the heat degree hours per year:

$$E_v = 4254 + 938.5 = 5,192 \text{ kWh per year}$$

4.2 Using heat recovery system

The heat exchanger reduces the heat demand by a factor $(1-\eta)$. However, the heat exchanger only affects the fan-driven supply air (90 percent of the exhaust air).

Equation (4) shows the energy demand of heating using heat exchanger:

$$Q_{\text{Hex}} = Q_s(1 - \eta_t) \tag{4}$$

$$Q_{\text{Hex}} = 10.24 \text{ W} \cdot \text{°C}^{-1}$$

$$E_{\text{Hex}} = 1106 \text{ kWh per year and } E_{\text{rec}} = E_s - E_{\text{Hex}} = 3148 \text{ kWh per year}$$

If it is considered, $0.25 \leq \lambda_v \leq 1$, $2,000 \leq \text{HDD} \leq 6,000$ and $0.7 \leq \eta_t \leq 0.85$, annual energy recovery is in the following ranges:

$$6 \leq E_{\text{rec}} \leq 90 \text{ kWh m}^{-2}, \text{ and for this case study } E_{\text{rec}} = 30 \text{ kWh m}^{-2}.$$

Ventilation losses of the house are summarized in Table II. Normal condition is defined as in which ventilation rate and infiltration rate are 0.5 and 0.05 Ach, respectively.

The other heat losses in the house are transmission loss and domestic hot water loss. The calculation results of transmission and domestic hot water losses are 8,240 and 3,186 kWh per year, respectively. This means that total heat loss for this house is about 10,284 kWh per year.

5. Results

5.1 Radon measurements

Radon concentrations were measured constantly during the winter. The measurement tools included a continuous radon meter (CRM) and α -track detectors (ATD). Table III shows the results of these measurements.

There are usually some errors in radon measurement, such as place of detectors, measuring period and electromagnetic fields for electronic radon meter. These factors can affect on measurement results.

| Heat loss types | | Specific heat loss (W °C) | Energy (kWh per year) | Recovered energy (kWh per year) |
|---|------------------------|---------------------------|-----------------------|---------------------------------|
| Table II. Ventilation losses of the house at normal condition | Exhaust fan (0.5 Ach) | 39.4 | 4,254 | – |
| | HRV (0.5 Ach) | 10.2 | 1,106 | 3,148 |
| | Air leakage (0.05 Ach) | 8.7 | 938.5 | – |

| | Date and period | ATD (Bq m ⁻³) | CRM (Bq m ⁻³) | Air change rate (h ⁻¹) | Ventilation type | Remedial action |
|--|---------------------|------------------------------|------------------------------|---------------------------------------|------------------|-------------------|
| Table III. Radon measurements results | 2-2008 (2 weeks) | 3,580 ± 380 | – | 0.25 | Exhaust fan | No action |
| | 2-10-2010 (1 week) | – | 150 ± 15 | 0.25 | HRV | 3 connected sumps |
| | 3-18-2010 (12 days) | – | 65 ± 6 | 0.5 | HRV | 3 connected sumps |
| | 4-22-2010 (12 days) | – | 36 ± 4 | 1 | HRV | 3 connected sumps |

5.2 Analytical analysis

If it is assumed that the rate of the radon generation (G) is constant, then the radon content of the indoor radon can be calculated as:

$$C = EA/V(\lambda + \lambda_v) \quad (5)$$

where $C(\text{Bq m}^{-3})$ accounts for the indoor radon at the steady state, $E(\text{Bq m}^{-3} \text{ h}^{-1})$ is the rate of radon exhalation, $A(\text{m}^2)$ is the area of the radon exhalation surface (the floor area in this case), $V(\text{m}^3)$ is the volume of the house, and $\lambda_v (\text{h}^{-1})$ is the ventilation rate of the house.

Using Equation (5) indoor radon can easily be calculated with $E = 65 \text{ Bq m}^{-3} \text{ h}^{-1}$ (Clavensjo and Akerblom, 1994), and the given data from the case study of the house for different ventilation rates. The results are as shown in Table IV.

It can be seen that measured data from Table III are comparable with the analytical results. The error between analytical analysis and measurement data is less than 14 percent at 0.5 Ach.

In order to show the impact of the ventilation rate on the radon level, and to have a qualitative comparison, the radon concentrations were measured by means of a CRM instrument at three different ventilation rates (Figure 4). However, this figure is not suitable for a quantitative comparison due to the short measurement time.

5.3 Dynamic simulation results

For a long-term assessment of the heat recovery ventilation efficiency it is necessary to consider the complete time series of outdoor temperature and all the losses and gains of the building during the heating period.

| Ventilation rate (Ach) | Indoor radon (Bq m^{-3}) |
|------------------------|-------------------------------------|
| 0.0 | 3,582 |
| 0.25 | 108 |
| 0.5 | 54 |
| 1.0 | 27 |

Table IV.
Analytical results
of indoor radon

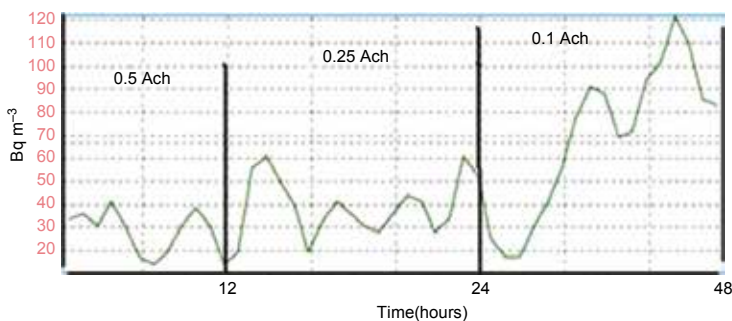


Figure 4.
Continuous radon
concentration levels
measured with CRM

The variations in outdoor temperature and ventilation rate may change the heat recovery temperature and humidity efficiencies. All these time-dependent effects were taken into account through using dynamic thermal simulation programs. These results are explained in this section.

Table V shows delivered energy overview of the simulation results. In this table, delivered energy for ventilation is related to electrical energy for supply and exhaust fans and heating refers to thermal losses of the house.

These values are comparatively close with the calculation results as seen in Section 4.

The annual results of the IDA dynamic simulation are shown in Table VI. This table compares the heat recovery ventilation system with an exhaust (traditional) fan ventilation system. Also using DC fan instead of AC fan can reduce electrical energy more than 50 percent.

The whole-year predicted result of the dynamic simulation is shown that the heat exchanger ventilation system can damp wide variations in the outdoor conditions and maintain the indoor air at a set point temperature with a small variation throughout the year.

The results of measurement and simulation showed that increasing ventilation rates decrease indoor radon levels (inversely proportional) but raise ventilation energy use (direct proportional). Table VII compares different ventilation rates, indoor radon levels and total ventilation losses quantitatively.

5.4 Economic analysis

5.4.1 Energy analysis. In order to install a radon mitigation system, the following aspects should be considered: ventilation loss, cost of the operational energy and the

Table V.
Delivered energy overview

| | kWh | kWh m ⁻² |
|------------------------|-------|---------------------|
| Domestic hot water | 3,386 | 31 |
| Ventilation at 0.5 Ach | 616 | 8 |
| Heating at 0.5 Ach | 9,977 | 93 |

Table VI.
Simulation results
of energy savings with
different ventilation rates

| Ventilation system | Air change rate (h ⁻¹) | Heat recovery (kWh) | AC fans energy use (kWh) | DC fans energy use (kWh) |
|--------------------|------------------------------------|---------------------|--------------------------|--------------------------|
| Heat | 1.0 | 7,163 | 1,227 | 514 |
| Recovery | 0.5 | 3,506 | 616 | 352 |
| Ventilation | 0.25 | 1,799 | 307 | 129 |
| Exhaust fan | 0.5 | 0 | 4,368 | – |

Table VII.
Comparison between
energy use and radon level

| Ventilation rate (Ach) | Fans energy use (kWh) | Ventilation thermal energy use (kWh) | Radon level (Bq m ⁻³) |
|------------------------|-----------------------|--------------------------------------|-----------------------------------|
| 0.25 | 350 | 2,630 | 150 |
| 0.5 | 616 | 5,192 | 65 |
| 1 | 1,400 | 10,384 | 36 |

future energy price, climate, fan(s) energy consumption, heat energy cost, indoor air temperature and ventilation rate (dependent on the life style of the occupants) and the initial and installation costs of the unit.

The heating and cooling degree day is a useful method which has been used in industry and academia for many years (Akander *et al.*, 2005).

In cold climates, high heating degree days are very important from the viewpoint of the energy recovery when proposing the ventilation system for radon mitigation. The energy loss and the initial costs of a ventilation system to reduce radon levels are usually the main concerns of the home owners.

In order to install a radon mitigation system, some costs and key factors such as the direct electrical energy cost, efficiency, noise and service lifetime of the ventilation unit should be considered. Since the ventilation system is installed indoors, the size of the system is also a concern for the homeowners.

A general and accepted approach to calculate the recovered energy is the outside temperature cumulative curve during the heating and cooling period. The seasonal recoverable energy at constant room temperature (20°C) was calculated.

5.4.2 Energy life cycle cost analysis. The net present value (NPV) method was used to evaluate the cost-effectiveness of an investment in the future.

Life cycle costs consist of the initial capital investment, the installation costs of the rotary heat exchanger unit, which is about 4,000 USD for this unit, and the energy and maintenance costs. The annual electrical consumption of the unit is 616 kWh. The annual cost of replacing two of the unit's filters is about 80 USD.

For the NPV analysis, the following assumptions were considered:

$i = 4$ percent, $q = 2$ percent, $n = 25$ years and energy cost in Sweden is roughly about 0.16 USD per kWh including all taxes.

In this method if the NPV of all the savings is larger than the initial capital cost, an investment is profitable (Nilsson, 2006).

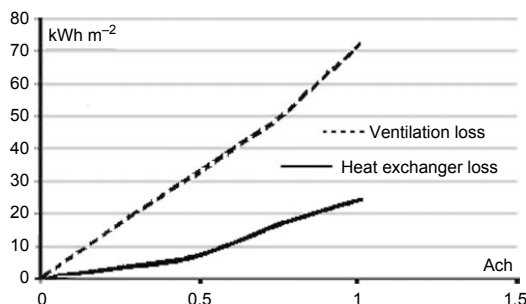
Based on analytical relations, the NPV of this heat recovery was calculated and the results of the life cycle cost are shown in Table VIII. The life cycle cost analysis shows that the use of a HRV system is cost-effective, and with regard to the annual increase of the energy cost, in this case the investment will have a payback period of about 12 years.

The annual energy saving varies with the ventilation rate; the amount of ventilation loss with and without the heat exchanger unit is shown in Figure 5. The two key factors which potentially add to the utility costs of a residential radon mitigation system are the outside environmental conditions and the house air exchange rate (Ach). Considering that there may be a 30-60 percent increase in energy consumption due to buildings ventilation (Awbi, 1998) and radon mitigation system, it is apparent that a huge amount of energy can be saved through a heat recovery ventilation system. Therefore, employing this type of radon mitigation system is quite cost-effective.

| Ventilation system | Capital cost (USD) | Annual costs (USD) | | Life cycle costs (USD) |
|--------------------|--------------------|--------------------|-------------|------------------------|
| | | Energy | maintenance | |
| Traditional fan | 100 | 702 | – | 13,605 |
| HRV with AC fan | 4,000 | 98 | 80 | 7,488 |
| HRV with DC fan | 4,000 | 56 | 80 | 6,655 |

Table VIII.
Ventilation systems life
cycle cost analysis

Figure 5.
Ventilation and heat
exchanger ventilation
system losses



6. Discussion

Heat recovery units are manufactured in Europe and small size units suitable for single-family buildings cost in the range 2,700-4,800 USD (FLEXIT, 2009).

This study showed that balanced ventilation with heat recovery provides better indoor air quality (lower radon level) due to balanced supply/exhaust airflows and in same time saves energy due to heat recovery. While results with “business as usual” solution, i.e. exhaust ventilation without heat recovery makes higher depressure (potential for radon inflow) and does not recover the heat of exhaust air.

The reduction in purchased energy after using heat exchanger unit is a clearly obvious. This is amounted to 2940 kWh per year which is almost near to calculation result. Also data concerning the energy use in Swedish Single-family houses has reported 102 kWh m⁻² for net heating (Hiller, 2003), which is close to 93 kWh m⁻², resulted from the simulation of this case study.

The analytical and dynamic simulation results indicate that by using this type of ventilation system to mitigate the radon level, Swedish buildings can save between 30-42 kWh m⁻² of energy per year for between 4,000 and 6,000 heating degree days. If it is considered that each of the 500,000 buildings has at least 50 m² of floor area, the annual energy savings would be roughly 1,000 GWh. These figures are rough estimates, and can vary widely due to a great number of factors. In practice, the energy saving through the heat recovery between the exhaust and the supply air “competes” to save energy with many other measures.

The economic evaluation of the heat exchanger from the exhaust air depends on the volume and duration of the ventilation. The payback increases with increasing annual utilization hours. This means that heat recovery ventilation systems are more advantageous for long and severe winters such as those in Sweden.

7. Conclusions

Nowadays HRVs systems are a well-known technology in Sweden as most energy efficient systems. But this study focussed on another aspect of this technology and showed that it could be applicable in order to reduce the indoor radon problem.

Contrastingly, an extractor fan ventilation system with a negative pressure draws outdoor air from all possible sources. Unfortunately using extract fan is a common method to mitigate indoor radon level in Sweden.

A heat recovery ventilation system because of controlling on pressure and outdoor ventilation rate has strong effects on radon mitigation and energy saving in residential

buildings. This technology enables improvement of both indoor air quality and energy efficiency without sacrificing either. A heat recovery ventilation system can give substantial final energy reduction, which it depends strongly on the initial cost, the annual costs of maintenance and electricity used for unit and the air tightness of buildings.

The first set of conclusions derived from using the balanced heat exchanger ventilation system relates to the indoor air quality and the radon concentration; the balance between the air supply and the exhaust air prevents radon from being sucked out of the ground and into buildings. Regarding the effects of air pressure condition due to air tightness and supply/exhaust airflow ratio, simulation results show that reducing air tightness of the house leads to reducing indoor radon and with increasing supply/exhaust airflow ratio at constant exhaust air flow rate, indoor radon is increased.

The second set of conclusions regarding the advantages of a heat exchanger relates to the energy savings. This study shows that in comparison to exhaust fan ventilation, a heat exchanger ventilation system could save 74 percent of the energy lost through ventilation and about 30 kWh m^{-2} can be saved per year. This means that the recovered energy for this case study is about 3,000 kWh per year based on analytical and simulation results.

The colder the climate is, the more energy can be saved and recovered. The economic calculations of the NPV method and the energy life cycle cost shows that the capital investment is cost-effective even if the energy price remains unchanged in future years.

From an indoor air quality point of view, a higher radon level requires a higher ventilation rate. Under these circumstances a heat recovery ventilation system can recover more energy and the investment payback time would be shorter. Where there is both a cold climate and high radon levels, the investment cost of installing a heat recovery ventilation system can indeed be balanced by the energy savings, since more heat degree days (more energy demand) and higher radon levels lead to more energy savings.

In Sweden, due to the long winters, the large number of heating degree days and the elevated radon levels in residential buildings, using heat exchanger ventilation systems can be a quite cost-effective strategy for both energy saving and indoor radon active remedy.

References

- Akander, J., Alvarez, S. and Johannesson, G. (2005), "Energy normalization techniques", in Santamouris, M. (Ed.), *Energy Performance of Residential Buildings: A Practical Guide for Energy Rating and Efficiency*, James & James, London, ISBN 1-902916-49-2.
- Awbi, H. (1998), "Chapter 7: ventilation", *Renewable and Sustainable Energy Reviews*, Vol. 2 Nos 1-2, pp. 157-188.
- Clavensjö, B. and Akerblom, G. (1994), *The Radon Book*, Swedish Council for Building Research, Stockholm.
- FLEXIT (2009), "Brochures", available at: www.flexit.no/Documents/Brosjyrer/E/BR_95220_E.pdf (accessed November 10, 2009).
- Hekmat, D., Feustel, H. and Modera, M.P. (1986), "Ventilation strategies and their impacts on the energy consumption and indoor air quality in single-family residences", *Energy and Buildings*, Vol. 9 No. 3, pp. 239-251.

-
- Hiller, C. (2003), "Sustainable energy use in houses", available at: www.sp.se/sv/index/research/effenergi/ongoing/.../CH-3041.pdf (accessed November 10, 2009).
- Hubbard, L.M., Mellander, H. and Swedjemark, G.A. (1996), "Studies on temporal variations of radon in Swedish single-family house", *Environment International*, Vol. 22 No. 1, pp. 715-722.
- Jokisalo, J., Kurnitska, J. and Torkki, A. (2003), "Performance of balanced ventilation with heat recovery in residential buildings in cold climate", *International Journal of Ventilation*, Vol. 2 No. 3, pp. 223-235.
- Kåberger, T., Lublin, Z. and Andersson, A. (2009), "Energimyndigheten", available at: energimyndigheten.se (accessed November 10, 2010).
- Lazzarin, R.M. and Gasparella, A. (1998), "Technical and economical analysis of heat recovery in building ventilation systems", *Applied Thermal Engineering*, Vol. 18 Nos 1-2, pp. 47-67.
- Ministry of Sustainable Development (2006), "Regeringen", available at: www.regeringen.se/sb/d/574/a/63635 (accessed November 10, 2010).
- Nilsson, P.E. (2006), *Achieving the Desired Indoor Climate*, Studentlitteratur, Lund.
- Oman, R. (2011), *Energy and Buildings*, Mälardalen University, Västerås.
- Radonelektronik (2009), "Electronic radon gas monitor", available at: www.Radonelektronik.se (accessed November 10, 2009).
- Swedish Energy Agency (2009), *Energy Efficiency Policies and Measures in Sweden*, Swedish Energy Agency, Eskilstuna.
- Swedjmark, G. and Mjones, L. (1987), "Radon and radon daughter concentration in Swedish dwellings", *Radon Protection Dosimetry*, Vol. 17 Nos 1-4, pp. 341-345.
- Taniplan (2009), "Rotary heat exchanger", available at: www.taniplan.fi/userData/taniplan-ky/en-rotary-heat-exchangers/TP-Rotary-exchangers.pdf (accessed November 10, 2009).
- Turiel, I., Fisk, W.J. and Seedall, M. (1983), "Energy saving and cost-effectiveness of heat exchanger use as an indoor air quality mitigation measure in the BPA weatherization program", *Energy*, Vol. 8 No. 5, pp. 323-335.
- Worldclimate (2009), "Climate data for stockholm", available at: www.worldclimate.com (accessed November 10, 2009).
- Zeeb, H. and Shannoun, F. (2009), *WHO Handbook on Indoor Radon*, WHO, Geneva.

Corresponding author

Keramatollah Akbari can be contacted at: keramatollah.akbari@mdh.se

Paper II



MEQ
24,3

394

Received 18 May 2012
Revised 14 July 2012
2 August 2012
Accepted 22 August 2012

Simulation of ventilation effects on indoor radon

Keramatollah Akbari and Jafar Mahmoudi

*School of Sustainable Development of Society and Technology,
Mälardalen University, Västerås, Sweden, and*

Mahdi Ghanbari

*Department of Energy Engineering, Sharif University of Technology,
Tehran, Iran*

Abstract

Purpose – The purpose of this paper is to describe the use of computational fluid dynamics (CFD) to simulate indoor radon distribution and ventilation effects. This technique was used to predict and visualize radon content and indoor air quality in a one-family detached house in Stockholm. The effects of intake fans, exhaust fans and doors on radon concentration were investigated.

Design/methodology/approach – In this study a mechanically balanced ventilation system and a continuous radon monitor (CRM) were used to measure the indoor ventilation rate and radon levels. In a numerical approach, the *FLUENT CFD* package was used to simulate radon entry into the building and ventilation effects.

Findings – Results of the numerical study indicated that indoor pressure created by ventilation systems and infiltration through doors or windows have significant effects on indoor radon content. The location of vents was found to affect the indoor radon level and distribution.

Research limitations/implications – It may be possible to improve any discrepancies found in this article by using a more refined representation of grids and certain boundary conditions, such as pressure and temperature differences between inside and outside and by considering some real situations in residential buildings and external situations.

Originality/value – From the viewpoints of indoor air quality (IAQ) and energy savings, ventilation has two opposing functions; on the positive side it enhances IAQ and the establishment of thermal comfort, and on the negative side it increases energy consumption. This paper describes the search for a solution to cope with this contradiction.

Keywords Housing, Residential property, Radon gas, Numerical simulation, Radon mitigation, Balanced ventilation, Residential buildings

Paper type Research paper

1. Introduction

Radon exposure is an international problem and attention to the problem and the associated health risks have been growing throughout the world. More than 50 countries currently have ongoing projects and have established mandatory regulation in the area (Ahmed, 1994). In most countries, such as in Scandinavia, the USA, UK, Hong Kong, etc., radon enters houses through building materials. Increasing insulation and air-tightness in buildings for increasing energy efficiency and lowering energy costs have led to indoor air quality (IAQ) problems. Thus, the study of radon problem is very important from the viewpoints of health and energy consumption.

Ventilation is a good method for controlling indoor radon and maintaining IAQ in existing residential buildings. Pollutant concentrations are inversely proportional to ventilation rates (Zhang, 2004). Increasing the amount of fresh air brought into the indoor environment from a non-polluted ambient source can increase the achievable IAQ. However, increasing the ventilation rate to control radon level is not permitted in



the building sector because of the energy implications. Therefore energy efficient solutions have to be considered.

From the viewpoints of IAQ and energy savings, ventilation has two opposing functions – on the positive side it enhances IAQ and the establishment of thermal comfort, and on the negative side it increases energy consumption. This paper describes possible solutions to cope with this contradiction.

Previous studies have been carried out on airflow in buildings and ventilation effects, employing computational fluid dynamics (CFD) techniques, and on radon modeling in soil and building materials (European Collaborative Action, 2003; Nilsson, 2003; Amissah, 2005; Pitarma *et al.*, 2004).

Wang and Ward (2000) used the CFD package FLUENT to develop a model of multiple radon entry in a house with a cellar. In order to develop the model, they applied methods such as using a subroutine to specify the radon generation rate in the soil cells and designed appropriate boundary conditions. The model was verified by a grid-independency test and convergence behavior analysis. The inter-model validation technique and comparison with analytical solutions were also used to validate the model.

Zhou *et al.* (2001) used CFD to study the concentrations and distributions of indoor radon in three dimensions (3D) in a ventilated room. According to the results of this simulation, the distribution of radon is uniform except at locations near air diffuser vents. He showed that the results of simulations of activities and their distributions agreed well with experimental results in a laboratory.

Rota *et al.* (1994) compared the results of numerical simulations and experiments. The results showed good agreement, but the simulation results showed elevated concentrations in the region with low ventilation rates compared to the experiments.

Cohlis *et al.* (1991) suggested the use of a numerical code based on the finite difference method. Based on the results and the code validation, they concluded that this method was a powerful tool that could predict and evaluate the performance of subfloor ventilation strategies.

Marley and Phillips (2001) investigated air-movement control of radon in a retail store. Mitigation of radon gas and radon progeny in buildings is based largely on reducing the pressure difference between the point of the radiation source and the point of entry to indoor air. However, this proved ineffective in reducing radon levels in a large retail store. They found that reduction in radon levels brought about by the operation of the system was in absolute terms, and the rate of reduction was a constant which allowed an accurate estimate of the levels at a point in time from the start-up of the system. Importantly, the operation of the air-movement system reduced the progeny level substantially, relative to the radon gas.

In this study, FLUENT, a CFD software package was used to simulate and predict radon levels and to visualize the effects of intake fans, exhaust fans and doors. An analytical solution and measurement method were also used for validation of the numerical model.

2. Problem specifications

The case study is a one family detached house located in Stockholm, built on bedrock in 1975. The house volume is $12 \times 9 \times 2.4 \text{ m}^3$. The house consists of three intake fans, three exhaust fans, one door and one window. The house does not contain any partition in this study. The radon level after some remedial techniques remains around 600 Bq/m^3 , mainly originating as soil gas from the building foundations.

This house is in direct contact with the ground, meaning that radon entry is driven by two disturbance pressures, along its route into the house. The house is occupied. But there is no energy source among furniture and they are not too large that can affect on radon concentration and distribution in the house. So we can neglect the effect of furniture in the model. The portion of the house above ground level represents the living area. The volume of soil included in the computational domain is $30 \times 30 \times 3 \text{ m}^3$. Such a volume has previously been demonstrated to be sufficient to represent the soil block in radon entry modeling (Loureiro, 1987). Figure 1 shows the geometry of the house and soil.

3. Materials and methods

Radon entry into a one family detached house and ventilation effects were modeled using FLUENT in 3D steady state model.

A heat recovery balanced ventilation system, a continuous radon monitor (CRM), and alpha track detectors (ATD) were used to measure the indoor ventilation rate and indoor radon levels.

Analytical analysis was also used to confirm the numerical results.

3.1 Measurement method

Radon concentrations were measured continuously during the winter and spring, both with a CRM and an ATD. Radon measurement instrument is an electronic radon monitor, which is an electronic device. Radon meter, R2, is an electronic meter manufactured by a Swedish company (Radonelektronik, 2012). It is suitable for short- and long-term measurements. This radon meter is used to identify problems with indoor radon and influences of physical and environmental factors such as ventilation effects and indoor conditions. Indoor temperature and relative humidity are also measured and logged, so that any influence from the measuring environment can be determined. This radon meter undergoes control irradiation at Swedish Radiation Safety Authority (SSM) and gives very reliable values with 10 percent accuracy.

To measure radon level, one CRM device was installed in the middle of the house at desktop position for short-term test. Table I shows the results of these measurements.

3.2 Analytical analysis

Indoor radon content can be calculated as (Man and Yeung, 1997; Petropoulos *et al.*, 2001):

$$C = \frac{EA}{V(\lambda_{Rn} + \lambda_v)} \tag{1}$$

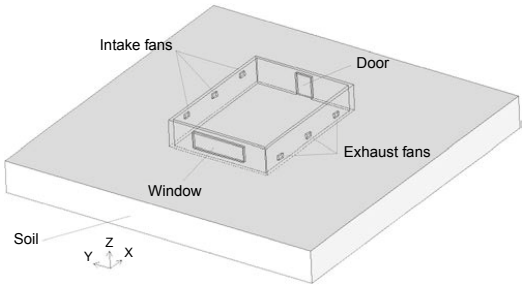


Figure 1.
Geometry of the house
and soil

where C (Bq/m^3) is indoor radon content at steady state, E ($\text{Bq/m}^2/\text{h}$) is radon exhalation rate, A (m^2) is radon exhalation surface (in this study, the house floor), V (m^3) is the volume of the house, λ_{Rn} is the radon decay constant ($2.1 \times 10^{-6} \text{ s}^{-1}$) and λ_v (h^{-1}) is the air change rate in the house.

Using $E = 65 \text{ Bq/m}^2/\text{h}$ (Clavensjo and Akerblom, 1994) and data provided for the case study house, with Equation (1) gives indoor radon levels for different ventilation rates; $C_{0.0} = 3,582$, $C_{0.25} = 106$, $C_{0.5} = 53$, $C_1 = 22 \text{ Bq/m}^3$. These analytical data showed close agreement with the measured data and was used to confirm numeric results at four distinct air change rates. The comparisons of analytical, numerical and measuring results are shown in Table VI.

3.3 Numerical simulation approach

CFD programs are based on solving the transport equations, which is the collective term for the conservation of mass (continuity), momentum (Navier-Stokes equations), thermal energy and concentrations of species. In a room with ventilation and radon, concentration is necessary to solve these partial differential equations. CFD programs are implemented to solve governing equations to calculate velocity, temperature and species transport numerically.

Indoor airflow with mechanical ventilation with presence of radon is a complicated problem. Even having access to new CFD packages and powerful computers, it is very often necessary to use simplifications and approximations. Similar methods have been used in several research studies (Tung and Burnett, 2004; Mora *et al.*, 2003; Arvela, 1995; Kokotti, 1995).

In this study, the 3D model is assumed to be turbulent, as airflow in a ventilated room, even with a ventilation rate lower than 0.2 m/s , usually has a turbulent regime, and the appropriate turbulent model is required to solve the governing equations (Wang and Ward, 2000).

3.3.1 Radon transport equation. Radon enters mostly through the larger air-filled pores in the building materials and a fraction reaches the building-air interface before decaying. Then radon enters into indoor air as a result of the airflow. This transport occurs by diffusion and advection (convection) mechanisms.

Radon gas flow, after entering the building, may be induced due to a pressure or temperature gradient. This gradient may be created mainly as a result of changes in environmental conditions due to natural or mechanical ventilation systems such as exhaust fans or suppliers, heating and air-conditioned systems in residential buildings (Spoel, 1998).

Basic governing equations include mass, momentum, energy and species transport conservation equations. These equations must be solved simultaneously for obtaining radon distribution at indoor environment. The general forms of these conservation equations have been given in the following paragraphs (FLUENT Incorporation, 2005).

| Date and period | ATD (Bq/m^3) | CRM (Bq/m^3) | ACH | Ventilation type | Remedial action |
|---------------------|-------------------------|-------------------------|------|------------------|------------------------|
| 2008-2 (2 weeks) | $3,580 \pm 380$ | — | 0.25 | Extractor fan | No action |
| 2010-1 (3 months) | $1,280 \pm 160$ | $1,580 \pm 158$ | 0.25 | HRV | Radon sump and sealing |
| 2010-3-18 (12 days) | — | 65 ± 6 | 0.5 | HRV | 3 connected sumps |
| 2010-4-22 (12 days) | — | 36 ± 4 | 1 | HRV | 3 connected sumps |

Table I.
Measurements of indoor
radon levels (Bq/m^3)

Mass conservation equation is as follow:

$$\frac{\partial \rho}{\partial t} + \frac{\partial(\rho u)}{\partial x} + \frac{\partial(\rho v)}{\partial y} + \frac{\partial(\rho w)}{\partial z} = 0 \quad (2)$$

Momentum conservation equations in three directions are as in the following equations:

$$\begin{aligned} & \frac{\partial(\rho u)}{\partial t} + \frac{\partial(\rho uu)}{\partial x} + \frac{\partial(\rho uv)}{\partial y} + \frac{\partial(\rho uw)}{\partial z} \\ &= -\frac{\partial p}{\partial x} + \frac{\partial}{\partial x} \left(\mu \frac{\partial u}{\partial x} \right) + \frac{\partial}{\partial y} \left(\mu \frac{\partial u}{\partial y} \right) + \frac{\partial}{\partial z} \left(\mu \frac{\partial u}{\partial z} \right) + S_{Mx} \end{aligned} \quad (3)$$

$$\begin{aligned} & \frac{\partial(\rho v)}{\partial t} + \frac{\partial(\rho vu)}{\partial x} + \frac{\partial(\rho vv)}{\partial y} + \frac{\partial(\rho vw)}{\partial z} \\ &= -\frac{\partial p}{\partial y} + \frac{\partial}{\partial x} \left(\mu \frac{\partial v}{\partial x} \right) + \frac{\partial}{\partial y} \left(\mu \frac{\partial v}{\partial y} \right) + \frac{\partial}{\partial z} \left(\mu \frac{\partial v}{\partial z} \right) + S_{My} \end{aligned} \quad (4)$$

$$\begin{aligned} & \frac{\partial(\rho w)}{\partial t} + \frac{\partial(\rho wu)}{\partial x} + \frac{\partial(\rho wv)}{\partial y} + \frac{\partial(\rho ww)}{\partial z} \\ &= -\frac{\partial p}{\partial z} + \frac{\partial}{\partial x} \left(\mu \frac{\partial w}{\partial x} \right) + \frac{\partial}{\partial y} \left(\mu \frac{\partial w}{\partial y} \right) + \frac{\partial}{\partial z} \left(\mu \frac{\partial w}{\partial z} \right) + S_{Mz} \end{aligned} \quad (5)$$

In Equations (3)-(5), S_M is the momentum source.

Energy conservation equation for a perfect gas is as follows:

$$\begin{aligned} & \frac{\partial(\rho C_v T)}{\partial t} + \frac{\partial(\rho C_v Tu)}{\partial x} + \frac{\partial(\rho C_v Tv)}{\partial y} + \frac{\partial(\rho C_v Tw)}{\partial z} \\ &= -p \left(\frac{\partial u}{\partial x} + \frac{\partial v}{\partial y} + \frac{\partial w}{\partial z} \right) + \frac{\partial}{\partial x} \left(k \frac{\partial T}{\partial x} \right) \\ &+ \frac{\partial}{\partial y} \left(k \frac{\partial T}{\partial y} \right) + \frac{\partial}{\partial z} \left(k \frac{\partial T}{\partial z} \right) + \Phi + S_{Energy} \end{aligned} \quad (6)$$

In Equation (6), S_{Energy} is the energy source and Φ is the dissipation function. Dissipation function for a gas is defined by the following equation:

$$\begin{aligned} \Phi = & \mu \left\{ 2 \left[\left(\frac{\partial u}{\partial x} \right)^2 + \left(\frac{\partial v}{\partial y} \right)^2 + \left(\frac{\partial w}{\partial z} \right)^2 \right] \right. \\ & + \left(\frac{\partial u}{\partial y} + \frac{\partial v}{\partial x} \right)^2 + \left(\frac{\partial u}{\partial z} + \frac{\partial w}{\partial x} \right)^2 + \left(\frac{\partial v}{\partial z} + \frac{\partial w}{\partial y} \right)^2 \Big\} \\ & - \frac{2}{3} \mu \left(\frac{\partial u}{\partial x} + \frac{\partial v}{\partial y} + \frac{\partial w}{\partial z} \right)^2 \end{aligned} \quad (7)$$

The conservation equation for the species transport model is in the following general form:

$$\begin{aligned} \frac{\partial}{\partial t}(\rho c) + \frac{\partial}{\partial x}(\rho u c) + \frac{\partial}{\partial y}(\rho v c) + \frac{\partial}{\partial z}(\rho w c) = \\ \frac{\partial}{\partial x}\left(D_e \frac{\partial c}{\partial x}\right) + \frac{\partial}{\partial y}\left(D_e \frac{\partial c}{\partial y}\right) + \frac{\partial}{\partial z}\left(D_e \frac{\partial c}{\partial z}\right) + S_c \end{aligned} \quad (8)$$

As the radon mixture (with air) is constant in the steady state condition, this equation reduces to:

$$\begin{aligned} \frac{\partial}{\partial x}(\rho u c) + \frac{\partial}{\partial y}(\rho v c) + \frac{\partial}{\partial z}(\rho w c) \\ = \frac{\partial}{\partial x}\left(D_e \frac{\partial c}{\partial x}\right) + \frac{\partial}{\partial y}\left(D_e \frac{\partial c}{\partial y}\right) \\ + \frac{\partial}{\partial z}\left(D_e \frac{\partial c}{\partial z}\right) + S_c \end{aligned} \quad (9)$$

$$S_c = \varepsilon(G - \lambda C) \quad (10)$$

In this equation, G is defined in Equation (11), where D_e represents effective diffusion coefficient, ρ is the mixture density, S_c is the generation rate of concentration and c is the mean radon concentration (Awbi, 2003).

The radon generation rate G is a function of soil specifications and is defined as:

$$G = f \rho_s A_{\text{Ra}} \lambda_{\text{Rn}} \frac{1 - \varepsilon}{\varepsilon} \quad (11)$$

where G is the volumetric radon generation rate in soil pores ($\text{Bq/m}^3/\text{s}$), f is the emanation fraction, ρ_s is the density of the soil grain, A_{Ra} (Bq/kg) is the radium activity concentration in the soil grain, λ_{Rn} is the radon decay constant and ε is the soil porosity.

The conservation equation of species transport, including convection and diffusion, is solved for each species C in the FLUENT package through the solution of a convection-diffusion equation for each species, with selected species transport model and individual species defined in the model. FLUENT then predicts the mass fraction of the species (FLUENT Incorporation, 2005).

3.3.2 Turbulence modeling. Airflows in ventilated rooms are generally turbulent. As the Reynolds number (Re) in this case is $>10^5$, airflow is assumed to be turbulent, and thus turbulence model is used for modeling this case study.

The $k-\varepsilon$ model family is the most popular turbulence model and has the largest number of variants. The standard $k-\varepsilon$ model developed by Launder and Spalding (1974) is one of the most prevalent models for indoor airflow simulation due to its simple format, robust performance, wide validations, its applicability to wide-ranging flow situations, stability during simulation time, good predictive accuracy for the flow and lower computational demand than other available and more complex models (Awbi, 2003; Cehlin and Moshfegh, 2002). The standard $k-\varepsilon$ model with wall functions can predict the airflow and turbulence in enclosed environments reasonably well. For example, Holmes *et al.* (2000) simulated two ideal rooms with several $k-\varepsilon$ models and found that the standard $k-\varepsilon$ model provides a reasonably good prediction.

Gadgil *et al.* (2003) also verified that the $k-\epsilon$ model predicted the indoor-pollutant mixing time in an isothermal closed room fairly well. Zhang and Chen (2006) successfully applied the standard $k-\epsilon$ model to predict the airflow and particle distribution in a room with an underfloor air distribution system.

Two-equation models are the simplest available means of calculating turbulent stresses in the recirculation flow where the length scale distribution cannot be calculated algebraically. As a two-equation model, the standard $k-\epsilon$ model is a semi-empirical model based on model transport equations for the kinetic energy k and its dissipation rate ϵ . When using this model it is assumed that the flow is fully turbulent and that the effects of molecular viscosity are negligible (Awbi, 2003).

In this work we have used standard $k-\epsilon$ model for numerical simulation of airflow in rooms.

3.3.3 Values and constants. Tables II and III show the values and constants used in this study, which are used to indicate parametric values of variables in FLUENT.

3.3.4 Boundary conditions. Table IV indicates the boundaries in the model, their locations and physical descriptions. The last column also lists the boundary condition options available in FLUENT.

At the minimum indoor air speed (0.5 m/s), the Reynolds number reaches the transition values and the flow becomes turbulent. The $k-\epsilon$ model is therefore used to simulate the turbulence.

3.3.5 Simulation procedure. In order to model the soil and house, three individual cases are defined to solve the governing equations. The simulation approach is repeated for these three cases to show the influences of changing ventilation rates and inlet and outlet locations.

The initial condition is applied to the temperature field to calculate the buoyancy effect of the flow and the disturbance pressure in the second run. The radon concentration in the case study house before remedial techniques were applied, was about 4,000 Bq/m³, equivalent to just 5.25×10^{-16} kg/m³.

Table II.
Radon properties

| Radon properties | Usage | Quantity |
|------------------------------|--------------------|----------|
| CP (J/kg K) | Energy equation | 96.35 |
| K (W/m K) | Energy equation | 0.00361 |
| M_W (kg/kmol) | Transport equation | 222 |
| Density (kg/m ³) | Transport equation | 7.13 |

Table III.
Constants used in
boundary conditions

| Variable | Quantity |
|---------------------------|---------------------------------------|
| Atmosphere pressure gage | 0 Pa |
| Air leakage from door | 0-0.2 m/s |
| Air leakage from window | 0-0.02 m/s |
| Intake fan-pressure jump | 0-20 Pa |
| Exhaust fan-pressure jump | -20-0 Pa |
| Radon source term | $2.6\text{e-}17$ kg/m ³ /s |
| Permeability of soil | $10\text{-}10$ m ² |
| Porosity | 0.4 |

| Location | Physical description | Option in FLUENT |
|--------------|--|------------------|
| Door | Mass and heat leakage | Velocity inlet |
| Exhaust fan | Pressure jump, no radon entry | Exhaust fan |
| Floor | No-flow and vertical radon diffusion only | Interior |
| Intake fan | Pressure jump, no radon entry | Intake fan |
| Roof | No-flow boundary (including soil gas, radon) | Wall |
| Room walls | No-flow boundary (including soil gas, radon) | Wall |
| Soil bottom | Fixed temperature; no-flow | Wall |
| Soil surface | Fixed temperature; fixed concentration; fixed pressure | Pressure inlet |
| Soil wall | No-flow boundary (including soil gas, radon and heat flux = 0) | Symmetry |
| Window | Mass and heat leakage | Velocity inlet |

Table IV.
Boundary conditions
of the model

3.3.6 Solution methods. The finite volume solution method can be used for solving governing equations. This method either uses a “segregated” or a “coupled” solution procedure.

With segregated methods an equation for a certain variable is solved for all cells, and then the equation for the next variable is solved for all cells, etc.

With coupled methods, for a given cell equations for all variables are solved, and that process is then repeated for all cells.

The segregated solution method is the default method in most commercial finite volume codes. It is best suited for incompressible flows or compressible flows at low Mach number.

Compressible flows at high Mach number, especially when they involve shock waves, are best solved with the coupled solver.

3.3.7 Grid refinement. Grid refinement is deemed necessary when the simulation grid cannot resolve the attributes accurately and is applied to minimize the numerical diffusion.

Grid refinement should be continued until the solution is reasonably grid independent. In order to achieve grid independency two aspects must be considered: grid distribution, and the total number of grid cells in the computational domain.

An acceptable grid with reasonable respect and aspect ratios results in fast convergence, and residual errors decrease with increasing cell number. However, increasing grid refinement usually creates greater demands on computing capacity and cost (Wang and Ward, 2000).

The independency of grids was checked by increasing the mesh size by six steps, and results of finer grids were approximately equal. Some of the grid systems tested and the numbers of cells in them are shown in Table V.

The computational load increased rapidly after step 4, which contained $40 \times 32 \times 10$ cells. This step was therefore used in all simulation modeling. A further reason for selecting step 4 was that 3D modeling generally requires many more calculations, as the parametric studies require a wide range of conditions in combination.

| | Grid 4 | Grid 5 |
|-------------|----------------------------|----------------------------|
| House | $40 \times 32 \times 10$ | $80 \times 64 \times 20$ |
| Soil | $120 \times 120 \times 12$ | $120 \times 120 \times 12$ |
| Total cells | 185,600 | 275,200 |

Table V.
Various grid systems
of 3D models

Larger numbers of grid cells were sometimes used to increase the accuracy of the results. Thus, grid density was maximized based on accuracy and affordability.

4. Results and discussion

Air conditioning in houses and living areas is an important consideration for design, operation and maintenance services. Study of its effect on radon distribution in house is therefore also important. However, its complexity limits the methods which can be used to study it. In this study we considered a simple and popular method of air conditioning and studied its behavior and effects on radon concentration. Fan-coils or fans are the most widely used class of air conditioning systems globally.

In this study we considered three intake fans and three exhaust fans in the room and set for them the conditions of fan-coils.

4.1 Exhaust fan

The figures below show the flow field in a house for a case study of an exhaust fan. In this case the pressure jump across the exhaust fan is set to 10 Pa. These figures clearly illustrate the mixing behavior in the house for this condition. The indoor air velocity and temperature are in the thermal comfort zone.

Figure 2 shows the velocity at the midpoint of the house in the case study for an exhaust fan with a pressure jump of 10 Pa.

Figures 3 and 4 show the variation of radon concentration in the house due to the effect of the exhaust fan pressure jump. Increasing the pressure jump in the fan, results in lower radon concentration. This is because the larger pressure jump and mass flow rate, force the radon out of the room and decreases radon level at indoor environment.

Figure 2.
Velocity contours for two perpendicular planes crossing the midpoint of the house in the case study for the exhaust fan with a pressure jump of 10 Pa from CFD model outputs

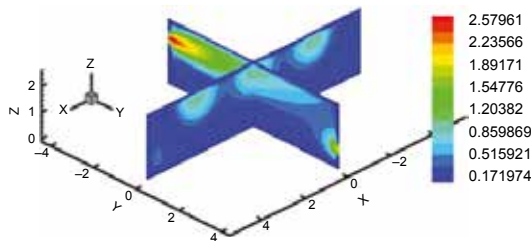
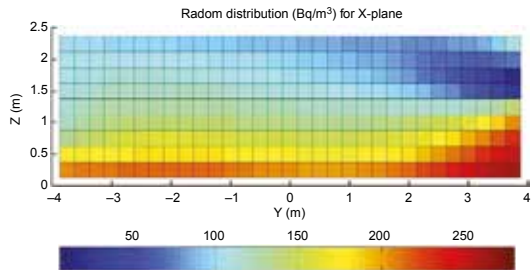


Figure 3.
Radon concentration at the midpoint of the house in the case study for the exhaust fan with a pressure jump of 10 Pa from CFD model outputs



4.2 Intake fan

In some houses, air conditioning is performed with inlet fans instead of exhaust fans. In this part of the study we considered a house with three intake fans. The pressure jump across the fans was between 2 and 20 Pa. The contours below investigate the flow field (air) properties throughout the house. The velocity and radon distribution are shown in Figures 5 and 6.

4.3 Doors

Figures 5 and 6 show that, the intake fans force air into the house causing the pressure inside to rise. Every house has doors and windows. Their effect is considered in air conditioning calculations for design and operation. Doors and windows result in

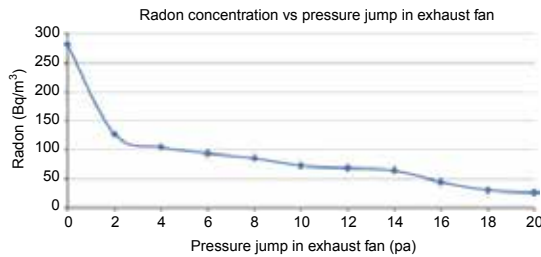


Figure 4.
Radon concentration in
the house vs pressure
jump in the exhaust fan
from CFD model outputs

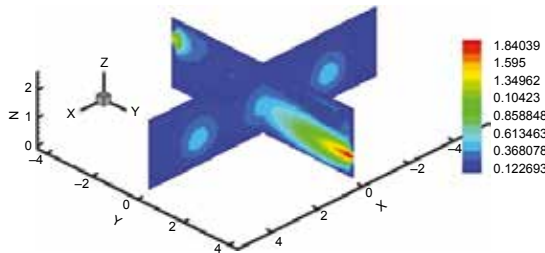


Figure 5.
Velocity contours for two
perpendicular planes
crossing the midpoint of
the house in the case study
for the intake fan with a
pressure jump of 10 Pa
from CFD model outputs

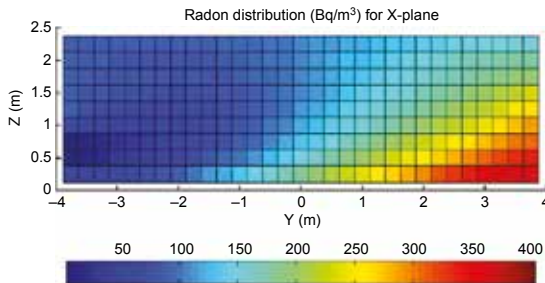


Figure 6.
Radon concentration at the
midpoint of the house in
the case study for the
intake fan with a pressure
jump of 10 Pa from CFD
model outputs

leakage of mass or heat or both. In this part of the study we examined the effect of doors on radon concentration and distribution in the house.

Figure 7 shows the effect of door leakage velocity on radon concentration in the house. Increasing the velocity or mass flow rate leaking through the door decreases the radon content of the house. The main reason for this is likely to be the increase in internal pressure in the house and therefore door effect will be like an intake fan. Increasing internal pressure has two effects. One, takes the radon out of the house by increasing leakage velocity. Two, decrease the difference pressure between indoor and outdoor environment, driving force, which decreases radon entry rate into the house.

The heating, ventilation and air conditioning systems, because of the changing pressure or temperature, create pressure-driven convective flow, in which the apparent velocity of fluid flow through a cross-sectional area is related to the pressure gradient (Spoel, 1998).

4.4 Analytical and measurements methods results

In this work an analytical solution and a measurement method have been used for validation of the numerical model. Each pressure jump in an intake fan or exhaust fan corresponds to a specific mass flow rate. In other words, different pressure jumps correspond to different ventilation rates. Here we have considered three air change rates for validation of the numerical model. Table VI shows the radon concentrations of the house from measurements, analytical calculation and numerical simulation techniques. Comparison of these analytical data with the measured data showed close agreement. This close agreement remained in spite of the errors inherent in all the techniques, such as the 10 percent uncertainty in measurement by the CRM. Results show that differences between analytical solution and numerical model are below 10 percent (Table VI).

Results of measurement method have also been plotted in Figure 8 which is measured with a CRM.

Figure 7.
Effect of air velocity
leakage through the door
on radon concentration
from CFD model outputs

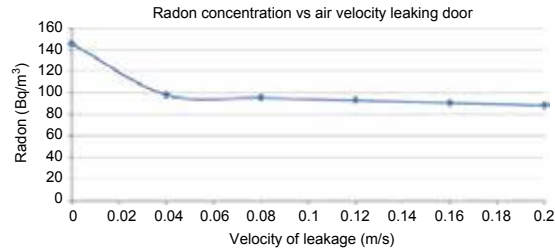


Table VI.
Indoor radon
concentrations results

| Ach (h ⁻¹) | Measurement (Bq/m ³) | Analytical (Bq/m ³) | Numerical (Bq/m ³) | Difference (%) |
|------------------------|----------------------------------|---------------------------------|--------------------------------|----------------|
| 0.25 | 90 | 106 | 100 | 0.9 |
| 0.5 | 45 | 53 | 65 | 3.6 |
| 1 | 25 | 22 | 30 | 10.0 |

This analytical solution along measurement method gives sufficient validation for the numerical model.

Results of the numerical study indicated that indoor pressure created by ventilation systems and infiltration through doors or windows has significant effects on indoor radon content. Comparison of Figures 3 and 6 shows that the location of vents can affect on indoor radon distribution and indoor radon level.

5. Conclusions

The method by which radon concentration is modeled in FLUENT software is a key factor for solving transports equations in turbulence modeling and enhancing accuracy of the results.

A model for radon entry through soil into a one family house in 3D was developed in FLUENT. The results indicate that indoor radon concentrations are dependent on ventilation specifications and indoor and outdoor conditions.

Verification of the model and its performance show that radon entry to the house and ventilation effects were well defined both physically and numerically.

The performance and sensitivity of the model were confirmed by changing a number of input parameters and boundary conditions.

According to the simulation results, distribution of radon is homogeneous except near exhaust or intake fans. The concentration of radon decreases exponentially with increasing indoor pressure and ventilation rate. The results of simulation, analytical analysis and measurement agreed well with each other.

Discrepancies found here between CFD simulation, measurement and mathematical methods may have resulted from insufficiently detailed representations of boundary and initial conditions. It may be possible to further improve CFD results by using a more refined representation of grids and certain boundary conditions, such as pressure and temperature differences between the inside and outside. Meanwhile, the use of CFD for quantitative estimation of indoor radon concentration requires careful validation of the CFD methods.

In conclusion, CFD is a powerful tool for exploring the factors that influence radon distribution in residential buildings. However, the accuracy of simulations of indoor radon and indoor conditions can only be confirmed for conditions that have been validated. This model may also be improved by considering some real situations in residential buildings, internal heating sources and external situations. The problem can be modeled by integration of all or specific combinations of parameters such as the outdoor weather or indoor conditions.

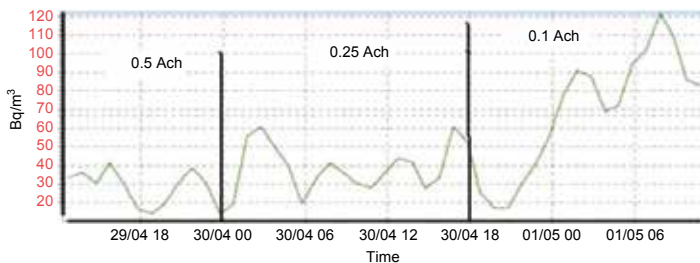


Figure 8.
Radon level vs ventilation
rate from measurement

References

- Ahmed, J.U. (1994), "Radon in the human environment: assessing the picture", *International Atomic Energy Agency Bulletin*, Vol. 36 No. 2, pp. 32-35.
- Amissah, P.K. (2005), "Indoor air quality: combining air humidity with construction moisture", working paper, Energy Systems and Research Unit, University of Strathclyde, Glasgow.
- Arvela, H. (1995), *Residential Radon in Finland: Sources, Variation, Modelling and Dose Comparisons*, Finnish Center for Radiation and Nuclear Safety, Helsinki.
- Awbi, H.B. (2003), *Ventilation of Buildings*, Taylor & Francis, London.
- Cehlin, M. and Moshfegh, B. (2002), "Numerical and experimental investigation of air flows and temperature patterns of a low velocity diffuser", *Indoor air 2002 Proceedings of 9th International Conference on Indoor Air Quality and Climate in Monterey, USA, Fraunhofer-Stuttgart*, pp. 765-770.
- Clavensjo, B. and Akerblom, G. (1994), *The Radon Book: Measures Against Radon*, The Swedish Council for Building Research, Stockholm.
- Cohilis, P., Wouters, P. and L'Heureux, D. (1991), "Prediction of the performance of various strategies of subfloor ventilation as remedial action for radon problems", *Ventilation System Performance Proceedings of AIVC 11th Conference, Belgirate, 1990, Vol. 2*, pp. 17-40.
- European Collaborative Action (2003), "Ventilation, good indoor air quality and rational use of energy", working paper (Report No. 23, EUR 20741 EN), Office of Official Publications of the European Communities, Luxembourg.
- FLUENT Incorporation (2005), *FLUENT User's Guide Version 6.3*, FLUENT Inc, Lebanon, NH.
- Gadgil, A.J., Lobscheid, C., Abadie, M.O. and Finlayson, E.U. (2003), "Indoor pollutant mixing time in an isothermal closed room: an investigation using CFD", *Atmospheric Environment*, Vol. 37 Nos 39-40, pp. 5577-5586.
- Holmes, S.A., Jouvray, A. and Tucker, P.G. (2000), "An assessment of a range of turbulence models when predicting room ventilation", *Healthy Buildings 2000 Proceedings of the International Conference in Espoo, Vol. 2*, pp. 401-406.
- Kokotti, H. (1995), *Dependence of Radon Level on Ventilation Systems in Residences*, Kuopio University Publication, Kuopio.
- Launder, B.E. and Spalding, D.B. (1974), "The numerical computation of turbulent flows", *Computer Methods in Applied Mechanics and Engineering*, Vol. 3 No. 2, pp. 269-289.
- Loureiro, C.O. (1987), *Simulation of the Steady-State Transport of Radon from Soil into Houses with Basements under Constant Negative Pressure*, Lawrence Berkeley National Laboratory, University of California, Berkeley, CA.
- Man, C.K. and Yeung, H.S. (1997), "The effects of cracks and holes on the exhalation of radon from concrete", *Building and Environment*, Vol. 32 No. 4, pp. 351-354.
- Marley, F. and Phillips, P.S. (2001), "Air-movement control of radon in a retail store", *Environmental Management and Health*, Vol. 12 No. 5, pp. 483-491.
- Mora, L., Gadgil, A.J. and Wurtz, E. (2003), "Comparing zonal and CFD model predictions of isothermal indoor airflows to experimental data", *Indoor Air*, Vol. 13 No. 2, pp. 77-85.
- Nilsson, P.E. (2003), *Achieving the Desired Indoor Climate: Energy Efficiency Aspects of System Design*, Studentlitteratur AB, Lund.
- Petropoulos, N.P., Anagnostakis, M.J. and Simopoulos, S.E. (2001), "Building materials radon exhalation rate: ERRICCA intercomparison exercise results", *Science of The Total Environment*, Vol. 272 Nos 1-3, pp. 109-118.
- Pitarma, R.A., Ramos, J.E., Ferreira, M.E. and Carvalho, M.G. (2004), "Computation fluid dynamics: an advanced active tool in environmental management and education",

-
- Management of Environmental Quality: An international Journal*, Vol. 15 No. 2, pp. 102-110.
- Radonelektronik (2012), "Electronic Radon Gas Monitor", available at: www.radonelektronik.se (accessed July 13, 2012).
- Rota, R., Canu, P., Carra, S. and Nano, G. (1994), "Ventilated enclosure with obstacles: experiments and CFD simulations", *Ventilation for Contaminant Control Proceedings of the 4th International Symposium in Cincinnati, OH, Vol. 1*, pp. 181-186.
- Spoel, W.H. (1998), "Radon transport in sand: a laboratory study", working paper, Technische Universiteit Eindhoven, Eindhoven, March 23.
- Tung, T.C.W. and Burnett, J. (2004), "Radon measurement protocol for residences with different ventilation rates", *Indoor and Built Environment*, Vol. 13 No. 2, pp. 133-138.
- Wang, F. and Ward, I.C. (2000), "The development of a radon entry model for a house with a cellar", *Building and Environment*, Vol. 35 No. 7, pp. 615-631.
- Zhang, Y. (2004), *Indoor Air Quality Engineering*, CRC Press, Boca Raton, FL.
- Zhang, Z. and Chen, Q. (2006), "Experimental measurements and numerical simulations of particle transport and distribution in ventilated rooms", *Atmospheric Environment*, Vol. 40 No. 18, pp. 3396-3408.
- Zhou, W., Iida, T., Moriizumi, J., Aoyagi, T. and Takahashi, I. (2001), "Simulation of the concentrations and distributions of indoor radon and thoron", *Radiation Protection Dosimetry*, Vol. 93 No. 4, pp. 357-367.

About the authors

Keramatollah Akbari is a PHD student at the Malardalen University, Sweden. He is also an academic member at ACECR – Fars Branch and trainer of Entrepreneurship in Shiraz University, Iran. He teaches such courses as General Mathematics, Statistics & Probability, Systems Analysis and Design, Management Principles and Entrepreneurship. He is also involved in the projects of radon reduction and energy consumption in buildings, priorities in electronic industries units, project considering the establishment of aggregation, processing and marketing information center, considering new job opportunities in the field of information technology (IT) and electronics, business plan of civil information and services center.

Jafar Mahmoudi is an Adjunct Professor at the Malardalen University, Department of Public Technology, Energy Tech, Vasteras, Sweden. His university chair is Process Optimization in Metal Industry. He is the head of directing board and president of MESET, Sweden. His major research focus is development of new technology and methods for industrial energy optimization with special focus on heat and mass transfer. He has years of theoretical and experimental experience on this. He also has a broad technical background encompassing thermodynamic, numerical methods and modeling (CFD computation), as well as materials science.

Mahdi Ghanbari graduated as Master of Science in Energy Systems Engineering in 2009. The studies were conducted at the Department of Energy Engineering at the Sharif University of Technology, Iran. He is now working on the projects at the ACECR – Sharif University Branch, primarily with computational fluid dynamics within a wide range of applications. He is also involved in the projects of energy auditing in industries and projects including CHP systems design, heat exchangers design, optimization using genetic algorithm and energy recovery systems.

Paper III

Effects of Heat Recovery Ventilation Systems on Indoor Radon

Keramatollah Akbari^a, Jafar Mahmoudi^b

^a*TDI researcher at ACECR, Iran and Mälardalen University, PhD student, School of Sustainable Development of Society and Technology, Västerås, Sweden*

keramatollah.akbari@mdh.se

^b*Mälardalen University, Adj Professor at School of Sustainable Development of Society and Technology, Västerås, Sweden* jafar.mahmoudi@mdh.se

Abstract

A heat recovery ventilation system enables us to control indoor conditions such as ventilation rate, temperature, relative humidity and pressure difference. These environmental conditions affect indoor radon levels.

Computational fluid dynamics (CFD) is a powerful tool for predicting and visualizing radon content and indoor air quality and is cost effective in comparison with other methods such as full scale laboratory and gas trace techniques.

In this study a mechanically balanced ventilation system and a continuous radon monitor (CRM) were used to measure the indoor ventilation rate and radon levels. In a numerical approach the FLUENT CFD package was used to simulate radon entry into the building and effects on indoor air conditions.

The effects of different ventilation rates, indoor temperature and relative humidity on indoor radon concentrations were investigated in a one family detached house in Stockholm. Results of numerical studies indicated that changes of ventilation rate, indoor temperature and moisture by means of ventilation systems have significant effects on indoor radon content. Ventilation rate was inversely proportional to indoor radon concentration. Minimum radon levels were estimated in the range of thermal comfort, i.e. at 21°C and relative humidity between 50-70%.

The analytical solution was used to validate numeric results at 3 distinct air change rates. Comparisons between numerical and analytical results showed good agreement but there was poor agreement between simulations and measurement results due to the short measuring period.

Keywords:

Numerical modeling, Radon mitigation, Balanced Ventilation, Residential buildings

Nomenclature

| | | | |
|---------------|--|----------------|--|
| A | surface(m^2) | λ_v | air change rate (h^{-1}) |
| C | radon concentration ($Bq.m^{-3}$) | λ_{Rn} | radon decay constant ($2.1 \times 10^{-6} s^{-1}$) |
| D | diffusion coefficient | ν | air kinematic viscosity($1.1 \times 10^{-5} m.s^{-1}$) |
| D_h | hydraulic diameter | ATD | alpha track detector |
| E | radon exhalation rate ($Bqm^{-2}h^{-1}$) | CFD | computational fluid dynamics |
| G | source term | CRM | continuous radon monitor |
| K | turbulence kinetic energy | HRV | heat recovery ventilation system |
| Pa | Pascal | Re | Reynolds number |
| T | temperature ($^{\circ}C$) | RH | relative humidity |
| V | volume of the house(m^3) | | |
| U_r | equivalent room velocity | | |
| ρ | density($kg.m^{-3}$) | | |
| ε | energy dissipation rate | | |

1.Introduction

Understanding indoor radon transport and distribution is a priority, and for this it is important to be able to predict indoor air quality and the exact value of radon level at different points and areas, especially in breathing zones in residential buildings.

Indoor radon distribution and treatments have been studied through measurements and full scale laboratory and tracer gas models. These methods are rather expensive and time consuming. Analytical methods are also limited to varying ventilation rates, and radon measurements are generally expressed as average monthly or annual levels.

A numerical modeling approach using computational fluid dynamics (CFD) techniques may be a powerful and cost-effective tool to study and predict indoor radon distribution. Numerical models can be used to estimate the importance of specific factors for radon entry. These models also can provide a cost-effective test bench for improved designs of radon prevention systems [1,2].

CFD techniques are based on solving the transport equations iteratively and are employed to solve equations involving velocity, temperature and species transport numerically in a finite volume. They describe the processes in the ventilated room, including the conservation of mass, energy, momentum and species such as radon [3, 4].

Numerous studies have used CFD to study the distribution of indoor air flow and radon concentration in two and three dimensions. Some of these studies are described in the following paragraphs.

Zhuo [5] used CFD to study the concentrations and distributions of indoor radon in three dimensions. According to the results of this simulation, the distribution of radon in a ventilated room is uniform except at locations near air diffuser vents. He showed that the results of simulations of activities and their distributions agreed well with experimental results in a laboratory. Feng and Persily [6] performed computer simulations of airflow and radon transport in a large building using the multi-zone airflow and pollutant transport model CONTAM88. This study investigated ventilation system factors including the operation of exhaust fans and variations in outdoor air intake.

Wang and Ward [7] used the CFD package FLUENT to develop a model of multiple radon entry in a house with a cellar. In order to develop the model, they applied methods such as using a subroutine to specify the radon generation rate in the soil cells and designed appropriate boundary conditions. The model was verified by a grid-independency test and convergence behavior analysis. The inter-model validation technique and comparison with analytical solutions were also used to validate the model.

Cohilis [8] suggested the use of a numerical code based on the finite difference method. Based on the results and the code validation, they concluded that this method was a powerful tool that could predict and evaluate the performance of subfloor ventilation strategies.

Rota [9] compared the results of numerical simulations and experiments. The results showed good agreement, but the simulation results showed elevated concentrations in the region with low ventilation rates compared to the experiments. Unlike the previous cited works, this study focuses on indoor radon concentration, in this case the diffusion and advection forces are considered and there is not any radon decay and generation rate.

1. Material and Methods

In this study a continuous radon monitor (CRM) and alpha track detectors (ATD) were used to measure indoor radon concentrations. A one family detached house with a rotary heat exchanger ventilation system was used in a case study. Numerical methods, measurement and analytical calculations were used to estimate radon levels, as detailed in the following section.

The house consists of eight rooms with a total volume of $12 \times 9 \times 2.4 \text{ m}^3$. Each room has its own vent except for Room 8, which shares a vent with Room 6. All doors are kept open. A rotary heat exchanger is placed in Room 4. The effect of the heat exchanger is ignored and an outlet vent is considered in Room 4 to play the role of the heat exchanger. Figure 1 shows the geometry of the house plan.

2.1. Numerical method

In the numerical approach the commercial CFD package including GAMBIT was used to define the geometry, and FLUENT 6.3 [10] was used as the solver for calculations to simulate radon entry into the building and ventilation effects.

The selected 3dimensional model was: species transport, pressure base and steady state, $k-\epsilon$ turbulence, and the SIMPLE algorithm were used to calculate and predict radon concentration at all grid locations numerically.

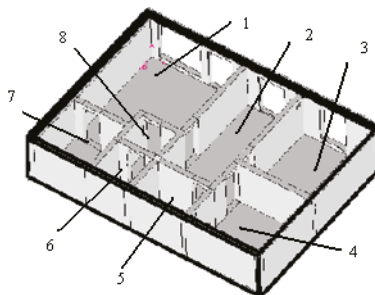


Fig.1. The geometry of the house plan

The model is meshed with 376238 hexahedral cells with 10 cm vertices in order to solve the conservation equations of various fluid properties within each cell. These equations are flow, energy, turbulence, radon and humidity.

Three criteria were considered to confirm the model convergence. The first criterion was the residuals of equations residuals could not change drastically through iterations and the residuals of all the conservation equations had to be less than 1×10^{-7} .

The second criterion was that the concentration of radon in one of the rooms (Room 1) could not change through iterations. The third criterion concerned the rate of radon passing through the outlet. As the model is solved for the steady state, all radon which is generated in the floor must also pass through the outlet, i.e. radon rate from the outlet must be equal to the radon generation rate. Specifically, radon rate through the outlet must be 2 bq/s and 3 bq/s for 1 Pa and 2 Pa pressure differences respectively. In order to avoid residual instability and oscillations, under relaxation factors were adjusted to speed up the convergence.

The results of using 376238 and 752476 cells were compared to ensure that the grid cells were sufficiently small to ensure accurate results.

The model was solved for four different air change rates. Specifically, Ach=0.05, 0.25, 0.5 and 1.2. Temperature and relative humidity were assumed to be fixed at 30 °C and 30% respectively in these cases. The difference pressure was set at 1kPa.

2.1.1. Initial values and boundary conditions

The materials used in the model are air, water vapor, radon as a fluid in a mixture and light concrete for the floor, dense concrete for walls, windows material and main door as solid materials. Internal doors are left open. Properties of radon are given in the previous sections. Properties of the other materials are as shown in Tables 1 and 2.

Table 1. Properties of Fluids

| Properties | Air | Water Vapor | Radon |
|------------------------------|-------------------------|-----------------------|----------------------|
| Density (kg/m ³) | 1.225 | 0.5542 | 9.73 |
| C _p (j/kg-k) | 1006.43 | 2014 | 96.35 |
| K (w/m-k) | 0.0242 | 0.026 | 0.0036 |
| Viscosity(kg/m.s) | 1.7894×10 ⁻⁵ | 1.34×10 ⁻⁵ | 1.8×10 ⁻⁵ |
| M _w (kg/kmol) | 28.966 | 18.0153 | 222 |

Table 2. properties of Solids

| Material | Density kg/m ³ | C _p j/kg-k | K w/m-k |
|----------------|------------------------------|--------------------------|------------|
| Light concrete | 1200 | 1000 | 0.4 |
| Dense concrete | 2100 | 840 | 1.4 |
| Windows | 2700 | 880 | 0.8 |
| Main Doors | 720 | 1250 | 0.16 |

Boundary conditions in the model are: 7 vents in rooms, outer surfaces, floor zone, outlet, walls zones and room zones. Characteristics of these boundaries are as follows.

The vent in each room is defined as the velocity inlet boundary. Specifications which must be defined for this type of boundary are velocity, hydraulic diameter, temperature and mass fraction of radon and mass fraction of water vapor.

2.2. Measuring method

Radon concentrations were measured continuously during winter and spring, both with a continuous radon meter (CRM) and an alpha track detector (ATD). The air change rates in the house also were measured by the heat recovery ventilation (HRV) system.

2.3. Analytical method

Indoor radon content can be calculated as

$$C = \frac{\frac{EA}{V(\lambda_{Rn} + \lambda_v)}}{\frac{E}{h(\lambda_{Rn} + \lambda_v)}} \quad (1)$$

Where $C(\text{Bqm}^{-3})$ is indoor radon concentration at the steady state, $E(\text{Bqm}^{-2}\text{h}^{-1})$ is radon exhalation rate, $A(\text{m}^2)$ is the radon exhalation surface (in this study the house floor), $V(\text{m}^3)$ is the volume of the house, $\lambda_{\text{Rn}}(2.1 \times 10^{-6} \text{ s}^{-1})$ is the radon decay constant and $\lambda_v(\text{h}^{-1})$ is the air change rate in the house and $h=2.4 \text{ m}$ is the height of the house. For $E = 65 \text{ Bqm}^{-2}\text{h}^{-1}$ (11) and the given data of the case study house, Equation (1) gives indoor radon levels for different ventilation rates (0, 0.25, 0.5 and 1).

3. Results and discussion

3.1. Numerical results

Graphical presentations of the three dimensional simulation data were prepared using FLUENT contours. These contours are a good tool for qualitative comparisons. From the FLUENT report, it is also possible to determine the numeric data for quantitative comparisons. This study investigated the effects of: 1. Ventilation rate, 2. Temperature, 3. Relative humidity, and 4. Pressure difference

1. Ventilation rate:

Contours of radon concentration in the house plan at position $y=210 \text{ cm}$ from the floor for various air change rates are shown in Figure 4. This figure shows qualitative comparisons of radon concentrations at four different hourly air change rates ranging from 0.05 to 1.2 Ach.

As evident from Figure 5, different ventilation rates have distinct effects on indoor concentration in Room 1. The quantitative comparisons are plotted in Figure 6, which shows that the radon concentration levels were inversely proportional to outdoor flow rate at steady state.

Numerical simulations were performed at different Reynolds numbers. The Reynolds number in the house was calculated using Equation (2):

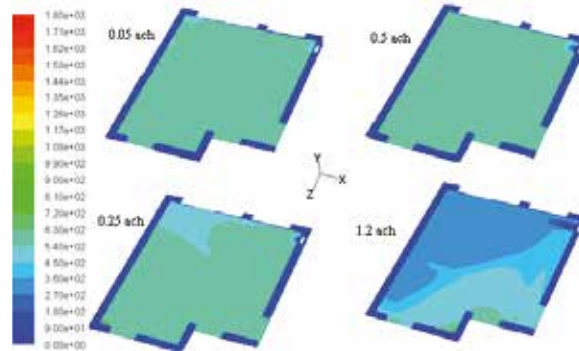


Figure 4. Contours of radon concentration in the house plan (Room1) with air change rates 0.05-1.2 Ach

$$\text{Re} = D_h \times U_r / \nu \quad (2)$$

where D_h is the hydraulic diameter of room and is defined as: $2WH/(W + H)$ (W = width, H = height), U_r is the equivalent room velocity (flow rate/cross-sectional area) and ν ($1.1 \times 10^{-5} m/s$) is the kinematic viscosity of air [3]. The Reynolds numbers were 2×10^4 and greater than 2×10^5 , corresponding to ventilation rates of 0.05 and greater than 0.5 Ach.

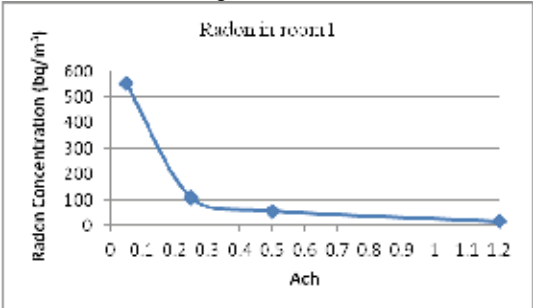


Figure 5. Radon concentrations in Room1 versus air change rate

2. Temperature:

In order to investigate the effects of temperature changes on radon concentration, air change and relative humidity were fixed and indoor temperature was varied between 15 °C to 25 °C. Air change and relative humidity were maintained at 0.5 and 30% respectively. The temperature effects are shown qualitatively in Figure 6. Indoor radon levels were inversely proportional to indoor temperature. This is because of the direct correlation between temperature and pressure as stated by the constant gas law. Thus, increasing temperature increases the pressure, and since the indoor radon concentration is driven by pressure, the amount of radon driven into the room decreases. From another perspective, increasing the house temperature increases indoor pressure and the outside acts a vacuum cleaner and sucks away the indoor air. This phenomenon is referred to as the "stack effect"[12].

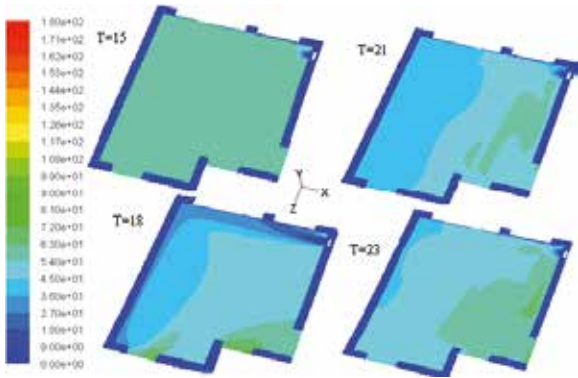


Figure 6. Contours of radon concentration in Room 1 at different temperatures

Figure 7 shows the contours of radon concentration at y=120 cm from the floor for various temperatures.

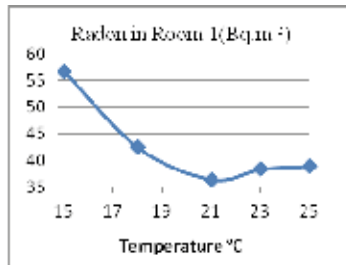


Fig.7. Radon concentrations in Room1 versus temperature

3. Relative humidity

The effect of varying relative humidity on radon concentration in Room 1 is shown in Figure 8. Relative humidity is varied between 30 to 80% and temperature and air change are maintained at 18°C and 0.25 respectively.

Figure 8 indicates that radon concentration decreases from RH 30% to 70%, and increases when RH rises from above 70%.

This is because increasing humidity from zero to a defined quantity below 50% increases the pressure gradient in air. This increases the driving force that draws the radon out of the ground. However, higher RH levels result in denser air, and radon is unable to rise to high altitudes. Increased moisture in air also decreases diffusion coefficient and hence reduces the diffusion length of radon, which reduces transfer of radon to areas of low radon concentration.

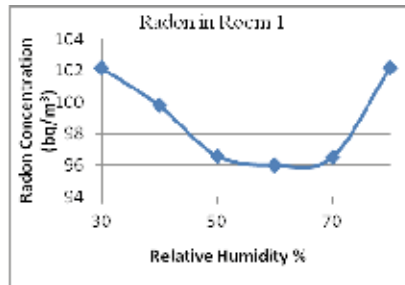


Fig. 8. Radon concentrations in Room1 versus relative humidity

4. Pressure difference

The model was solved for 1 Pa and 2 Pa difference pressures. Radon entry rate varies with pressure difference. Previous work in the field has established entry rates of 2 Bq/s and 3 Bq/s for pressure differences of 1 Pa and 2 Pa respectively [1].

Air change rate, temperature and relative humidity are maintained at 0.25, 18 °C and 40% respectively.

Contours of radon concentration in a plane at y=120 cm from the floor are shown in Figure 9, and clearly show that pressure difference affects indoor radon levels.

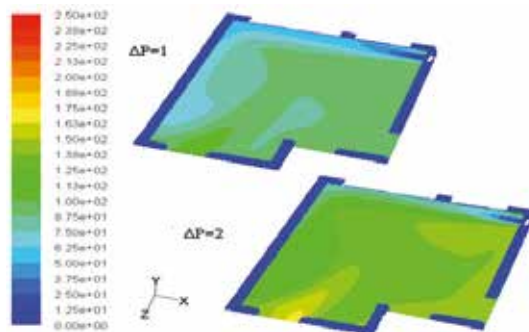


Figure 9. Contour of radon concentration for $\Delta p=1\text{Pa}$ and 2 Pa

3.2 Measuring results

The results of measurements are shown in Table 3. In order to show the impact of ventilation rate on radon level, radon concentrations were measured at three different ventilation rates. Figure 10 shows the results at three different air change rates, measured with a CRM. The figure shows that measured radon levels were inversely proportional to air exchange rate.

Continuous radon measurements using a CRM also confirmed that in the indoor temperature range, fluctuating radon levels in the house have a strong indirect correlation with temperature (Figure 11).

Table 3. Measured indoor radon levels (Bq.m^{-3})

| Date and period | ATD | CRM | Ventilation rate | Ventilation type | Remedial action |
|----------------------|----------|----------|------------------|------------------|----------------------|
| 2008-2 (2weeks) | 3580 380 | ----- | 0.25 | Extract fan | No action |
| 2010-1 (3months) | 1280 160 | 1580 158 | 0.25 | HRV | Radon sump & sealing |
| 2010-04 (3 weeks) | 100 20 | ----- | 0.5 | HRV | 3connected sumps |
| 2010-3 (12days) | ----- | 97 10 | 0.5 | HRV | 3connected sumps |
| 2010-3 (12days) | ----- | 65 6 | 0.5 | HRV | 3connected sumps |
| 2010-4 (12 days) | ----- | 36 4 | 1 | HRV | 3connected sumps |

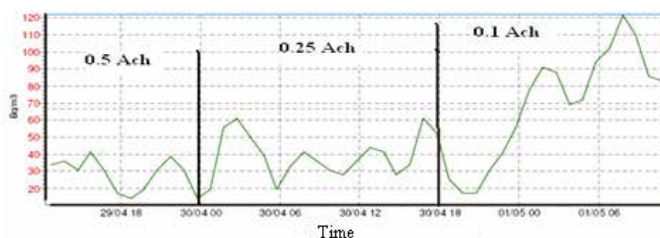


Fig.10. Measured radon level measurements versus ventilation rate

3.3. Analytical results

As previously mentioned, Equation (1) was used for analytical calculation and air change rates were set at 0.25, 0.5, and 1.2 h⁻¹. The results are shown in Table 4.

4. Defined Functions

In our estimates, radon concentrations are given in bq.m⁻³, whereas the FLUENT package gives molar concentration of radon in kmol.m⁻³. We therefore define a Custom Field Function to calculate radon concentration (bq.m⁻³) in term of molar radon concentration as follows:

$$C_{Rn} \left(\frac{bq}{m^3} \right) = \frac{C_{Rn,molar} \left(\frac{kmol}{m^3} \right) \times M_{Rn} \left(\frac{kg}{kmol} \right)}{1.75 \times 10^{-19} \left(\frac{kg}{bq} \right)} \quad (3)$$

Where $M_{Rn} = 222 \frac{kg}{kmol}$ is the molecular weight of radon.

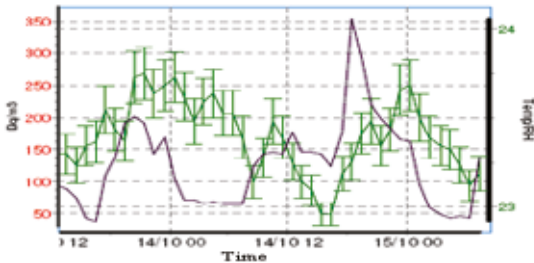


Fig. 11. Radon level (green) versus temperature (black)

5. Model Validation

Model validation was performed using analytical solution. The numeric differences between numerical simulation and analytical calculation results are shown in Table 4.

For quantitative comparisons, the percentage difference between the results of estimation by FLUENT and the analytical calculations were computed at each ventilation rate. The maximum difference was found to be below 10%. Measurement data were not suitable for comparison, because the measuring period was too short to obtain an acceptable average radon level.

Table 4. Indoor radon concentrations result in Bq.m⁻³

| Ach | Measurement | Analytic | Numeric |
|------|-------------|----------|---------|
| 0.0 | 3580 | 3582 | ----- |
| 0.25 | 90 | 106 | 107 |
| 0.5 | 45 | 53 | 55 |
| 1.2 | 25 | 22 | 20 |

6. Conclusion

The models were developed in FLUENT with simulated radon entry through the floor into a one family house in three dimensional models. The results support the hypothesis that indoor radon concentrations are indoor temperature and moisture dependent.

The verification of the model and its performance indicate that radon entry to the house and the effects of temperature and moisture have been well defined physically and numerically. The performance and sensitivity of the model was confirmed by varying input parameters and boundary conditions. The effects of different parameters of indoor air such as ventilation rate, indoor-outdoor pressure difference, indoor temperature and relative humidity on indoor radon concentrations were investigated. The value of mass flow rate at the air inlet outlet affected the distribution patterns of indoor radon, both qualitatively and quantitatively.

Discrepancies were found here between CFD simulation, numerical calculations and measurement data. These may have resulted from insufficiently detailed representation of boundary conditions and inaccuracies of measured data due to the short measurement period.

In conclusion, CFD is a powerful research tool for predicting the factors that influence indoor radon distribution. However, further improvement of the accuracy of the quantitative estimations of radon concentration will require more detailed consideration of turbulence, near wall effects, grid refinement near the vents, and development of a robust validation method.

References

- [1] Andersen C. E., Numerical modeling of radon-222 entry into houses: an outline of techniques and results, the science of total environment, 2001, Vols. 272: 33-42.
- [2] Wang F., Ward I. C., Radon entry, migration and reduction in houses with cellars, 2002, Vols. 37 (2002) 1153 – 1165.
- [3] Awbi H.B., Ventilation of building,. 2003.
- [4] Loureiro C.O., Simulation of the steady-state transport of radon from soil into houses with basement under constant negative pressure. s.l. Report no. LBL-24378. Lawrence Berkeley Laboratory, Berkeley, CA., 1987.
- [5] Zhuo W., Iida T., Moriizumi J., Aoyagi T. and Takahashi I., Simulation of the concentrations and distributions of indoor radon and thoron, 2000.
- [6] Fang J. B., Persily A. K., Computer Simulations of Airflow and Radon Transport in Four Large Buildings, Building and Fire Research Laboratory, 1995.
- [7] Wang F., and Ward I. C., Development of a radon entry model for a house with a cellar, 2000, Vols. 35 (2000) 615-631.
- [8] Cohilis P., Wouters P., and L'Heureux D., Prediction of The Performance of Various Strategies of Subfloor Ventilation as Remedial Action For Radon Problems. 2004.
- [9] Rota, R., Ventilated enclosure with obstacles: experiments and CFD simulations. Cincinnati, OH: NIOH. pp. 181–6. : s.n., 1994. In Proceedings of the 4th International Symposium on Ventilation for Contaminant Control. Vol. 1.
- [10] FLUENT Incorporated. FLUENT. User's Guide Version 6.3. Linux Format, Cavendish Court, Lebanon, NH 03766, USA: s.l. FLUENT, 2005. 2005.
- [11] Goto M., Estimation of Global Radon Exhalation Rate Distribution. 2008.
- [12] Hoffmann R. L., Radon contamination of residential structure, an overview of factors influence infiltration rates. s.l. Illinois Central College, 1997.

Paper IV



Contents lists available at SciVerse ScienceDirect

Journal of Environmental Radioactivity

journal homepage: www.elsevier.com/locate/jenvrad



Influence of indoor air conditions on radon concentration in a detached house

Keramatollah Akbari^{a,b,*}, Jafar Mahmoudi^b, Mahdi Ghanbari^c

^a ACECR, Fars Branch, Shiraz, Iran

^b Mälardalen University, School of Sustainable Development of Society and Technology, Box 724 80, Västerås, Sweden

^c Sharif University of Technology, Tehran, Iran

ARTICLE INFO

Article history:

Received 11 February 2012

Received in revised form

28 July 2012

Accepted 23 August 2012

Available online

Keywords:

Numerical modeling

Radon mitigation

Air change rate

Temperature

Relative humidity

ABSTRACT

Radon is released from soil and building materials and can accumulate in residential buildings. Breathing radon and radon progeny for extended periods hazardous to health and can lead to lung cancer. Indoor air conditions and ventilation systems strongly influence indoor radon concentrations. This paper focuses on effects of air change rate, indoor temperature and relative humidity on indoor radon concentrations in a one family detached house in Stockholm, Sweden.

In this study a heat recovery ventilation system unit was used to control the ventilation rate and a continuous radon monitor (CRM) was used to measure radon levels. FLUENT, a computational fluid dynamics (CFD) software package was used to simulate radon entry into the building and air change rate, indoor temperature and relative humidity effects using a numerical approach.

The results from analytical solution, measurements and numerical simulations showed that air change rate, indoor temperature and moisture had significant effects on indoor radon concentration. Increasing air change rate reduces radon level and for a specific air change rate (in this work $Ach = 0.5$) there was a range of temperature and relative humidity that minimized radon levels. In this case study minimum radon levels were obtained at temperatures between 20 and 22 °C and a relative humidity of 50–60%.

© 2012 Elsevier Ltd. All rights reserved.

1. Introduction

Indoor air change rate, temperature and relative humidity have significant effects on radon levels in residential buildings. Active and appropriate ventilation can control the ventilation rate and maintain indoor conditions in order to mitigate radon in residential buildings (Clever, 1979; Surbeck, 1996).

Numerous studies have found that indoor radon generally correlates with indoor and outdoor air conditions, and factors such as indoor and outdoor pressure, temperature, moisture, ventilation rate and precipitation can affect radon entry into buildings (Andersen, 2001; Van der Pal and Van der Spoel, 2001). In this study we focus on the effects of indoor air change rate, temperature and relative humidity on indoor radon.

Computational fluid dynamics (CFD) is a powerful tool that can simulate and predict airflow patterns, indoor air conditions and concentration distributions of pollutants in a space at low cost. In this study, FLUENT, a CFD software package was used to simulate

and predict radon distribution and visualize the effects of indoor air temperature and moisture. Analytical solution and measurements were also performed for validation of numerical simulation.

2. Problem specifications

The case study is a one family detached house located in Stockholm, built on bedrock in 1975. The house plan comprises of 8 rooms and its volume is $12 \times 9 \times 2.4 \text{ m}^3$. Each room has its own vent, except Room 8, which shares a vent with Room 6. All doors are supposed to be kept open. A rotary heat exchanger is placed in Room 4. Here the effect of the heat exchanger is ignored and an outlet vent is considered instead to play the role of the heat exchanger in Room 4. The house is occupied but there is no energy source among furniture and they are not too large that can affect on radon concentration and distribution in the house. So we can neglect the effects of furniture in the model. Fig. 1 presents the house plan. The air change rate in each of the rooms corresponds to the volume of that room, and all inlet air from the rooms passes through the unique outlet.

The radon level after some remediation was around 600 Bq/m^3 , mainly originating as soil gas from the building's foundations. The house is in direct contact with the ground, and radon entry is driven by two disturbance pressures along its route into the house.

* Corresponding author. Mälardalen University, School of Sustainable Development of Society and Technology, Box 724 80, Västerås, Sweden.

E-mail addresses: keramatollah.akbari@mdh.se (K. Akbari), jafar.mahmoudi@mdh.se (J. Mahmoudi), ma.ghanbari@gmail.com (M. Ghanbari).

Nomenclature

| | |
|-----------|--|
| k | Kinetic energy |
| C_p | Specific heat (J/kg K) |
| ν | Kinetic viscosity (kg/m s) |
| u, v, w | Velocity components in x, y, and z – coordinates |
| A | Area (m ²) |
| M_w | Molecular weight (kg/k mol) |
| RH | Relative humidity |
| C | Radon concentration (Bq/m ³) |
| L | Characteristic length (m) |
| Ach | Air change |
| CRM | Continuous radon monitor |

| | |
|---------------|---|
| Grad | Gradient |
| K | Thermal conductivity (W/m K) |
| ε | Dissipation rate |
| S | Source term |
| \mathbf{V} | Velocity vector (m/s) |
| ρ | Density (kg/m ³) |
| D | Radon diffusion coefficient (m ² /s) |
| T | Temperature (°C) |
| Δp | Pressure difference (Pa) |
| V | Velocity (m/s), Volume (m ³) |
| Re | Reynolds number |
| CFD | Computational fluid dynamics |
| Div | Divergence |

The research methods include analytical solution, measurements and numerical simulation.

Radon entry into a one family detached house and effects of ventilation rate, temperature and moisture are modeled using the FLUENT package in a three dimensional steady state model. A continuous radon monitor (CRM) was used to measure the indoor radon and check the numerical modeling method. Analytical solution was also performed for validating of numerical simulation.

3. Numerical simulation approach

FLUENT software can model the mixing and transport of chemical species by solving conservation equations describing convection and diffusion. For all flows, FLUENT solves conservation equations of mass and momentum. In this work, flows involve heat and species transfer, thus additional equations of energy and species conservation must be solved (FLUENT Incorporation, 2005).

In this study, a turbulent model is used, because airflow in a ventilated room even with ventilation rates below 0.2 m/s is usually in the turbulent regime, and the turbulent $k-\varepsilon$ model is used to solve the governing equations (Wang and Ward, 2000). The standard $k-\varepsilon$ model is a popular method for numerical simulation of airflow in a room. In FLUENT we define the model as species transport with a mixture of air, radon and water vapor.

3.1. Determining flow pattern

Flow pattern can be determined by calculating Reynolds number. Reynolds number can be obtained from the following expression:

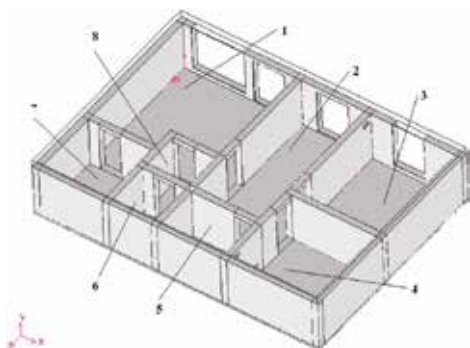


Fig. 1. The geometry of the house plan.

$$Re = \frac{VL}{\nu} \quad (1)$$

Where, ν is the kinetic viscosity of the mixture, V is the velocity at a vent and L is the characteristic length, for example the channel width (Andersen, 2001). Because there are several rooms and therefore several vents, here we use the highest velocity to calculate the Reynolds number. The critical Reynolds number of 2000, at which transient flow becomes turbulent, is used to determine the flow pattern (Lesieur, 1990; Sun et al., 2002).

$$Re_{0.5} = \frac{VL}{\nu} = \frac{0.16389 \frac{m}{s} \times 0.3 m}{1.115 \times 10^{-5} \frac{m^2}{s}} = 4409.6 > 2000 \xrightarrow{\text{yields}} \text{Turbulent flow}$$

3.2. Radon transport equation

For the steady state condition and constant density of radon, the transport equation is written as:

$$\text{div}(\rho C \mathbf{V}) = \text{div}(\rho D \text{grad}(C)) + S \quad (2)$$

In the above expression, C is the radon concentration, S is the source term and \mathbf{V} is the velocity vector, ρ is the density of the radon and D is the diffusion coefficient (Surbeck, 1996). As radon is transported to the air and there is no radon generation and decay in the air itself, $S = 0$, and Equation (2) reduces to Equation (3) in three dimensions. FLUENT solves this equation using numerical methods.

$$\frac{\partial(Cu)}{\partial x} + \frac{\partial(Cv)}{\partial y} + \frac{\partial(Cw)}{\partial z} = \frac{\partial}{\partial x} \left(D \frac{\partial C}{\partial x} \right) + \frac{\partial}{\partial y} \left(D \frac{\partial C}{\partial y} \right) + \frac{\partial}{\partial z} \left(D \frac{\partial C}{\partial z} \right) \quad (3)$$

This equation calculates the radon content at any point in the house.

3.3. Temperature and relative humidity effects on radon properties

Some radon properties, such as radon diffusion coefficient, radon emanation coefficient and radon exhalation rate correlate with temperature, relative humidity and pressure field.

The radon emanation factor is moisture dependent and reaches a constant maximum value as moisture content increases to between 0.1 and 0.5. Since radon exhalation rate is a function of radon emanation coefficient, radon exhalation rate is also moisture dependent.

The radon exhalation rate increases with temperature, but this effect is smaller than the effect of moisture (Stranden et al., 1984).

The radon diffusion coefficient in air and water are $1.1 \times 10^{-5} \text{ m}^2/\text{s}$ and $1.2 \times 10^{-9} \text{ m}^2/\text{s}$ respectively. The radon diffusion coefficient in water is thus much smaller than in air.

The relationship between temperature and radon diffusion coefficient is shown in Equation (4). This equation shows that increasing temperature increases radon diffusion coefficient.

$$D = D_0 e^{\frac{Q}{RT}} \quad (4)$$

Where:

D_0 = Open air radon diffusivity in m^2/s

Q = Activation energy in J mol^{-1}

R = Gas constant $8.31 \text{ J mol}^{-1} \text{ K}^{-1}$

T = Temperature in Kelvin

The dependence of the diffusion coefficient on the relative humidity was reported by Kotrappa et al. (1976), who showed that the maximum value of the diffusion coefficient occurs at 20–80% relative humidity.

Humidity is the amount of water vapor or moisture contained within the air. Relative humidity is defined as:

$$\text{Relative humidity (RH)} = \frac{P_{\text{actual}}}{P_{\text{Water}}} \times 100\% \quad (5)$$

Where:

P_{actual} = Actual partial vapor pressure

P_{Water} = Saturation vapor pressure of water

The saturation vapor pressure of water (P_{water}) can be expressed as (Sonntag, 1990):

$$P_{\text{water}} = ae^{\left(\frac{bT}{c+T}\right)} \quad (6)$$

where, a , b and c are constants; $a = 6.112$, $b = 17.62$ and $c = 243.12$ and $-45 < T < 50^\circ \text{C}$.

This equation demonstrates the effect of temperature on saturation vapor pressure of water. The balance between the condensation and evaporation of water leads to vapor pressure, which depends on the temperature. Air can hold more vapor at high temperatures than at low temperatures.

The total pressure of air (P) is related to P_{water} and defined as follows:

$$P = P_{\text{dry air}} + P_{\text{water}} \quad (7)$$

Where:

P = Pressure disturbance field (relative to absolute pressure) (Pa)

On the other hand, P and V have a direct correlation. As in the radon transport equation (Equation (2)), the term V is pressure field dependent because of the advection mechanism ($V \nabla C = -k/\mu \nabla P \nabla C$) of the indoor radon transport.

This relation indicates that relative humidity due to changing the total pressure has an influence on indoor radon concentration.

3.4. Model meshing

The model is meshed with 10 cm hexahedral elements. All states were solved with this mesh. In order to perform a grid

independency check in the later sections, a second mesh was constructed for the model (see Fig. 2).

3.5. Materials

The materials considered in the model are air, water vapor, radon, light concrete for the floor, dense concrete for walls, windows material and main door material. Internal doors are supposed to be open. Properties of materials are shown in Table 1.

3.6. Boundary conditions

Boundary conditions in the model are: 7 vents in rooms, outer surfaces, floor zone, outlet, walls zones and rooms zones. Characteristics of these boundaries are as follows:

The vent in each room is defined as the velocity inlet boundary. Specifications that must be defined for this type of boundary are velocity, hydraulic diameter, temperature, mass fraction of radon and mass fraction of water vapor.

Each room has the same type of vent, each with an area of 0.06 m^2 . Velocity can be obtained from the following expression.

$$V = \frac{\text{Ach} \times \text{Volume}_{\text{Room}}}{\text{Area}_{\text{Vent}}} \quad (8)$$

For example for Room 1 and the following specification: Ach = 0.5, $V_{\text{Room 1}} = 70.8 \text{ m}^3$, $T = 21^\circ \text{C}$, RH = 30, $\Delta p = 1 \text{ Pa}$, Turbulent flow

$$V = \frac{\text{Ach} \times \text{Volume}_{\text{Room}}}{\text{Area}_{\text{Vent}}} = \frac{0.5 \frac{1}{\text{h}} \times 70.8 \text{ m}^3 \times \frac{1 \text{ h}}{3600 \text{ s}}}{0.06 \text{ m}^2} = 0.16389 \frac{\text{m}}{\text{s}}$$

3.7. Solution methods

The finite volume solution method can be used for solving governing equations. This method either uses a "segregated" or a "coupled" solution procedure.

With segregated methods an equation for a certain variable is solved for all cells, and then the equation for the next variable is solved for all cells, etc.

With coupled methods, for a given cell equations for all variables are solved, and that process is then repeated for all cells.



Fig. 2. Top view of the meshed model.

Table 1
Properties of fluids and solids.

| Properties | Air | Water vapor | Radon | Light concrete | Dense concrete | Windows | Main doors |
|------------------------------|-------------------------|-----------------------|----------------------|----------------|----------------|---------|------------|
| Density (kg/m ³) | 1.225 | 0.5542 | 9.73 | 1200 | 2100 | 2700 | 720 |
| C _p (J/kg K) | 1006.43 | 2014 | 96.35 | 1000 | 840 | 880 | 1250 |
| K (W/m K) | 0.0242 | 0.026 | 0.0036 | 0.4 | 1.4 | 0.8 | 0.16 |
| Viscosity (kg/m s) | 1.7894×10^{-5} | 1.34×10^{-5} | 1.8×10^{-5} | — | — | — | — |
| M _w (kg/k mol) | 28.966 | 18.0153 | 222 | — | — | — | — |

Table 2
Radon concentration (Bq/m³) for various temperatures when Ach = 0.5 and RH = 30% from CFD model outputs.

| | Room 1 | Room 2 | Room 3 |
|-----------|--------|--------|--------|
| T = 15 °C | 56.6 | 54.3 | 51.0 |
| T = 18 °C | 42.4 | 47.0 | 51.7 |
| T = 21 °C | 36.4 | 45.3 | 40.3 |
| T = 23 °C | 38.3 | 18.0 | 41.9 |
| T = 25 °C | 38.9 | 46.6 | 43.4 |

The segregated solution method is the default method in most commercial finite volume codes. It is best suited for incompressible flows or compressible flows at low Mach number.

Compressible flows at high Mach number, especially when they involve shock waves, are best solved with the coupled solver.

In this work, we have used from segregated solution method.

3.8. Convergence test

Three criteria are considered in assessing the model for convergence. For convergence to occur, all three criteria must be confirmed. The first criterion is the residuals of equations which are defined and must not change drastically through iterations. The second criterion is the concentration of radon in one of the rooms. Here we examine the radon concentration in Room 1. Concentration must not change through iterations. The third criterion is the rate of radon passing through the outlet. As all the radon that is generated in the floor must pass through the outlet, and as the model is solved for the steady state, the radon rate through the outlet must be equal to the radon generation rate. Specifically, the radon rate through the outlet must be 2 Bq/s and 3 Bq/s for 1 Pa and 2 Pa pressure differences respectively.

4. Measuring method

The experimental system comprises of a one family detached house, radon measurement tools, including an electronic radon monitor and alpha track detectors, a heat exchanger unit and some information about the indoor radon levels in recent years. Radon measurement instrument is an electronic radon monitor (CRM),

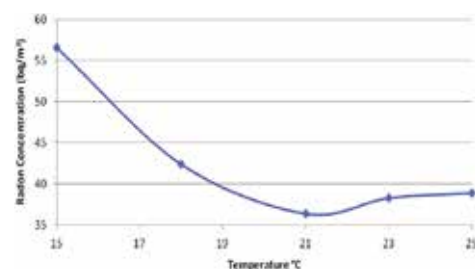


Fig. 3. Radon concentrations in Room 1 versus temperature from CFD model outputs.

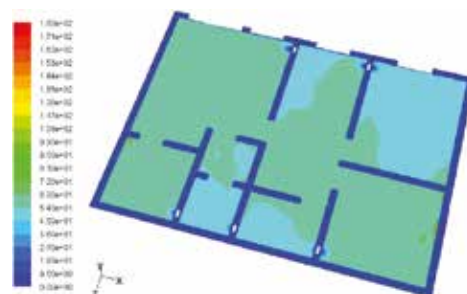


Fig. 4. Contours of radon concentration in the house plan for T = 15 °C from CFD model outputs.

which is an electronic device. It is used for long and short term test. This radon meter, R2, is manufactured by a Swedish company (Radonelektronik, 2012). It is used to identify problems with indoor radon and influences of physical and environmental factors such as ventilation effects and indoor conditions. Indoor temperature and relative humidity are also measured and logged, so that any influence from the measuring environment can be determined. This radon meter undergoes control irradiation at Swedish Radiation Safety Authority (SSM) and gives very reliable values with 10% accuracy.

For measurement, one CRM device was installed in the middle of Room 1 (seating room) at desktop position for short and long term test. In general radon detectors measure the average level of indoor radon.

5. Analytical method

Indoor radon content can be calculated as (Man and Yeung, 1997; Petropoulos et al., 2001):

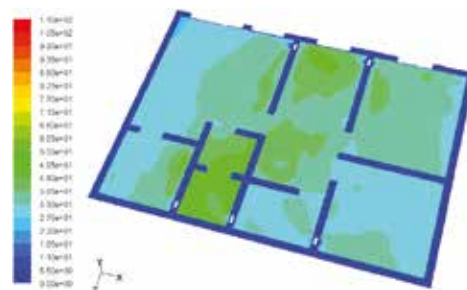


Fig. 5. Contours of radon concentration in the house plan for T = 25 °C from CFD model outputs.

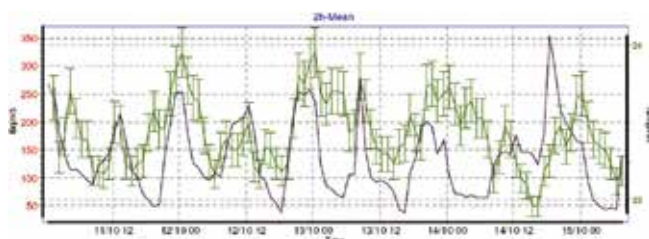


Fig. 6. Radon levels (green) versus temperature (purple) from measurement. (For interpretation of the references to colour in this figure legend, the reader is referred to the web version of this article.)

Table 3

Radon concentration (Bq/m³) for various relative humidities with Ach = 0.25 and T = 18 °C from CFD model outputs

| | Room 1 | Room 2 | Room 3 |
|----------|--------|--------|--------|
| RH = 30% | 102.2 | 94.3 | 105.3 |
| RH = 40% | 99.8 | 92.5 | 106.5 |
| RH = 50% | 96.6 | 93.8 | 106.7 |
| RH = 60% | 96.0 | 93.5 | 106.6 |
| RH = 70% | 96.5 | 97.4 | 106.8 |
| RH = 80% | 102.2 | 93.8 | 104.6 |

$$C = \frac{EA}{V(\lambda_{Rn} + \lambda_v)} \quad (9)$$

Where C (Bq m⁻³) is indoor radon content at steady state, E (Bq m⁻² h⁻¹) is radon exhalation rate, A (m²) is the radon exhalation surface (in this study the house floor), V (m³) is the volume of the house, λ_{Rn} (2.1×10^{-6} s⁻¹) is the radon decay constant and λ_v (h⁻¹) is the air change rate in the house.

For $E = 65$ Bq m⁻² h⁻¹ (Goto et al., 2008) and the given data of the case study house, Equation (9) gives indoor radon levels for different ventilation rates (0.0, 0.25, 0.5 and 1.0). These results are shown in Table 5.

6. Results

6.1. Temperature changes

In order to investigate the effect of temperature on radon concentration, in CFD model, air change rate and relative humidity

are fixed and temperature is varied from 15 °C to 25 °C. Start values for air change rate and relative humidity are 0.5 and 30% respectively. Outside temperature is set at 18 °C in the model.

When inside temperature is less than outside temperature, heat is transferred from the outside to the inside. Inside temperature therefore increases. This causes a decrease in relative humidity and therefore radon concentration also decreases. On the other hand, when inside temperature is greater than outside temperature, heat is transferred from inside to the outside, causing the inside temperature to fall, increasing relative humidity. This increases radon concentration. Therefore, we would expect radon concentration to decrease and then increase as temperature rises from 15 °C to 25 °C. Results of CFD model are shown in Table 2.

Radon concentration transport is essentially pressure based (convection mechanism), and higher indoor temperature acts like a weak vacuum cleaner and creates a stack effect phenomenon (Lesieur, 1990). In higher indoor temperatures, diffusion mechanism will also increase and boosts the effect of convection mechanism in radon transport and will decrease indoor radon content.

This behavior is clearly demonstrated in Fig. 3, where radon concentration from CFD model in Room 1 (seating room) is plotted against temperature.

Figs. 4 and 5 show contours of radon concentration at $y = 210$ cm from the floor at various temperatures from CFD model outputs. These figures show the effects of temperature on both radon concentration and distribution.

Radon measurement with the CRM radon meter provides confirmation that radon levels show strong correlation with indoor temperature. These results are shown in Fig. 6. This figure is plotted based on measurement results at air exchange rate Ach = 0.05.

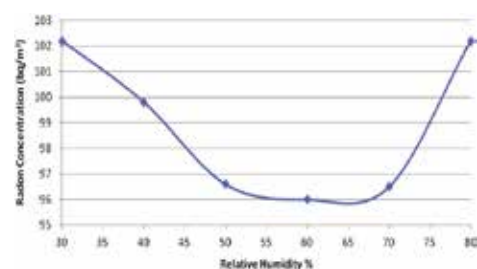


Fig. 7. Radon concentration in Room 1 versus relative humidity from CFD model outputs.

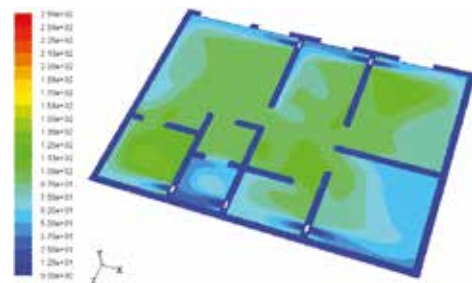


Fig. 8. Contours of radon concentration in the house plan for RH = 30% from CFD model outputs.

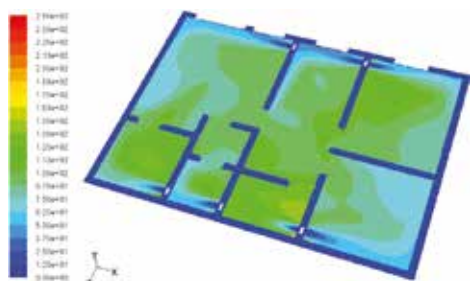


Fig. 9. Contours of radon concentration in the house plan for RH = 70% from CFD model outputs.

6.2. Relative humidity changes

In order to investigate the effect of relative humidity on indoor radon concentration, six values of relative humidity are considered for a given temperature and air change rate. The relative humidity values are 30%, 40%, 50%, 60%, 70%, and 80% and temperature and air change rate are set at 18 °C and 0.25 respectively. The model is solved for these cases and the results of CFD model are shown in Table 3.

Fig. 7 is plotted based on CFD model outputs. This figure shows the effect of relative humidity on radon concentration in Room 1 (seating room). This figure shows that increasing relative humidity increases water content in the house and decreases the radon concentration. However, as relative humidity increases further, air density increases, and radon in the room cannot rise upwards. Increasing water content in air also leads to lower diffusion coefficients and hence shorter diffusion length for radon. The shorter radon length also restricts the height that radon can rise to.

Fig. 7 shows that radon concentration falls as relative humidity increases from 30% to 60%, and radon concentration increases as relative humidity increases above 70%.

Figs. 8 and 9 show contours of radon concentration at a position $y = 210$ cm from the floor for various relative humidity values.

Figs. 8 and 9 clearly indicate that the relative humidity influences both radon concentration and distribution.

Radon measurement with the CRM radon meter also show strong correlation with indoor relative humidity. These results are shown in Fig. 10 at Ach = 0.05.

6.3. Air change rate effects

Contours of radon concentration in the house plan at position $y = 210$ cm from the floor for various air change rates, from CFD model outputs, are shown in Fig. 11. This figure shows qualitative comparisons of radon concentrations at four different hourly air change rates ranging from 0.05 to 1.2 Ach. As evident from Fig. 12,

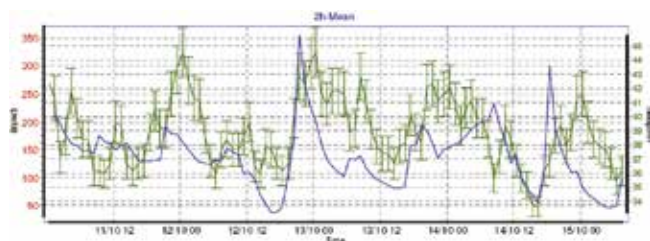


Fig. 10. Radon levels (green) versus relative humidity (blue) from measurement. (For interpretation of the references to colour in this figure legend, the reader is referred to the web version of this article.)

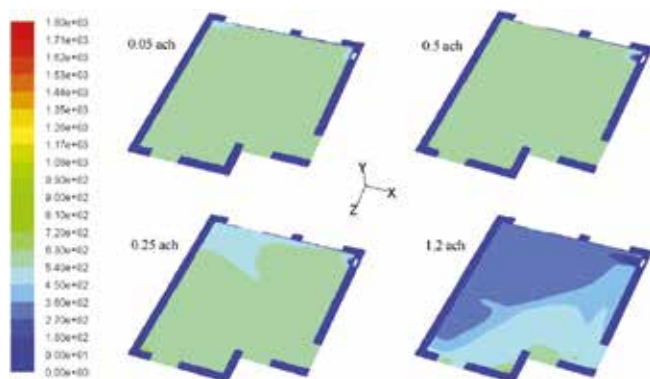


Fig. 11. Contours of radon concentration in the house plan (Room 1) with air change rates 0.05–1.2 Ach from CFD model outputs.

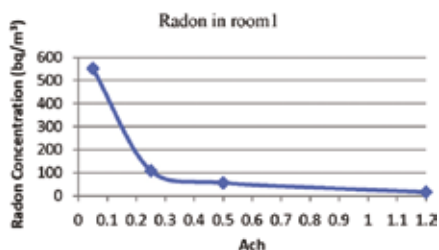


Fig. 12. Radon concentrations in Room 1 versus air change rate from CFD model outputs.

different ventilation rates have distinct effects on indoor concentration in Room 1 (seating room).

The results of measurements are also shown in Table 4. In order to show the impact of ventilation rate on radon level, radon concentrations were measured at three different ventilation rates. Different remedial actions were also considered during measurements. Fig. 13 shows the results at three different air change rates and using of 5 connected sumps, measured with a CRM. The figure shows that measured radon levels were inversely proportional to air exchange rate.

Continuous radon measurements using a CRM also confirmed that in the indoor temperature range, fluctuating radon levels in the house have strong indirect correlation with temperature.

7. Model validation

Model validation was performed using analytical solution from Equation (9). The numeric differences between numerical simulation and analytical calculation results are shown in Table 5.

For quantitative comparisons, the percentage difference between the results of estimation by FLUENT and the analytical calculations were computed at each ventilation rate. The maximum difference was found to be below 10%. Measurement data for the

Table 5

Indoor radon concentration results in Bq m^{-3} .

| Ach | Measurement | Analytical solution | Numerical simulation | Difference (%) |
|------|-------------|---------------------|----------------------|----------------|
| 0.0 | 3580 | 3582 | — | — |
| 0.25 | 90 | 106 | 107 | 0.9 |
| 0.5 | 45 | 53 | 55 | 3.6 |
| 1.2 | 25 | 22 | 20 | 10.0 |

specified house plan were also in good agreement with numerical simulation results.

8. Discussion

This study shows that indoor conditions, i.e. ventilation rate, temperature and moisture can have a significant effect on indoor radon concentration. These effects are described and demonstrated theoretically, by numerical simulation and through measurement and are also validated by analytical solution.

Equation (4) shows that increasing indoor temperature results in increasing radon diffusion coefficient. Radon transport within indoor environment is a result of two mechanisms, convection mechanism and diffusion mechanism. Radon transport by convection mechanism is due to pressure gradient and airflow. For a specific air change rate, convection mechanism is constant and therefore only diffusion mechanism will affect on radon concentration and distribution. Increasing diffusion coefficient increases diffusion mechanism effect and therefore it boosts the convection mechanism effect on radon depletion from indoor environment and reduces radon concentration. Therefore increasing temperature in a specific air change rate and constant relative humidity by increasing radon diffusion coefficient reduces indoor radon content. However, in high diffusion values the situation of radon transport will be complicated and many other parameters should also be considered. The numerical results shown in Fig. 3 confirm the inverse relationship between temperature and radon level in the house.

From the relative humidity viewpoint, maximum diffusion coefficient value occurs within 20%–80% of relative humidity

Table 4

Measured indoor radon levels (Bq m^{-3}).

| Date and period | ATD | CRM | Ventilation rate | Ventilation type | Remedial action |
|-------------------|----------------|----------------|------------------|------------------|----------------------|
| 2008–2 (2 weeks) | 3580 ± 380 | — | 0.25 | Extract fan | No action |
| 2010–1 (3 months) | 1280 ± 160 | 1580 ± 158 | 0.25 | HRV | Radon sump & sealing |
| 2010–04 (3 weeks) | 100 ± 20 | — | 0.5 | HRV | 3 connected sumps |
| 2010–3 (12 days) | — | 97 ± 10 | 0.5 | HRV | 3 connected sumps |
| 2010–3 (12 days) | — | 65 ± 6 | 0.5 | HRV | 3 connected sumps |
| 2010–4 (12 days) | — | 36 ± 4 | 1 | HRV | 3 connected sumps |

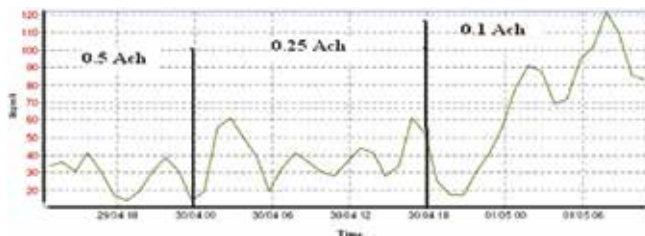


Fig. 13. Radon concentrations versus ventilation rate from measurement (5 connected sumps were used).

(Kotrappa et al., 1976). The affection mechanism of diffusion coefficient on radon concentration has been explained in the previous paragraph. Increasing diffusion coefficient leads to decreasing of radon content. Therefore within mentioned range of relative humidity, minimum radon concentration will be obtained. The same results have been obtained from the numerical simulation which is plotted in Fig. 7. In addition, Equation (6) shows that increasing indoor temperature increases the saturation vapor pressure, which has a direct effect on total pressure, leading to lower radon levels.

Increasing ventilation rate increases air change rate which decreases radon level. In this case, increasing ventilation rate, convection mechanism which is due to pressure gradient will be dominant mechanism in depletion of radon from indoor environment.

Results of numerical modeling indicate a strong relationship between ventilation rate, relative humidity, temperature and indoor radon in the thermal comfort range.

9. Conclusions

It is seen that ventilation rate has direct effect on radon level. In addition to maintaining a specific ventilation rate and establishing the desired indoor pressure using a balanced ventilation system, it is necessary to maintain indoor air temperature and relative humidity within a specific range to minimize radon levels. These ranges can be determined and depend on radon level, ventilation rate and type, radon mitigation system and climatic conditions.

In this case study, it is shown that setting temperature between 20 and 22 °C and relative humidity between 50 and 60% in a specific air change rate can affect on indoor radon levels.

The 3D models developed with FLUENT simulated radon entry through the floor into a one family house. The overall results indicate that indoor radon concentrations are dependent on ventilation rate, indoor temperature and moisture levels. The verification of the model and its performance support the idea that radon entry to the house and effects of ventilation rate, temperature and moisture can be defined well physically and numerically. The performance and sensitivity of the model was confirmed by varying input parameters and boundary conditions. The results indicate that the considered conditions and assumptions provided acceptable modeling of this environment. This model may therefore be useful and applicable for other similar problems under a similar range of conditions.

This model may be improved by considering additional parameters that occur in real situations in residential buildings, such as wall temperature, internal heating sources and external situations and temperature differences between the inside and outside. The problem can be modeled with the integration of all or some combinations of these to reflect real weather conditions. In addition, more detailed treatment of turbulence and wall effects and a finer grid near the source may also improve CFD performance.

In conclusion, CFD is a powerful tool for exploring the factors that influence radon distribution in a residential building. However, the accuracy of indoor radon and indoor conditions simulation results can only be confirmed for conditions that have been validated.

References

- Andersen, C.E., 2001. Numerical modeling of radon-222 entry into houses: an outline of techniques and results. *J. Sci. Total Environ.* 272, 33–42.
- Clever, H.L., 1979. Solubility Data Series. In: Krypton, Xenon and Radon Gas Solubility, vol. 2. Pergamon Press, Oxford.
- FLUENT Incorporation, 2005. FLUENT User's Guide Version 6.3. FLUENT Inc., Lebanon, NH, USA.
- Goto, M., Moriizumi, J., Yamazawa, H., Iida, T., Zhuo, W., 2008. Estimation of global radon exhalation rate distribution. In: *Proc. of 8th Int. Symp. Natural Radiation Environment-AIP Conference*, Buzios, Brazil, vol. 1034, pp. 169–172.
- Kotrappa, P., Bhanti, D.P., Raghunath, B., 1976. Diffusion coefficients for unattached decay products of thoron-dependence on ventilation and relative humidity. *J. Health Phys.* 31, 378–380.
- Lesieur, M., 1990. *Turbulence in Fluids*. Kluwer Academic Publisher, Dordrecht, The Netherlands.
- Man, C.K., Yeung, H.S., 1997. The effects of cracks and holes on the exhalation of radon from concrete. *J. Build. Environ.* 32 (4), 351–354.
- Petropoulos, N.P., Anagnostakis, M.J., Simopoulos, S.E., 2001. Building materials radon exhalation rate: ERRICCA intercomparison exercise results. *J. Sci. Total Environ.* 272 (1–3), 109–118.
- Radonelektronik, 2012. Available at: www.radonelektronik.se (accessed 10.05.12.).
- Sonntag, D., 1990. Important new values of physical constants of 1986, vapour pressure formulations based on the ITS-90, and Psychrometer Formulae. *J. Z. Meteorol.* 40 (5), 340–344.
- Stranden, E., Kolstad, A.K., Lind, B., 1984. The influence of moisture and temperature on radon exhalation. *J. Radiat. Protect. Dosim.* 7 (1–4), 55–58.
- Sun, H., Stowell, R.R., Keener, H.M., Michel, F.C., 2002. Two-dimensional computational fluid dynamics (CFD) modeling of air velocity and ammonia distribution in a high-rise (TM) Hog building. *Trans. ASAE* 45 (5), 1559–1568.
- Surbeck, H., 1996. A radon in water monitor based on fast gas transfer membranes. In: *Proc. Int. Conf. on Technologically Enhanced Natural Radioactivity*, Poland, pp. 16–19.
- Van der Pal, M., Van der Spoel, W.H., 2001. A simple method for measuring radon adsorption in porous materials. In: *Proc. Workshop Radon in the Living Environment*, Liege, Belgium.
- Wang, F., Ward, I.C., 2000. The development of a radon entry model for a house with a cellar. *J. Build. Environ.* 35, 615–631.

